


July 2016

Photolysis of Triazenylbenzoic Acids for Click Chemistry

Adam Gann

Follow this and additional works at: https://scholarworks.umass.edu/dissertations_2

 Part of the [Molecular Biology Commons](#), and the [Organic Chemistry Commons](#)

Recommended Citation

Gann, Adam, "Photolysis of Triazenylbenzoic Acids for Click Chemistry" (2016). *Doctoral Dissertations*. 661.

https://scholarworks.umass.edu/dissertations_2/661

This Open Access Dissertation is brought to you for free and open access by the Dissertations and Theses at ScholarWorks@UMass Amherst. It has been accepted for inclusion in Doctoral Dissertations by an authorized administrator of ScholarWorks@UMass Amherst. For more information, please contact scholarworks@library.umass.edu.

PHOTOLYSIS OF TRIAZENYLBENZOIC ACIDS FOR CLICK CHEMISTRY

A Dissertation Presented

By

ADAM WILLIAM GANN

Submitted to the Graduate School of the
University of Massachusetts Amherst in partial fulfillment
of the requirements for the degree of

DOCTOR OF PHILOSOPHY

May 2016

Department of Chemistry

© Copyright by Adam William Gann 2016

All Rights Reserved

PHOTOLYSIS OF TRIAZENYLBENZOIC ACIDS FOR CLICK CHEMISTRY

A Dissertation Presented

By

ADAM WILLIAM GANN

Approved as to style and content by:

James Chambers, Chair

Nathan Schnarr, Member

Sankaran Thayumanavan, Member

Richard Vachet, Member

E. Bryan Coughlin, Member

Craig T. Martin, Department Head

Department of Chemistry

DEDICATION

To my mother and father, Kellie and Gary Gann, for raising me to think before I speak, for supplementing my desire to build and create with countless LEGO sets, and for giving me the foundations in life necessary to pursue academic rigors. To my brother and sister, Matt and Shannon, for teaching me all the things I needed to do to get in trouble, and how to grow as a person. And to my ever-so-patient girlfriend, Kaitlyn Flenke, for listening to me speak in what could only be perceived as gibberish for the several months of proposal and dissertation writing and defending. I could never had made this happen without the support from the people close to me.

ACKNOWLEDGMENTS

I would like to thank my advisor, Nathan Schnarr for his guidance, encouragement on a seemingly-impossible project, and teaching me to always doubt my results; the mark of a true scientist. In addition to Nate, I would also like to thank my collaborative advisor, Jim Chambers for helping ease the pressure associated with a mid-PhD-career transition. I would also like to thank my committee for their valuable advice, experimental ideas, and presentation critique. Not only do my advisors and committee deserve recognition, but all those who assisted in my education throughout my life. If there is one thing I have learned through all the TA'ing, it is that teaching is best left to the professionals.

I cannot leave out my group members who made enormous contributions to the success of this project. Jon Amoroso assisted in getting the photochemistry off the ground and helped establish the basics behind the photolysis. Amanda Hussey helped with the implementation of our final design onto our most complicated system, cells.

ABSTRACT

PHOTOLYSIS OF TRIAZENYLBENZOIC ACIDS FOR CLICK CHEMISTRY

May 2016

ADAM WILLIAM GANN, B.S., BAYLOR UNIVERSITY

Ph.D., UNIVERSITY OF MASSACHUSETTS AMHERST

Directed by Dr. Nathan Schnarr

Copper catalyzed cycloaddition of terminal alkynes and azides has revolutionized the field of bioconjugate chemistry. Unfortunately, typical copper catalysts are known to disrupt relevant biological systems, so it has become necessary to develop new, copper-free methods that are less cytotoxic. particular interest are "click" probes which can be activated with an outside light source, giving the user spatial and temporal control over the system being investigated. We have developed a method in which an aryl diazonium salt is rapidly generated using photolysis of the triazene functional group, and subsequently coupled with an electron rich aromatic nucleophile to yield an azobenzene. Benefits of this method over current photo-click methods include the fast rate of photolysis and almost instantaneous reaction times with subsequent reaction partners, allowing for minimal exposure to a UV light source and little to no incubation time with reactive partners, respectively.

TABLE OF CONTENTS

	Page
ACKNOWLEDGMENTS.....	v
ABSTRACT.....	vi
LIST OF TABLES.....	xi
LIST OF FIGURES.....	xii
CHAPTER	
I. INTRODUCTION AND BACKGROUND OF CLICK CHEMISTRY, BIO-ORTHOAGONAL CLICK CHEMISTRY, AND PHOTO-INDUCED CLICK CHEMISTRY	1
A. Introduction to Click Chemistry.....	1
B. Copper(I)-Catalyzed Azide-Alkyne Cycloaddition	2
C. Traditional Tools for Cu-Free Click Chemistry	3
D. Benzyne Chemistry	7
E. Photochemical-based Click Reactions	10
F. References	15
II. DEVELOPMENT OF A PHOTO-INDUCED, BENZYNE CLICK REACTION	22
A. Introduction.....	22
B. Results and Discussion.....	24
C. Experimentals	34
1. General.....	34
2. Synthetic Procedures	35
a. 2-(3-Acetyl-3-methyltriaz-1-en-1-yl)benzoic acid (1a).....	35
b. (E)-2-(morpholinodiazenyl)benzoic acid (1b)	36
c. (Azidomethyl)benzene (15).....	37
d. (E)-(3-Azidoprop-1-en-1-yl)benzene (16)	38
e. Azidobenzene (17)	38
f. 1-Azido-4-methoxybenzene (18)	39

g. 1-Azido-4-nitrobenzene (19).....	39
h. 4-(<i>tert</i> -Butyl)benzyl 2-azidoacetate (20)	40
i. Ethyl 2-azidoacetate (21)	41
j. 2-Azido-1-morpholinoethanone (22).....	41
k. <i>N</i> -(3-Azidopropyl)acetamide (23)	42
l. 3-Azidopropan-1-ol (24).....	43
m. Synthesis of Benzotriazoles using Photolysis of Compound 1.....	43
n. 1-Benzyl-1 <i>H</i> -benzo[<i>d</i>][1,2,3]triazole (5)	44
o. 1-Cinnamyl-1 <i>H</i> -benzo[<i>d</i>][1,2,3]triazole (6).....	44
p. 1-Phenyl-1 <i>H</i> -benzo[<i>d</i>][1,2,3]triazole (7).....	45
q. 1-(4-Methoxyphenyl)-1 <i>H</i> -benzo[<i>d</i>][1,2,3]triazole (8).....	45
r. 1-(4-Nitrophenyl)-1 <i>H</i> -benzo[<i>d</i>][1,2,3]triazole (9).....	45
s. 4-(<i>tert</i> -Butyl)benzyl 2-(1 <i>H</i> -benzo[<i>d</i>][1,2,3]triazol-1-yl)acetate (10) ...	46
t. Ethyl 2-(1 <i>H</i> -benzo[<i>d</i>][1,2,3]triazol-1-yl)acetate (11)	46
u. 2-(1 <i>H</i> -Benzo[<i>d</i>][1,2,3]triazol-1-yl)-1-morpholinoethanone (12)	47
v. <i>N</i> -(3-(1 <i>H</i> -Benzo[<i>d</i>][1,2,3]triazol-1-yl)propyl)acetamide (13)	47
w. 3-(1 <i>H</i> -Benzo[<i>d</i>][1,2,3]triazol-1-yl)propan-1-ol (14)	47
 3. Functionalized Benzyne Precursor Synthesis	
a. Methyl 4-(hydroxymethyl)-2-nitrobenzoate (25)	48
b. Methyl 2-amino-4-(hydroxymethyl)benzoate (26).....	48
c. Methyl 2-amino-4-(chloromethyl)benzoate (27).....	49
d. Methyl 2-amino-4-(azidomethyl)benzoate (28)	50
e. (2-Amino-4-(azidomethyl)phenyl)methanol (29)	50
f. (E)-1-(3-(5-(azidomethyl)-2-(hydroxymethyl)phenyl)-1-methyltriazol-2-en-1-yl)ethanone (30).....	51
g. (E)-2-(3-acetyl-3-methyltriaz-1-en-1-yl)-4-(azidomethyl)benzaldehyde (31)	52
h. (E)-2-(3-acetyl-3-methyltriaz-1-en-1-yl)-4-(azidomethyl)benzoic acid (32)	53

i. (E)-4-((carboxymethyl)amino)-4-oxobut-2-enoic acid (33).....	53
j. 2-(2,5-dioxo-2,5-dihydro-1H-pyrrol-1-yl)acetic acid (34)	54
k. 2-(2,5-dioxo-2,5-dihydro-1H-pyrrol-1-yl)-N-(prop-2-yn-1-yl)acetamide (35)	55
l. (E)-2-(3-acetyl-3-methyltriaz-1-en-1-yl)-4-((4-((2-(2,5-dioxo-2,5-dihydro-1H-pyrrol-1-yl)acetamido)methyl)-1H-1,2,3-triazol-1-yl)methyl)benzoic acid (36)	55
4. Spectroscopic Yield Determinations	56
a. General procedure for Benzotriazole Authentic Standard preparation using Larock Method	56
b. Percent Conversion to Benzotriazole	57
c. Molar Ratio, Irradiation Time, and Solvent Effect Experiments	59
d. Water Tolerance Experiments	60
e. Photolysis of TBA and Diazonium with no azide partner.....	61
D. References	61
III. PHOTOLYSIS OF <i>ORTHO</i> -TRIAZENYLBENZOIC ACIDS TO YIELD <i>ORTHO</i> -DIAZONIUM CARBOXYLATE	63
A. Introduction	63
B. Results and Discussion.....	66
C. Experimentals	72
1. General.....	72
2. Synthetic Procedures	73
a. (E)-2-((2,4,6-trihydroxyphenyl)diazenyl)benzoic acid (37)	73
3. Quantum Yield Determination.....	73
4. Kinetics.....	74
a. Addition of Diazonium to Phloroglucinol (420 nm)	75
b. Addition of Diazonium to Morpholine (305 nm)	76
c. Addition of Diazonium to Phenol (347 nm)	76
D. References	76

IV. BIOLOGICAL APPLICATIONS AND FUTURE DIRECTIONS OF PHOTO-GENERATED <i>ORTHO</i> - DIAZONIUM CARBOXYLATE	79
A. Introduction	79
B. Results and Discussion	80
C. Future Directions	90
1. Bioorthogonal Development	91
2. Improving Kinetics	92
D. Experimentals	94
1. General	94
2. Synthetic Procedures	94
a. (E)-methyl 4-(hydroxymethyl)-2-(morpholinodiazenyl) benzoate (39)	94
b. (E)-4-(azidomethyl)-2-(morpholinodiazenyl)benzoic acid (40)	95
c. (E)-4-((4-((2-(2,5-dioxo-2,5-dihydro-1H-pyrrol-1- yl)acetamido)methyl)-1H-1,2,3-triazol-1-yl)methyl)-2- (morpholinodiazenyl)benzoic acid (41)	96
d. (Z)-N-(prop-2-yn-1-yl)heptadec-9-enamide (42)	97
e. 4-((4-((Z)-heptadec-9-enamidomethyl)-1H-1,2,3-triazol-1-yl)methyl)- 2-((E)-morpholinodiazenyl)benzoic acid (43)	98
f. tert-butyl 4-(3,5-dihydroxyphenyl)piperazine-1-carboxylate (44)	99
g. 2-((1E,3E)-3-(1-(6-(4-(3,5-dihydroxyphenyl)piperazin-1-yl)-6- oxohexyl)-3,3-dimethylindolin-2-ylidene)prop-1-en-1-yl)-1,3,3- trimethyl-3H-indol-1-ium chloride (45)	100
h. 4-(5-(4-(3,5-dihydroxyphenyl)piperazin-1-yl)-5- oxopentyl)tetrahydro-1H-thieno[3,4-d]imidazol-2(3H)-one (46)	101
3. Protein Labeling	102
4. Cell Labeling	102
E. References	103
BIBLIOGRAPHY	106

LIST OF TABLES

Table	Page
2.1 Solvent, irradiation time, and molar ratio optimization for irradiation of 1a in the presence of benzylazide	27
2.2 Percent conversion to 5	57
2.3 Percent conversion to 6	58
2.4 Percent conversion to 7	58
2.5 Percent conversion to 8	58
2.6 Percent conversion to 9	58
2.7 Percent conversion to 10	58
2.8 Percent conversion to 11	59
2.9 Percent conversion to 12	59
2.10 Percent conversion to 13	59
2.11 Percent conversion to 14	59
2.12 Solvent effects	60
2.13 Water tolerance on conversion	61
2.14 Monitoring consumption during photolysis	61
3.1 Reaction completions for quantum yield determination	75
3.2 Extinction coefficients and subsequent relative quantum yields	75
3.3 Double exponential constants for phloroglucinol kinetics	76
3.4 Linear constants for morpholine kinetics	77
3.5 Linear constants for phenol kinetics	77

LIST OF FIGURES

Figure	Page
1.1 Idea behind click chemistry.....	1
1.2 The prevalence of biological nucleophiles make traditional electrophilic labeling techniques an unattractive option for specificity.	2
1.3 Azide-Alkyne Cycloadditions.....	3
1.4 Electron deficient alkynes have proven capable targets of azides for Huisgen cycloadditions	4
1.5 Strain-promoted azide-alkyne cycloadditions	4
1.6 Variants of cyclooctynes developed for copper-free click chemistry in order to increase kinetics of the cycloaddition step	5
1.7 Tetrazene-transcyclooctene (TCO) inverse-demand Diels-Alder ligation.....	6
1.8 Benzyne, the most basic aryne	7
1.9 Mystery surrounding aryl halide substitutions.....	8
1.10 Various methods used to generate the highly reactive benzyne intermediate	9
1.11 Proposed idea to generate benzyne in a bioorthogonal manner and trap with azides in an aqueous environment.....	10
1.12 Recently photo-induced click techniques.....	11
1.13 Development of the nitrile imine-alkene cycloaddition	13
1.14 <i>o</i> -Nitro hydrazide as a benzyne precursor is slow	14
2.1 Comparison of fluoride-induced benzyne click A with a photochemical approach B	22
2.2 Decomposition pathways of aryl triazenes.....	23
2.3 The desired triazenylbenzoic acid could not be obtained by using <i>N</i> -methylacetamide as a nucleophile towards the terminal diazonium nitrogen	24
2.4 The target compound 1a is available in four straightforward synthetic steps from commercially available <i>o</i> -aminobenzyl alcohol in 40% overall yield.....	24
2.5 Synthesis of morpholinyl triazene	25
2.6 Comparison of rates of photolysis for 1a and 1b in acetonitrile	26
2.7 Scope of the photoinduced, benzyne click reaction.....	28
2.8 Water tolerance of our photoinduced, benzyne click reaction	29
2.9 Synthesis of a maleimide linker-functionalized triazenylbenzoic acid	31
2.10 Irradiation of a 50 μ L solution of 15 mM maleimide triazenylbenzoic acid 36 (pre-conjugated to methyl thioglycolate).....	32

2.11 Irradiation of 1a in 9:1 water/acetonitrile (2 mM, 50 μ L)	33
2.12 Synthesis of 1a	35
2.13 Synthesis of 1b	37
2.14 Synthesis of 15	37
2.15 Synthesis of 16	38
2.16 Synthesis of 17	38
2.17 Synthesis of 18	39
2.18 Synthesis of 19	39
2.19 Synthesis of 20	40
2.20 Synthesis of 21	41
2.21 Synthesis of 22	41
2.22 Synthesis of 23	42
2.23 Synthesis of 24	43
2.24 Synthesis of benzotriazoles using photolysis.....	43
2.25 Synthesis of 5	44
2.26 Synthesis of 6	44
2.27 Synthesis of 7	45
2.28 Synthesis of 8	45
2.29 Synthesis of 9	45
2.30 Synthesis of 10	46
2.31 Synthesis of 11	46
2.32 Synthesis of 12	47
2.33 Synthesis of 13	47
2.34 Synthesis of 14	47
2.35 Synthesis of 25	48
2.36 Synthesis of 26	48
2.37 Synthesis of 27	49
2.38 Synthesis of 28	50
2.39 Synthesis of 29	50
2.40 Synthesis of 30	51
2.41 Synthesis of 31	52
2.42 Synthesis of 32	53

2.43 Synthesis of 33	53
2.44 Synthesis of 34	54
2.45 Synthesis of 35	55
2.46 Synthesis of 36	55
2.47 Synthesis of benzotriazoles via the Larock method.....	56
2.48 Example standard curve prep using 5.....	57
3.1 Making use of the rapidly photo-generated diazonium carboxylate	65
3.2 Proposed diazonium click reaction core	66
3.3 Proposed explanation for slower photolysis of 1b in acetonitrile than in water	68
3.4 Support for recombination	69
3.5 Kinetic analysis of photogenerated diazonium carboxylate's coupling.....	71
3.6 Synthesis of 37	74
3.7 Equation for converting reaction completion to relative quantum yield.....	75
4.1 Design of click reaction using photo-generated diazonium carboxylate.....	80
4.2 Synthesis of functionalized triazenylbenzoic acids.....	82
4.3 Phloroglucinol tautomerization	83
4.4 Deprotected Boc-DHPP coupling with Cyanine-3	83
4.5 Labeling <i>h</i> ACP2 with 10x Mal-TBA 41 followed by irradiation in the presence of 10x Cy3-DHPP 45	84
4.6 Removing TCEP prior to labeling <i>h</i> ACP2 with 10x Mal-TBA 41 followed by irradiation in the presence of 10x Cy3-DHPP 45	85
4.7 Labeling of PHD2.....	86
4.8 Labeling array of proteins	87
4.9 Proposed experiment for labeling cellular membranes	88
4.10 Two biotin analogs functionalized with different electron-rich aromatic rings	89
4.11 Labeling of CHO cells.....	90
4.12 Proposed synthetic pathway to a triazenylbenzoic acid unnatural amino acid	92
4.13 Variations of the triazenylbenzoic acid core that could improve rates of photolysis and/or rates of electron-rich aromatic ring addition	94
4.14 Synthesis of 39	96
4.15 Synthesis of 40	97
4.16 Synthesis of 41	98

4.17 Synthesis of 42	99
4.18 Synthesis of 43	100
4.19 Synthesis of 44	101
4.20 Synthesis of 45	102
4.21 Synthesis of 46	103

CHAPTER I

INTRODUCTION AND BACKGROUND OF CLICK CHEMISTRY, BIO-ORTHOLOGICAL CLICK CHEMISTRY, AND PHOTO-INDUCED CLICK CHEMISTRY

A. Introduction to Click Chemistry

The term "click chemistry" was coined to describe a reaction which meets a demanding set of criteria which include modularity, broad scope, high yielding, fast kinetics, and limited by-product formation or interference¹. Click reactions typically involve an addition-type reaction between two compounds which each contain a specific and orthogonal functionality (**Figure 1.1**). Reactions which meet this definition, and can tolerate an aqueous solvent may find extremely useful applications in biological systems, primarily biomacromolecular labeling.

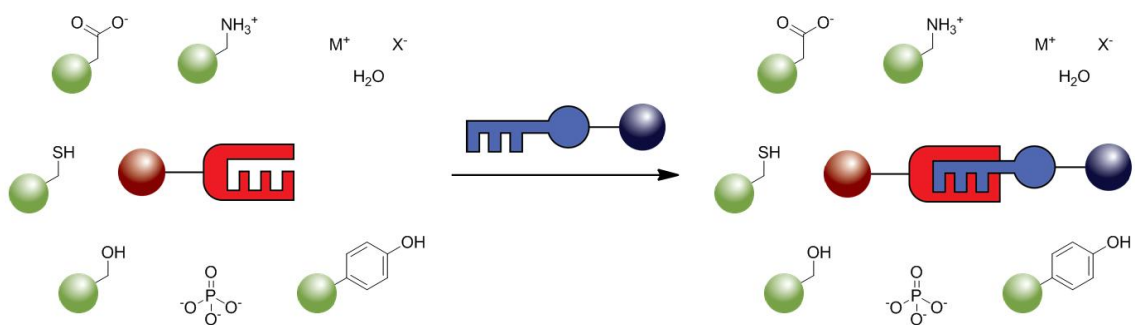


Figure 1.1: Idea behind click chemistry. The coupling of two orthogonal functional groups, joining two molecules together

Due to the complex chemical environment typically found within biology, the potential for undesired side reactions is quickly realized as the primary antagonist for biological labeling. Electrophilic addition of isocyanate⁻², isothiocyanate⁻³, acrylamide⁻⁴, and maleimide-bound⁵ labels to biological nucleophiles is prevalent, but limited in use to small, controlled systems due to a vast presence of potential targets (**Figure 1.2**).

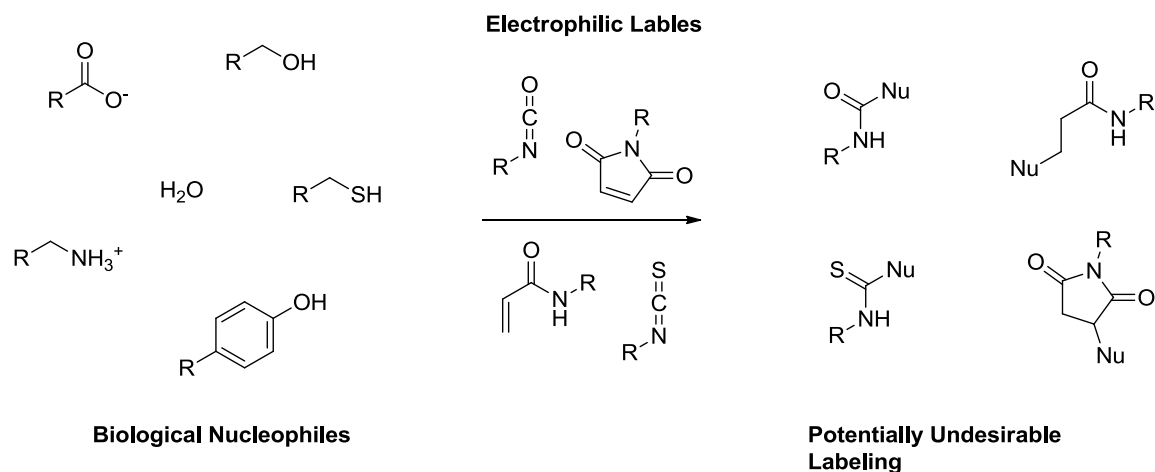


Figure 1.2: The prevalence of biological nucleophiles make traditional electrophilic labeling techniques an unattractive option for specificity.

Due to the non-specific nature of nucleophile-electrophile additions, click reactions used in biology often utilize cycloaddition reactions. Among these reactions, the copper(I)-catalyzed 1,3-dipolar azide-alkyne cycloaddition has become the golden standard to which many innovative click chemistry techniques are compared.

B. Copper(I)-Catalyzed Azide-Alkyne Cycloaddition

Cycloadditions between azido compounds and alkynes has been known to exist since their first introduction by Rolph Huisgen in 1961⁶, however this reaction was not useful for chemical biologists due to the higher temperatures and prolonged reaction times, and control over regiochemistry proved to be a difficult for synthetic chemists. In 2002, two separate publications^{7,8} were released which both highlighted the discovery of a copper catalyst which greatly increased the kinetics of the cycloaddition and allowed the reaction to proceed at room temperatures in an aqueous environment (**Figure 1.3**).

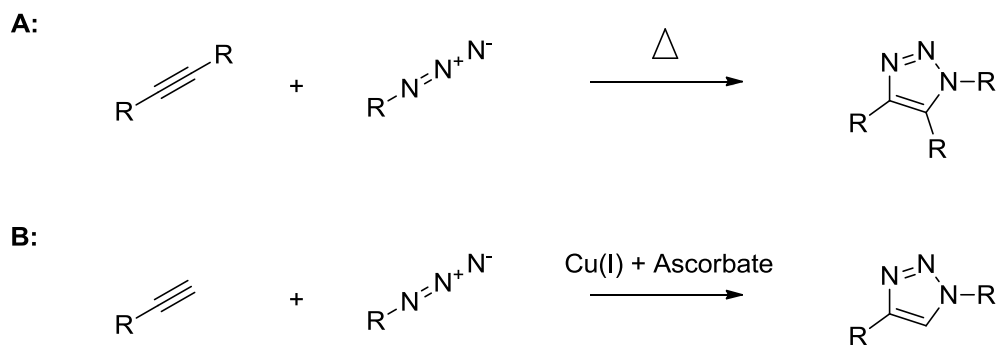


Figure 1.3: Azide-Alkyne Cycloadditions. A) The cycloaddition between an alkyne and organic azide compound demonstrated by Huisgen forms a 1,2,3-triazole under harsh conditions. B) The additions of a copper(I) catalyst by Meldal and Sharpless achieves a Huisgen cycloaddition under ambient conditions with rapid kinetics.

The now-dubbed Copper(I)-Catalyzed Azide-Alkyne Cycloaddition (CuAAC) was further discovered to also be catalyzed by a ruthenium complex⁹ and ligated silver.¹⁰ Most remarkably, presence of aliphatic or aromatic azide compounds and terminal alkynyl compounds are virtually absent in the natural world, leading to unprecedented selectivity for biological labeling. Additionally, azides are an attractive target due to their high stability and small size. Due to the small size, it is possible to engineer a native biological system to incorporate azide moieties into macromolecules with little issue due to down-stream processing.¹¹ While the impact the addition of a copper catalyst was great and continues to remain so, the CuAAC was not truly bioorthogonal. Copper salts are known to be cytotoxic, which greatly reduces the utility of CuAAC for *in vivo* experiments.¹² Additionally, previous work done in this lab had shown copper to be destructive towards proteins of interest^{13,14}, which drove the inspiration of this entire project; develop a new copper-free, bioorthogonal click reaction.

C. Traditional Tools for Cu-Free Click Chemistry

Shortly after the introduction of the CuAAC, the task of removing copper was undertaken by the bioconjugate community. In 2004, a copper-free Huisgen cycloaddition

between an azide and an electron deficient alkyne was demonstrated, however the alkynes became electrophilic due to the electron deficiency, and were susceptible to attack via Michael additions (**Figure 1.4**).¹⁵

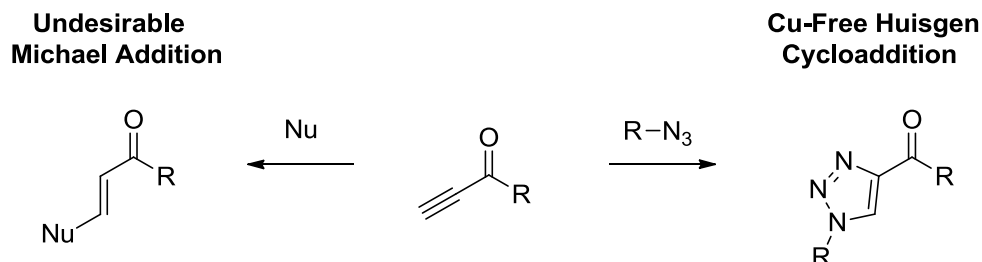


Figure 1.4: Electron deficient alkynes have proven capable targets of azides for Huisgen cycloadditions. However, the electron deficiency increases likelihood of 1,4 Michael additions.

Having realized that increasing the reactivity of the alkyne by decreasing its electron density was going to be inadequate, the Bertozzi group from U. C. Berkeley (now Stanford) sought to use ring strain of cyclic alkynes as a driving force to undergo efficient cycloaddition with azides, a reaction pioneered in 1961 by Wittig and Krebs (**Figure 1.5 A**).¹⁶

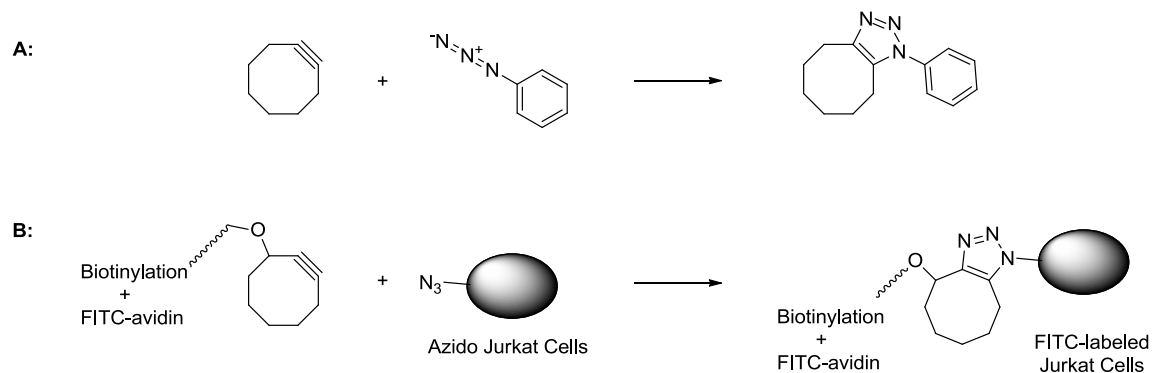


Figure 1.5: Strain-promoted azide-alkyne cycloadditions. A) Initial inspiration for cyclooctyne click chemistry demonstrated by Krebs and Wittig. B) First demonstration of cyclooctyne copper-free click chemistry in biological setting by Bertozzi.

Initial success was achieved when a biotin-conjugated cyclooctyne (OCT) successfully labeled the azide-modified glycoprotein, GlyCAM-IgG, and again when azide-modified surfaces of Jurkat cells (**Figure 1.5 B**).¹⁷ Although OCT showed no apparent cytotoxicity, the kinetics of

cycloaddition left much to be desired. Due to such a low secondary rate constant for the cycloaddition ($k_2 = 0.0024 \text{ M}^{-1}\text{s}^{-1}$), labeling of azido-proteins had to be incubated overnight, and labeling of azido-cells had to be done at an OCT concentration as high as 100 μM . Using higher concentrations could potentially accelerate the reaction, however OCTs showed limited water solubility, and increasing concentrations in this manner was previously shown to have unwanted side effects.

In order to increase the reactivity of the alkyne to improve kinetics, several modifications were made to the cyclooctyne core ring (**Figure 1.6**). Initial attempts to increase water solubility by removing aromatic rings led to a version with decreased kinetics, albeit improved water solubility was achieved.¹⁸ An increase in kinetics was observed when the propargyl position was mono- (MOFO, $k_2 = 0.0043 \text{ M}^{-1}\text{s}^{-1}$)¹⁸ and later difluorinated (DIFO, $k_2 = 0.076 \text{ M}^{-1}\text{s}^{-1}$)¹⁹. A similar rate was observed with a dibenzo- derivative (DIBO, $k_2 = 0.057 \text{ M}^{-1}\text{s}^{-1}$)²⁰,

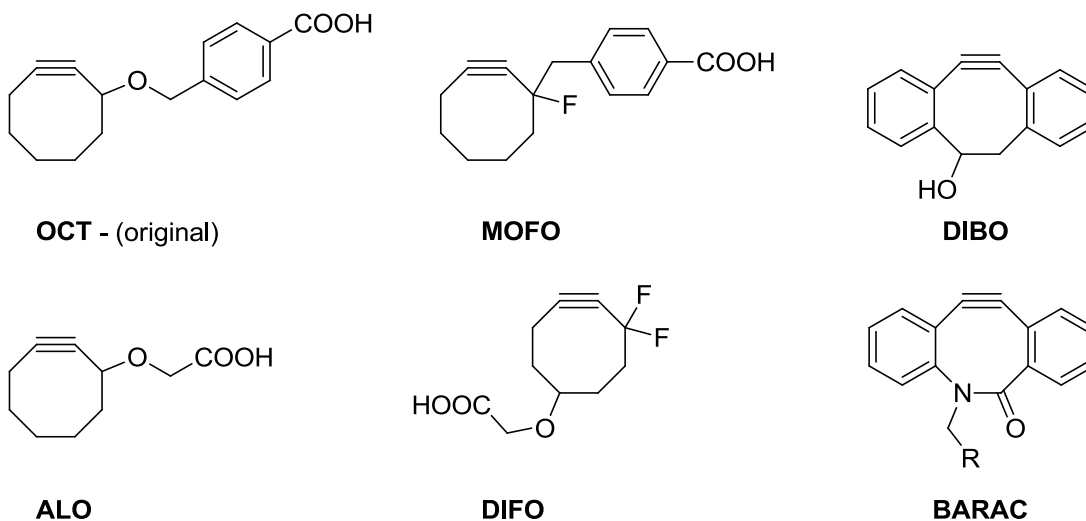


Figure 1.6: Variants of cyclooctynes developed for copper-free click chemistry in order to increase kinetics of the cycloaddition step.

and to even further increase the rate by an order of magnitude, an amide bond was included as part of the cyclooctyne ring of a dibenzo- derivative (BARAC, $k_2 = 0.96 \text{ M}^{-1}\text{s}^{-1}$).²¹ It would be

theoretically possible in greatly increase the reaction rate of cycloaddition by using a smaller scaffold than cyclooctyne, such as cycloheptyne, but the latter has been shown as too unstable for storage and non-ligated use.²²

Looking from a purely kinetic standpoint, the fastest bioorthogonal click-type reaction reported to date is an inverse-demand Diels-Alder reaction between a tetrazine and a trans-cyclooctene (TCO) (**Figure 1.7 A**). Initially reported in 2008²³ as a bioorthogonal reaction with a second order rate constant of $2000 \text{ M}^{-1}\text{s}^{-1}$, further improvements have yielded tetrazine-TCO reactions with second order rate constants as high as $3.3 \times 10^6 \text{ M}^{-1}\text{s}^{-1}$ (**Figure 1.7 B**).²⁴ Developments of this reaction have even taken roots in bioconjugate chemistry, as a tetrazine

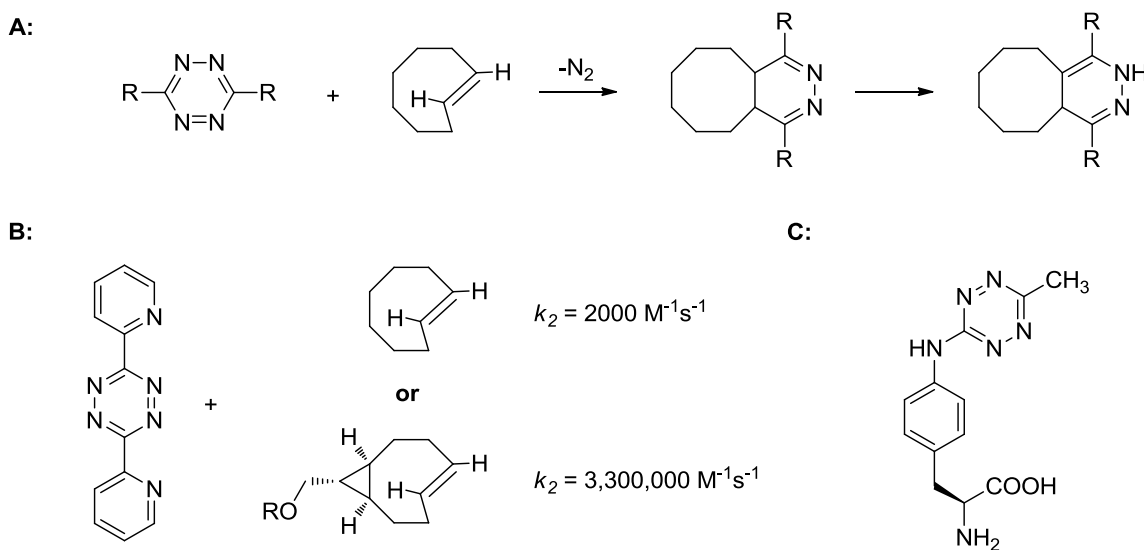


Figure 1.7: Tetrazine-transcyclooctene (TCO) inverse-demand Diels-Alder ligation. A) Reaction scheme of the ligation showing loss of nitrogen after the initial reaction, followed by a rearrangement. B) Reaction kinetics were initially fast, but further strain on the TCO made drastic improvements. C) Tetrazine unnatural amino acid which has been successfully incorporated into GFP.

amino acid was genetically incorporated into GFP while still displaying rapid cycloaddition with a TCO-conjugated rhodamine dye.²⁵ Although the tetrazine-TCO ligations proved to be dramatic improvements over cyclooctyne-azide-based click chemistry in terms of kinetics, the latter still

had the benefit of being targets for stable aliphatic azides. While improvements are being made, tetrazines reveal their unstable dark side by being potential targets for biological nucleophiles.²⁶ While impressed by the abilities of the tetrazine-TCO ligation, we were still interesting in finding a reaction in which some moiety undergoes cycloaddition with azides more rapidly than cyclooctynes. However, the bar had been set by the tetrazine-TCO ligation for desirable kinetics

D. Benzyne Chemistry

Instead of expanding the field of cyclooctynes, which has already been established to a large degree, we were interested in exploring a largely unexplored field of chemistry which has potential relevance to copper-free click chemistry - arynes.²⁷ Arynes are a highly reactive, non-isolable class of molecules which exhibit as a highly strained triple bond character within a six-membered aromatic ring. Benzyne, the benzene analog of arynes, represents the most basic

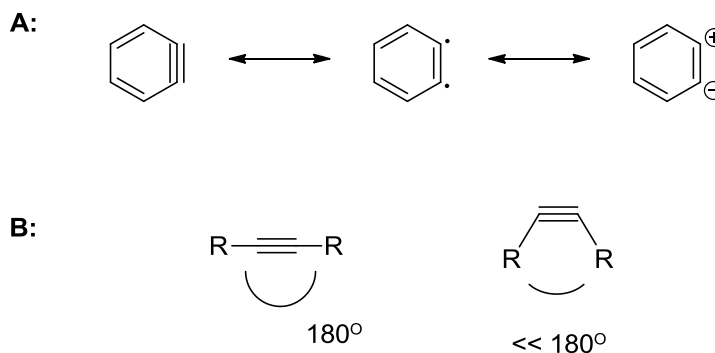


Figure 1.8: Benzyne, the most basic aryne. A) multiple ways of showing the nature of benzyne's triple bond. B) Reason for such high reactivity is attributed to the drastic amount of ring strain.

and classic example when discussing aryne chemistry. Initially, benzyne's existence sprang out of a mystery surrounding nucleophilic additions to aryl halides under strongly basic conditions. What was expected to be relatively simple substitutions at the halo-carbon turned out to yield a mix of isomers with addition occurring not only to the halo-carbon, but the alpha carbons as

well (**Figure 1.9 A**).²⁸ A proposed benzyne intermediate, formed from abstraction of a proton alpha to the halo-carbon leading to elimination (**Figure 1.9 B**), was suggested to be electrophilic towards the strong organo-lithium and amine bases.²⁹⁻³¹ If this was the case, the nucleophile could potentially add to either side of the triple bond of benzyne, leading to the observed substitution patterns.

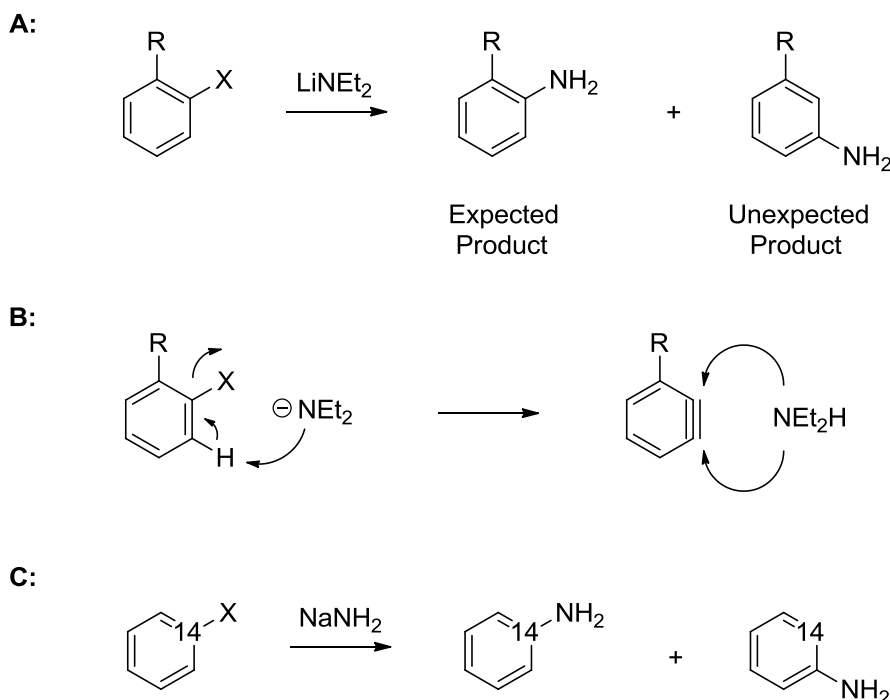


Figure 1.9: Mystery surrounding aryl halide substitutions. A) Direct substitution at the halo carbon not observed, 1:1 mixture of alpha substitution as well. B) Proposed mechanism explaining the observed substitution patterns containing intermediate benzyne. C) Intermediate confirmed by isotope-labeling experiment.

However, this was not confirmed until an isotope-labeling experiment was done using a C¹⁴-labeled halo carbon.³² Treatment with an amine base lead to a near 1:1 ratio of substitution at the isotope labeled carbon and substitution at a carbon alpha to the isotope label, suggesting that benzyne was an intermediate with two possible substitution locations (**Figure 1.9 C**).

Further exploration of lead to the discovery that benzyne was capable of cycloaddition reactions³³, and most importantly, 1,3-dipolar cycloadditions with phenyl azides as early as 1962.³⁴ We considered how useful benzyne could be in bioorthogonal click chemistry due to its potential to be an extremely fast reaction partner with azides due to its nature as an extraordinarily strained alkyne, but quickly realized one of the most difficult challenges would be how to generate benzyne in a bioorthogonal manner. The earliest methods typically involved very strong bases²⁸⁻³¹, metalated aryl species³⁵, or extreme temperatures.³⁶ Gradually, more mild methods were introduced (**Figure 1.10**), with the most prominent being the fluoride-activated aryl

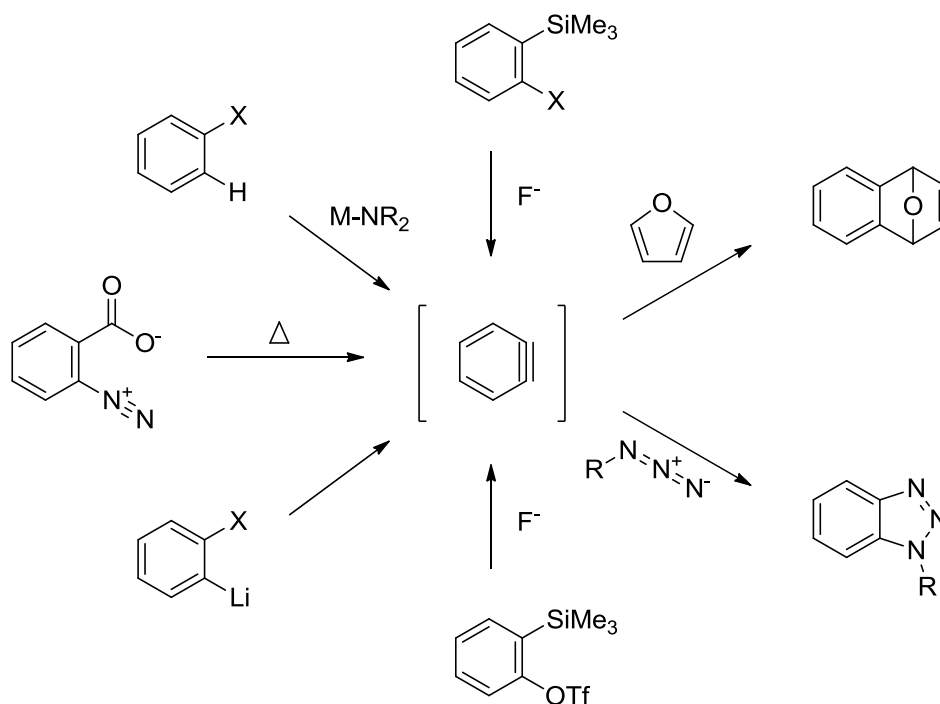


Figure 1.10: Various methods used to generate the highly reactive benzyne intermediate. Possible ways to utilize benzyne is to trap it with azido compound or in a pericyclic reaction.

trimethylsilyl derivatives.³⁷ Of great inspiration to our efforts was the work published by Larock in 2008 which highlighted efficient generation of benzotriazoles using *ortho*-trimethylsilylphenyl triflate treated with fluoride in the presence of azides to yield benzotriazoles.³⁸ However, this

work would still prove inadequate for bioorthogonal chemistry for two reasons. Although the cycloaddition with azides is generally considered very rapid, the generation of benzyne itself with the Larock method is slow, requiring several hours or days for completion. This process was accelerated with the use of crown ethers, but still required up to an hour.³⁹ Also, acetonitrile was the optimal solvent for benzyne generation, and attempts with an aqueous solvent inhibited the reaction completely. The blame for this inhibition is largely the fault of fluoride's inability to act as an effective nucleophile in water towards the silyl group due to its strong hydrogen-bonding character. In order to utilize benzyne as a bioorthogonal click partner, there

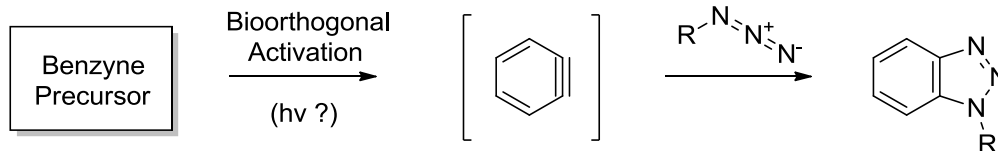


Figure 1.11: Proposed idea to generate benzyne in a bioorthogonal manner and trap with azides in an aqueous environment.

was need for a bioorthogonal generation method. In order to achieve this, we envisioned a photochemical method based on previous reports which suggested photochemically generated benzyne may be generated at wavelengths appropriate for biological applications (**Figure 1.11**).⁴⁰

E. Photochemical-based Click Reactions

Photochemical induced reactions offer several great opportunities for click chemistry and bioorthogonal chemistry. For one, photochemistry has a large following in chemical biology which is primarily populated with examples of photo-induced deprotections or cleavages.⁴¹ Due to the nature of photo-initiation, this type of chemistry offers something that traditional click chemistry cannot; spatial and temporal control over the subject of interest. It is possible to probe dynamic systems using narrowed optics after some perturbation. Secondly,

photochemistry has the potential to generate highly reactive intermediates which can be rapidly combined with specific partners to afford kinetics faster than that of typical cyclooctyne-azide cycloadditions. While photo-uncaging and photo-deprotection reactions in chemical biology are undoubtedly useful, photo-initiated addition or combination reactions with controlled specificity remain largely underdeveloped.

In recent years, a few reactions have been investigated for use as a photochemical click reaction. Among these are a photo-induced Diels-Alder reaction⁴² (**Figure 1.12 A**) and a photo-induced azirine-alkene cycloaddition (**Figure 1.12 B**).⁴³ However, both of these reactions suffer

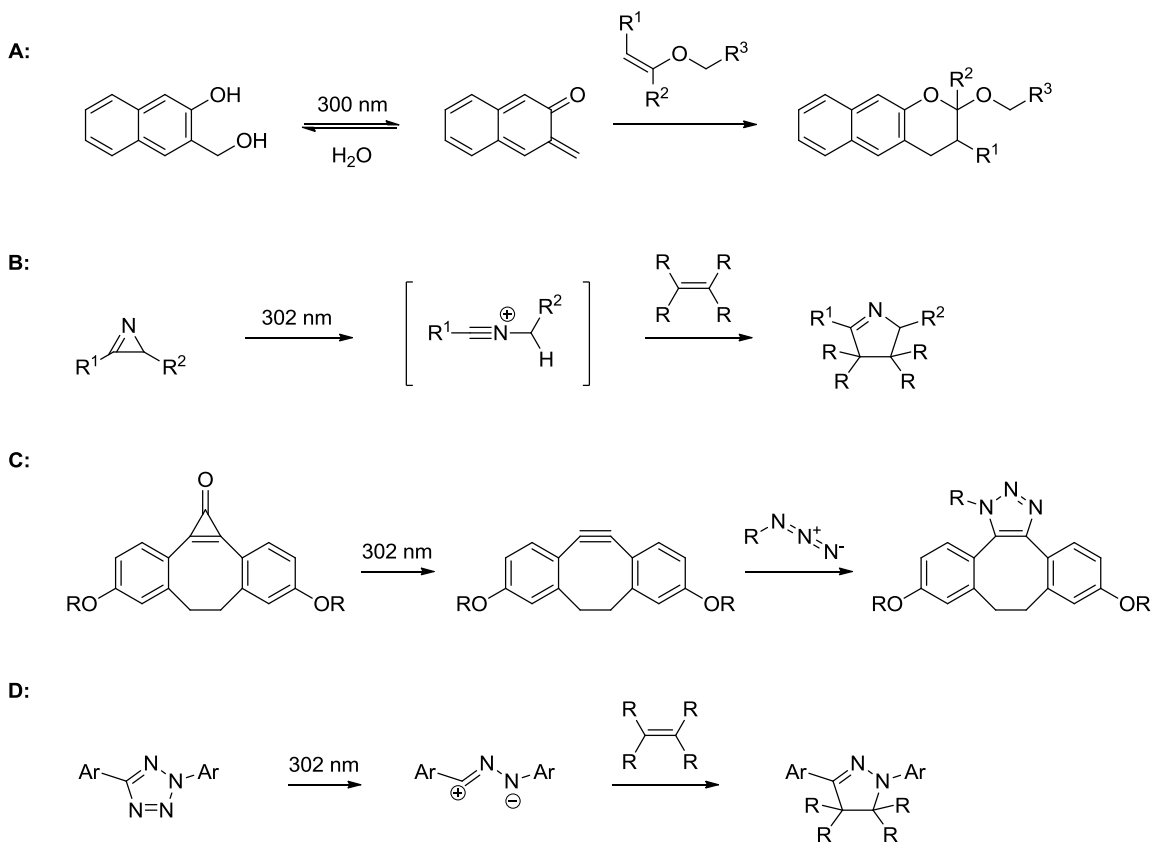


Figure 1.12: Recently photo-induced click techniques. A) Photo-induced Diels-Alder. B) Photo-induced azirine-alkene cycloaddition. C) Caged cyclooctyne. D) Photo-induced nitrile imine-alkene cycloaddition.

from requiring several minutes of irradiation at low wavelengths of around 300 nm; a combination that could prove extremely detrimental to studying live cells and tissues. A photocaging of a cyclooctyne was demonstrated to be capable of labeling live cells by Popik in 2009 (**Figure 1.12 C**).⁴⁴ The cyclooctyne approach benefits from targeting the desirable azide functionality and the required wavelength for uncaging was much higher at 350 nm. However, this reaction still suffers from lengthy irradiation times of up to a minute, and more importantly, the subsequent cycloaddition was rather slow ($k^2 = 0.0763 \text{ M}^{-1}\text{s}^{-1}$), requiring up to an hour of incubation with the partner azide. One reaction that has stood out as very adaptable as a photoclick tool has been the cycloaddition between alkenes and photo-generated nitrile imines from tetrazoles (**Figure 1.12 D**).

First introduced as a potentially useful photoreaction in 2007, easily synthesized di-aryl tetrazoles were irradiated at 302 nm in several solvent systems in the presence of excess alkene to efficiently yield pyrazolines, even in an aqueous solvent.⁴⁵ The reaction was soon adapted to label live *Escherichia coli* cells using an engineered allyl-tyrosine protein on the cell surface (**Figure 1.13 A**).⁴⁶ Although the photo-click reaction had been demonstrated, the reaction required four minutes of irradiation at 302 nm and proved to have an incredibly slow rate of cycloaddition ($k^2 = 0.00202 \text{ M}^{-1}\text{s}^{-1}$). Modifications to the tetrazole to red-shift the absorbance to allow for more biologically friendly wavelengths only achieved limited success.⁴⁷ Newer, red-shifted tetrazoles which yielded nitrile imines at 365 nm irradiation required up to 20 minutes of irradiation for successful conversion (**Figure 1.13 B**). Modifications of the tetrazole electronics to increase cycloaddition rates met with much greater success (**Figure 1.13 C**).⁴⁸ Again, *Escherichia coli* cells with engineered allyl-tyrosine containing surface proteins were irradiated in the presence of the new class of tetrazoles to yield labeled bacterial cells, but did not require significant incubation times after irradiation. However, the cycloaddition rate remained

relatively slow ($k^2 = 0.95 \text{ M}^{-1}\text{s}^{-1}$) which required a large excess, (100 μM) of tetrazole to be present for efficient labeling, and still required potentially harmful 302 nm irradiation.

Cycloaddition rates were further improved in 2012 by changing out the allylic reaction partner

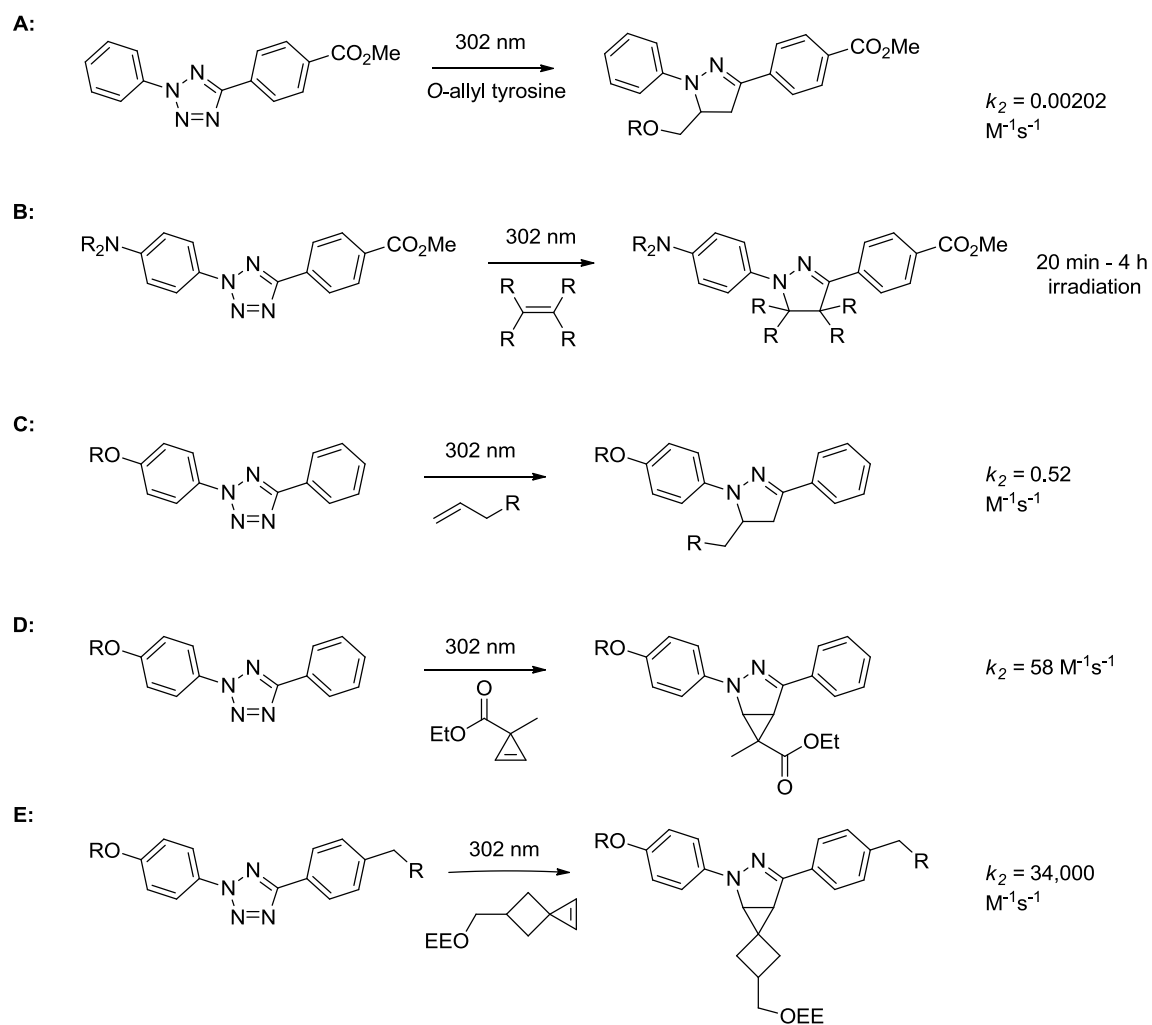


Figure 1.13: Development of the nitrile imine-alkene cycloaddition. A) Initial introduction as photoclick tool on cells. B) Attempt at red-shifting the absorbance. C) Increasing the kinetics by changing tetrazole. D) Improving kinetics by increasing reactivity of alkene. D) Current best method.

with acrylamide or more strained alkenes such as cyclopropenes and norbornenes (**Figure 1.13**

D).⁴⁹ Effective labeling of mammalian cells was achieved at 302 nm irradiation or 365 nm irradiation (tetrazole dependent) with cycloaddition rates of up to $58 \text{ M}^{-1}\text{s}^{-1}$ and $9.2 \text{ M}^{-1}\text{s}^{-1}$,

respectively. Although this was a drastic improvement in kinetics, lengthy irradiation times of up to 2 minutes were required. Kinetics were further improved again by using a super strained spiro cyclopropene ($k^2 = 34,000 \text{ M}^{-1}\text{s}^{-1}$), which is on par with the tetrazine-TCO ligations (**Figure 1.13 E**).⁵⁰ However, the synthesis of necessary probes is quite involved (up to 8 steps for the spiro compound), irradiation still requires damage 302 nm light, and the reaction has yet to be tested in an *in vivo* experiment.

While the nitrile imine-alkene cycloadditions remain the most advanced photo-click technique to date, there remains a need for an efficient photo-click reaction that proceeds efficiently with azides at more biological friendly wavelengths above 350 nm. For this reason, we wished to investigate the possibility to photochemically generate benzyne based on a scaffold published by Maki *et. al.* in 1971.⁴⁰ It was highlighted that an ortho-nitrobenzaldehyde based hydrazones underwent a series of photochemically driven rearrangements to yield

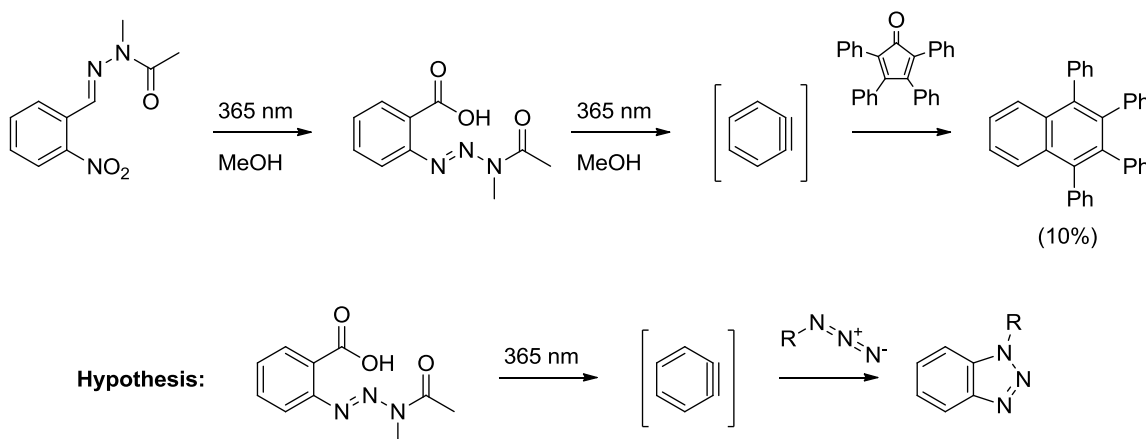


Figure 1.14: *o*-Nitro hydrazone as a benzyne precursor is slow. However, use of the triazenebenzoic acid intermediate may prove much more useful.

benzyne in methanol. Although benzyne was only generated in small quantities (trapped by tetracyclone in 10% yield), we were impressed by the ability of benzyne to perform cycloaddition chemistry in a protic, nucleophilic solvent due to benzyne's electrophilic nature.

The reaction took up to 30 hours, but the investigators reported that the slow step was the initial rearrangement of the hydrazone to a key intermediate; an *ortho*-triazenylbenzoic acid with an acetylated terminal nitrogen. The triazenyl benzoic acid scaffold became the basis of our investigations for developing a photo-chemically induced click reaction with the goal of photo-chemically generating benzyne to trap azide compounds in an aqueous solvent system (**Figure 1.14**).

Biological processes occur on the seconds time scale, and their effects can rapidly diffuse across the cell. In order to fully understand how these processes work and how the chemistry of the cell is affected, we aimed to develop a tool which would allow us and future scientists to monitor important metabolic and disease events. The tool we aim to develop would allow for rapid conjugation of a visualization marker on a biological macromolecule of interest on the order of seconds.

F. References

1. Kolb, H. C., Finn, M. G. & Sharpless, K. B. Click Chemistry: Diverse Chemical Function from a Few Good Reactions. *Angew. Chemie - Int. Ed.* **40**, 2004–2021 (2001).
2. Brown, W. E., Green, A. H., Cedel, T. E. & Cairns, J. Biochemistry of Protein-Isocyanate Interactions: A comparison of the Effects of Aryl vs. Alkyl Isocyanates. *Environ. Health Perspect.* **72**, 5–11 (1987).
3. Griffin, C. W., Carski, T. R. & Warner, G. S. Labeling Procedures Employing Crystalline Fluorescein Isothiocyanate. *J. Bacteriol.* 534–537 (1961).
4. Vytla, D., Combs-Bachmann, R. E., Hussey, A. M., Hafez, I. & Chambers, J. J. Silent, fluorescent labeling of native neuronal receptors. *Org. Biomol. Chem.* **9**, 7151 (2011).

5. Wang, X. *et al.* New method for effectively and quantitatively labeling cysteine residues on chicken eggshell membrane. *Org. Biomol. Chem.* **10**, 8082 (2012).
6. Huisgen, R. 1,3-Dipolar Cycloadditions. *Proc. Chem. Soc.* 357–369 (1961).
7. Rostovtsev, V. V., Green, L. G., Fokin, V. V. & Sharpless, K. B. A stepwise huisgen cycloaddition process: Copper(I)-catalyzed regioselective ‘ligation’ of azides and terminal alkynes. *Angew. Chemie - Int. Ed.* **41**, 2596–2599 (2002).
8. Tornøe, C. W., Christensen, C. & Meldal, M. Peptidotriazoles on solid phase: [1,2,3]-Triazoles by regiospecific copper(I)-catalyzed 1,3-dipolar cycloadditions of terminal alkynes to azides. *J. Org. Chem.* **67**, 3057–3064 (2002).
9. Boren, B. C. *et al.* Ruthenium-catalyzed azide– alkyne cycloaddition: scope and mechanism. *J. Am. Chem. Soc.* **130**, 8923–8930 (2008).
10. McNulty, J., Keskar, K. & Vemula, R. The first well-defined silver(I)-complex-catalyzed cycloaddition of azides onto terminal alkynes at room temperature. *Chem. - A Eur. J.* **17**, 14727–14730 (2011).
11. Laughlin, S. T. & Bertozzi, C. R. Metabolic labeling of glycans with azido sugars and subsequent glycan-profiling and visualization via Staudinger ligation. *Nat. Protoc.* **2**, 2930–2944 (2007).
12. Prescher, J. A. & Bertozzi, C. R. Chemistry in living systems. *Nat. Chem. Biol.* **1**, 13–21 (2005).
13. Amoroso, J. W., Borketey, L. S., Prasad, G. & Schnarr, N. A. Direct Acylation of Carrier Proteins with Functionalized β -Lactones. *Org. Lett.* **12**, 2330–2333 (2010).

14. Prasad, G., Amoroso, J. W., Borketey, L. S. & Schnarr, N. A. N-Activated β -lactams as versatile reagents for acyl carrier protein labeling. *Org. Biomol. Chem.* **10**, 1992–2002 (2012).
15. Li, Z., Seo, T. S. & Ju, J. 1,3-Dipolar cycloaddition of azides with electron-deficient alkynes under mild condition in water. *Tetrahedron Lett.* **45**, 3143–3146 (2004).
16. Wittig, G. & Krebs, A. Zur Existenz niedergliederiger Cycloalkyne. *Chem. Ber.* **94**, 3260–3275 (1961).
17. Agard, N. J., Prescher, J. a & Bertozzi, C. R. A Strain-Promoted [3 + 2] Azide - Alkyne Cycloaddition for Covalent Modification of Biomolecules in Living Systems. *J. Am. Chem. Soc.* **126**, 15046–15047 (2004).
18. Agard, N. J., Baskin, J. M., Prescher, J. A., Lo, A. & Bertozzi, C. R. A Comparative Study of Bioorthogonal Reactions with Azides. *ACS Chem. Biol.* **1**, 644–648 (2006).
19. Baskin, J. M. *et al.* Copper-free click chemistry for dynamic in vivo imaging. *Proc. Natl. Acad. Sci. U. S. A.* **104**, 16793–16797 (2007).
20. Mbuja, N. E., Guo, J., Wolfert, M. a., Steet, R. & Boons, G. J. Strain-Promoted Alkyne-Azide Cycloadditions (SPAAC) Reveal New Features of Glycoconjugate Biosynthesis. *ChemBioChem* **12**, 1912–1921 (2011).
21. Jewett, J. C., Sletten, E. M. & Bertozzi, C. R. Rapid Cu-free click chemistry with readily synthesized biarylazacyclooctynones. *J. Am. Chem. Soc.* **132**, 3688–3690 (2010).
22. Green, J. R. (Cycloheptyne)dicobalt Complexes in Organic Synthesis. *European J. Org. Chem.* **2008**, 6053–6062 (2008).

23. Blackman, M. L., Royzen, M. & Fox, J. M. Tetrazine ligation: fast bioconjugation based on inverse-electron-demand Diels-Alder reactivity. *J. Am. Chem. Soc.* **130**, 13518–9 (2008).
24. Darko, A. *et al.* Conformationally strained trans-cyclooctene with improved stability and excellent reactivity in tetrazine ligation. *Chem. Sci.* **5**, 3770 (2014).
25. Blizzard, R. J. *et al.* Ideal Bioorthogonal Reactions Using A Site-Specifically Encoded Tetrazine Amino Acid. *J. Am. Chem. Soc.* **137**, 10044–10047 (2015).
26. Karver, M., Weissleder, R. & Hilderbrand, S. A. Synthesis and Evaluation of a Series of 1,2,4,5-Tetrazines for Bioorthogonal Conjugation Conjugation Center for Systems Biology. *Bioconjug. Chem.* 2263–2270 (2011). doi:10.1021/bc200295y
27. Wenk, H. H., Winkler, M. & Sander, W. One Century of Aryne Chemistry . *Angew. Chemie Int. Ed.* **42**, 502–528 (2003).
28. Bergstrom, F. W. & Horning, C. H. The Action of Bases on Organic Halogen Compounds. V. The Action of Potassium Amide on Some Aromatic Halides. *J. Org. Chem.* **11**, 334–340 (1946).
29. Gilman, H. & Avakian, S. Dibenzofuran. XXIII. Rearrangement of Halogen Compounds in Amination by Sodamide¹. *J. Am. Chem. Soc.* **67**, 349–351 (1945).
30. Wittig, G. Phenyl-lithium, der Schlüssel zu einer neuen Chemie metallorganischer Verbindungen. *Naturwissenschaften* **30**, 696–703 (1942).
31. Roberts, J. D., Semenow, D. A., Simmons, H. E. & Carlsmith, L. A. The Mechanism of Aminations of Halobenzenes. *J. Am. Chem. Soc.* **78**, 601–611 (1956).
32. Roberts, J. D., Simmons, H. E., Carlsmith, L. A. & Vaughan, C. W. Rearrangement in the

- Reaction of Chlorobenzene-1-C¹⁴ With Potassium Amide. *J. Am. Chem. Soc.* **75**, 3290–3291 (1953).
33. Wittig, G. & Pohmer, L. Intermediäre Bildung von Dehydrobenzol (Cyclohexa-dienin). *Angew. Chemie* **67**, 348 (1955).
34. Wittig, G. & Hoffmann, R. W. Dehydrobenzol aus 1.2.3-Benzothiadiazol-1.1-dioxyd. *Chem. Ber.* **95**, 2718–2728 (1962).
35. Matsumoto, T., Hosoya, T., Katsuki, M. & Suzuki, K. New efficient protocol for aryne generation. Selective synthesis of differentially protected 1,4,5-naphthalenetriols. *Tetrahedron Lett.* **32**, 6735–6736 (1991).
36. Stiles, M., Miller, R. G. & Burckhardt, U. Reactions of Benzyne Intermediates in Non-basic Media. *J. Am. Chem. Soc.* **85**, 1792–1797 (1963).
37. Himeshima, Y., Sonoda, T. & Kobayashi, H. Fluoride-induced 1,2-elimination of o-trimethylsilylphenyl triflate to benzyne under mild conditions. *Chem. Lett.* 1211–1214 (1983). doi:10.1246/cl.1983.1211
38. Shi, F., Waldo, J. P., Chen, Y. & Larock, R. C. Benzyne click chemistry: synthesis of benzotriazoles from benzyne and azides. *Org. Lett.* **10**, 2409–2412 (2008).
39. Campbell-Verduyn, L., Elsinga, P. H., Mirfeizi, L., Dierckx, R. A. & Feringa, B. L. Copper-free 'click': 1,3-dipolar cycloaddition of azides and arynes. *Org. Biomol. Chem.* **6**, 3461 (2008).
40. Maki, Y., Takashi, F. & Suzuki, M. Photochemical Reactions. Part 10. Photolysis of o-Nitrobenzaldehyde N-Acylhydrazones leading to Benzyne and 5-Nitrothalazines. *J. Chem. Soc. Perkins Trans. I* 553–557 (1979).

41. Klán, P. *et al.* Photoremovable protecting groups in chemistry and biology: Reaction mechanisms and efficacy. *Chem. Rev.* **113**, 119–191 (2013).
42. Arumugam, S. & Popik, V. V. Light-Induced Hetero-Diels À Alder Cycloaddition : A Facile and Selective Photoclick Reaction. *J. Am. Chem. Soc.* 5573–5579 (2011).
43. Lim, R. K. V & Lin, Q. Azirine ligation: fast and selective protein conjugation via photoinduced azirine-alkene cycloaddition. *Chem. Commun. (Camb)*. **46**, 7993–7995 (2010).
44. Poloukhine, A. a., Mbua, N. E., Wolfert, M. a., Boons, G. J. & Popik, V. V. Selective labeling of living cells by a photo-triggered click reaction. *J. Am. Chem. Soc.* **131**, 15769–15776 (2009).
45. Wang, Y., Rivera Vera, C. I. & Lin, Q. Convenient synthesis of highly functionalized pyrazolines via mild, photoactivated 1,3-dipolar cycloaddition. *Org. Lett.* **9**, 4155–4158 (2007).
46. Song, W., Wang, Y., Qu, J. & Lin, Q. Selective functionalization of a genetically encoded alkene-containing protein via ‘photoclick chemistry’ in bacterial cells. *J. Am. Chem. Soc.* **130**, 9654–9655 (2008).
47. Wang, Y., Hu, W. J., Song, W., Lim, R. K. V & Lin, Q. Discovery of long-wavelength photoactivatable diaryltetrazoles for bioorthogonal 1,3-dipolar cycloaddition reactions. *Org. Lett.* **10**, 3725–3728 (2008).
48. Wang, Y., Song, W., Hu, W. J. & Lin, Q. Fast alkene functionalization in vivo by photoclick chemistry: HOMO lifting of nitrile imine dipoles. *Angew. Chemie - Int. Ed.* **48**, 5330–5333 (2009).

49. Yu, Z., Pan, Y., Wang, Z., Wang, J. & Lin, Q. Genetically encoded cyclopropene directs rapid, photoclick-chemistry-mediated protein labeling in mammalian cells. *Angew. Chemie - Int. Ed.* **51**, 10600–4 (2012).
50. Yu, Z. & Lin, Q. Design of spiro[2.3]hex-1-ene, a genetically encodable double-strained alkene for superfast photoclick chemistry. *J. Am. Chem. Soc.* **136**, 4153–4156 (2014).

CHAPTER II

DEVELOPMENT OF A PHOTO-INDUCED, BENZYNE CLICK REACTION

A. Introduction

We were initially inspired by impressive work from Larock and co-workers where benzyne served as the reactive alkyne species for click chemistry via treatment of appropriately functionalized benzene with a fluoride ion (**Figure 2.1**).¹ Despite generally good yields and a broad substrate scope, several hours to days were required for completion, presumably due to

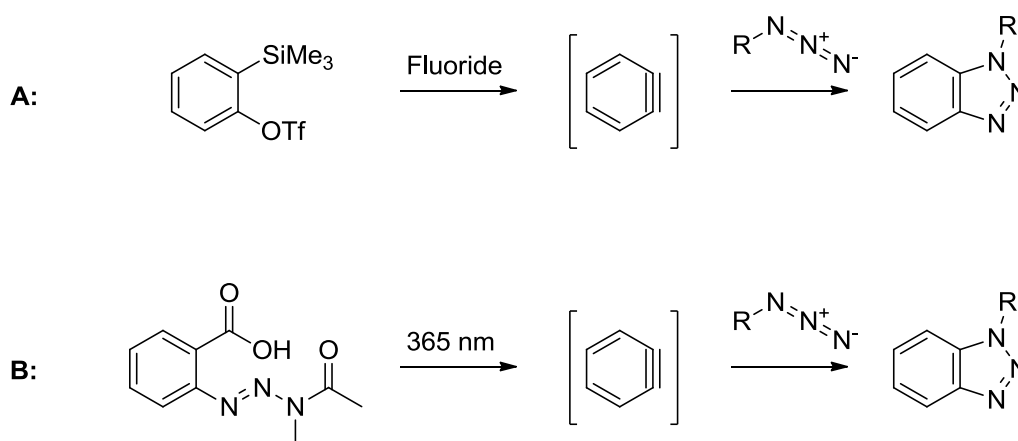


Figure 2.1: Comparison of fluoride-induced benzyne click **A** with a photochemical approach **B**. Fast benzyne formation via photolysis of appropriately substituted benzenes will vastly improve click reaction kinetics.

sluggish benzyne formation. Addition of crown ethers led to faster reaction times, but most of these reactions still required at least one hour for completion.² To improve kinetics, we envisioned fast photochemical generation of benzyne in the presence of an azide click partner to achieve the desired coupling. The use of light as an initiator also offers the potential for spatiotemporal control of the reaction, a highly desired feature for examining dynamic systems. Our goals for development of this reaction were (1) reaction times on the minute scale, (2) reliable and synthetically straightforward preparation of the benzyne photoprecursor, and (3) yields consistent with those observed for the previously reported chemical methods.

Based on a scaffold presented by Maki *et. al.* in the late 1970's, we decided to use *ortho*-triazenylbenzoic acids as photo-activated precursors to generate benzyne *in situ*.³ The triazene functional group typically undergoes one of three chemical transformations: protolysis, photolysis, or thermolysis (**Figure 2.2**).⁴ Protolysis involves protonation of the terminal nitrogen, followed by expulsion of the terminal nitrogen as an amine, leaving behind a diazonium salt. The photolysis of the triazene functional group is usually associated with release of the terminal nitrogen species, nitrogen gas, and an aryl radical which is rapidly quenched. Thermolysis is also

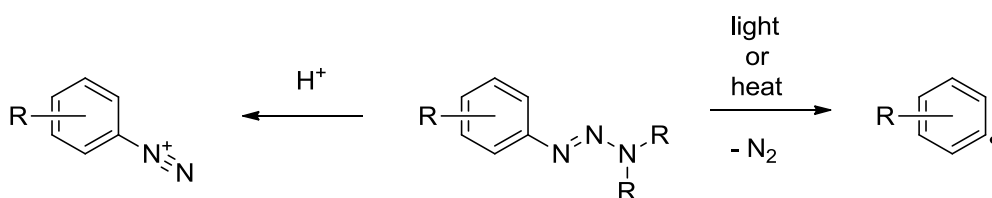


Figure 2.2: Decomposition pathways of aryl triazenes. Photolysis or thermolysis causes loss of nitrogen and generates an aryl radical. Protolysis generates a diazonium ion.

shown decomposition of the triazene in a radical pathway. Interestingly, if *ortho*-triazenylbenzoic acids were to undergo photolysis, it would be expected that they follow a radical pathway leaving an aryl radical. If this were the case, then the carboxylate would also have to undergo radical decomposition at a similar rate under the same photolysis conditions to yield another aryl radical in order to form benzyne. If we consider that *ortho*-diazoniumbenzoic acids (highly unstable, explosive, non-isolable) have shown to be photolytic precursors to benzyne⁵, then *ortho*-triazenylbenzoic acids may undergo a photo-induced self-protolysis to yield *ortho*-diazoniumbenzoic acid which undergoes further photolysis to benzyne.

Going forward, we decided to investigate the ability to photolytically generate benzotriazoles from an *ortho*-triazenylbenzoic acid in the presence of an azide coupling partner. Initially, investigations were carried out in an organic solvent in order to establish optimal

parameters, and secondly in an aqueous environment to explore the potential bioorthogonality of this reaction.

B. Results and Discussion

The synthesis of *ortho*-triazenylbenzoic acids bearing two alkyl groups on the terminal nitrogen is known, and can be carried out relatively easily in essentially one step from the diazotization of anthranilic acid, followed by treatment with a secondary amine under neutral or

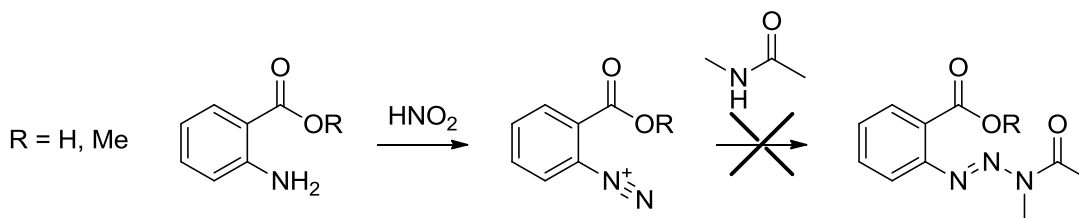


Figure 2.3: The desired triazenylbenzoic acid could not be obtained by using *N*-methylacetamide as a nucleophile towards the terminal diazonium nitrogen.

basic conditions.⁶ However, the *ortho*-triazenylbenzoic acid reported by Maki *et. al.* contained a terminal nitrogen which was acetylated. All attempts at direct synthesis of an *N*-Acetyl *ortho*-triazenylbenzoic acid compound using the anthranilic acid diazotization followed by treatment with an acetamide method failed (**Figure 2.3**), probably due to the inherent low nucleophilicity of amide nitrogens. Instead, it was determined that an indirect route using methylamine as the diazonium-aminating reagent, followed by acetylation would be preferred. However, this

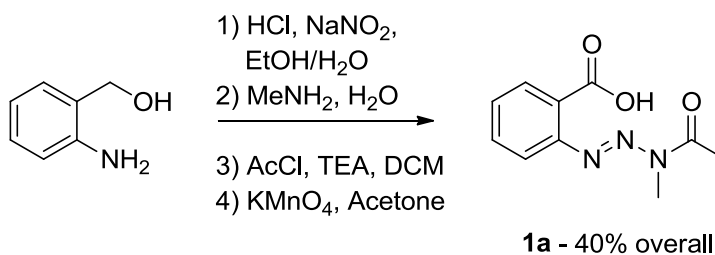


Figure 2.4: The target compound **1a** is available in four straightforward synthetic steps from commercially available *o*-aminobenzyl alcohol in 40% overall yield.

method fell short when we realized that the oxidation state of the carboxylate carbon would interfere with the stability of the mono-alkylated triazene product. Carboxylic acids would lead

to decomposition of the mono-methyl triazene and protection of the carboxylate as an ester would lead to an intramolecular ring-closure where the mono-methyl triazene's terminal nitrogen would attack the ester to yield a triazenone.⁷ Finally, the *N*-Acetyl *ortho*-triazenylbenzoic acid was prepared from *ortho*-aminobenzyl alcohol (**Figure 2.4**). Following diazotization, diazo-amination was achieved with methylamine. The mono-methyltriazene was then acetylated, and the benzyl alcohol was neatly oxidized to the acid using potassium permanganate.

Due to the ease of synthesis of the *N*-dialkyl *ortho*-triazenylbenzoic acids (**Figure 2.5**), they became tempting targets of investigation over of the originally reported acetylated derivatives. Upon further literature searching, we also discovered that the *N*-dialkyl derivatives

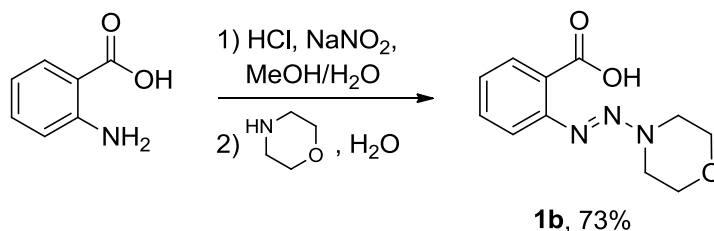


Figure 2.5: Synthesis of morpholinyl triazene. The target compound **1b** is available in essentially just one step from commercially anthranilic acid in 73% overall yield.

had been used as thermally-activated aryne precursors with the possibility of photochemical activation, as well.⁸ We became interested in the effective rate of photolysis for each version, *N*-dialkyl vs. *N*-acetyl. If the proposed diazonium intermediate is correct, we would expect the functionality of terminal-nitrogenous leaving group to have an effect on the rate of N-N bond cleavage of the triazene. Since the acetyl moiety is more electron withdrawing than alkyl, we would expect the triazene to cleave faster in the case of the *N*-acetyl triazene. A relatively large amount of each compound (15 mM, 5 mL) was irradiated in acetonitrile with no additional coupling partner and disappearance of the compound was monitored by TLC versus time (**Figure 2.6**). After 15 minutes, we observed almost complete consumption of the *N*-acetyl

triazenylbenzoic acid, while even after 60 minutes, a significant portion of the *N*-dialkyl

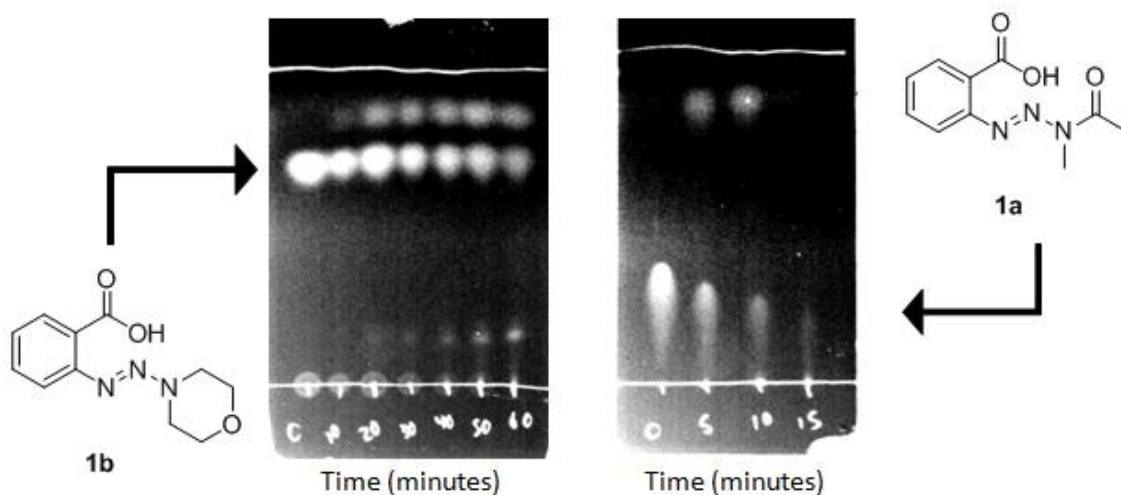


Figure 2.6: Comparison of rates of photolysis for **1a** and **1b** in acetonitrile. 5 mL of a 50 mM solution of each compound was subjected to irradiation and presence of the respective triazenylbenzoic acid was assayed via TLC.

triazenylbenzoic acid remained. It was decided that the faster kinetics of photolysis of the *N*-acetyl derivative outweighed the ease of synthesis of the *N*-dialkyl derivative.

With the target compound decided upon, we began to explore optimal parameters for the photoclick reaction using benzyl azide as a coupling partner for the *ortho*-triazenylbenzoic acid. To our delight, the reaction nears completion after only 3 min of irradiation and good yields can be achieved using a mere 1 equivalent of azide (**Table 2.1**). Yields can be improved by using higher azide equivalents when necessary. In addition, a variety of solvents are tolerated although acetonitrile appears the most suitable of those examined. Satisfied with the optimized

Entry	Solvent	Irradiation time (min)	Azide Equivalents	Yield
1	THF	3	1	3%
2	THF	3	2	3%
3	THF	3	5	13%
4	THF	3	10	23%

5	CHCl ₃	3	1	47%
6	CHCl ₃	3	2	56%
7	CHCl ₃	3	5	65%
8	CHCl ₃	3	10	61%
9	Dioxane	3	1	25%
10	Dioxane	3	2	28%
11	Dioxane	3	5	39%
12	Dioxane	3	10	46%
13	MeCN	3	1	82%
14	MeCN	3	2	90%
15	MeCN	3	5	97%
16	MeCN	3	10	98%
17	MeCN	0.1	1	2%
18	MeCN	1	1	56%
19	MeCN	5	1	83%

Table 2.1: Solvent, irradiation time, and molar ratio optimization for irradiation of **1a** in the presence of benzylazide. Reactions carried out at 15 mM, 50 μ L, analyzed by HPLC-MS. Compared to synthetic standards.

reaction conditions, we set out to explore the reaction scope. Yields were generally good (68–88%) with the notable exception of the phenyl azide series with p-nitrophenyl azide managing only a 3% yield of the expected product (**Figure 2.7**). These lower yields are potentially due to formation of nitrenes upon photolysis of the azides.^{9–11} Overall, the reaction appears to be quite tolerant of common functional groups including alcohols, amides, esters, alkenes, and ethers, and in all cases both LC retention times and mass profiles matched perfectly with authentic standards prepared via the Larock method.

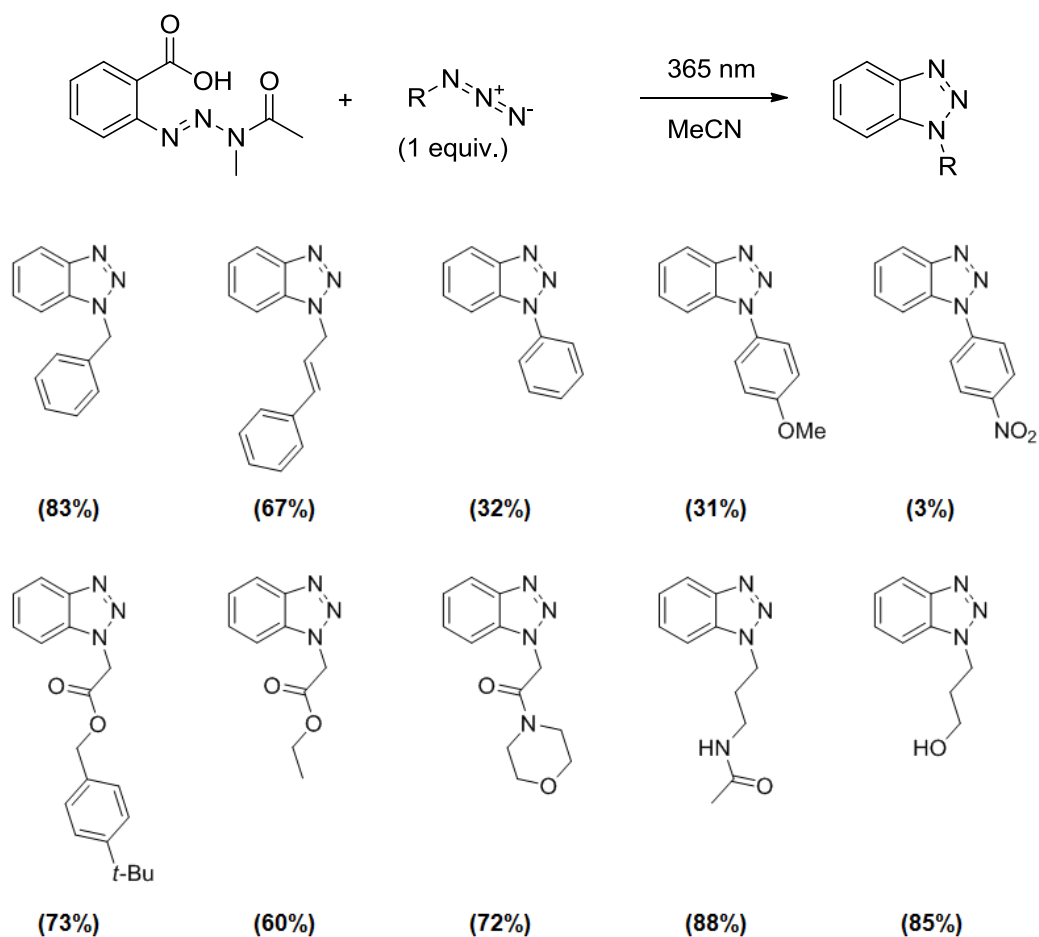


Figure 2.7: Scope of the photoinduced, benzyne click reaction. All reactions were executed on 15 mM (0.75 μ M compound 1) scale at room temperature using an LED light source (3 min irradiation) and 1 equiv of azide. Yields were obtained from fitting spectroscopic data to standard curves for each compound. Each yield is an average of three reactions.

With an eye for potential downstream applications, we were motivated to examine the water tolerance of this chemistry. In our hands, the fluoride induced benzyne click reaction was effectively stalled when even small amounts (~5%) of water were introduced presumably due to fluoride sequestration. Therefore, we were pleasantly surprised to find detectable product formation in acetonitrile solution with up to 70% water content (**Figure 2.8**), the limit of solubility for *ortho*-triazenylbenzoic acid. As above, these results were obtained using only 1 equivalent of azide, which boded well for future development of this chemistry aimed at applications in aqueous environments.

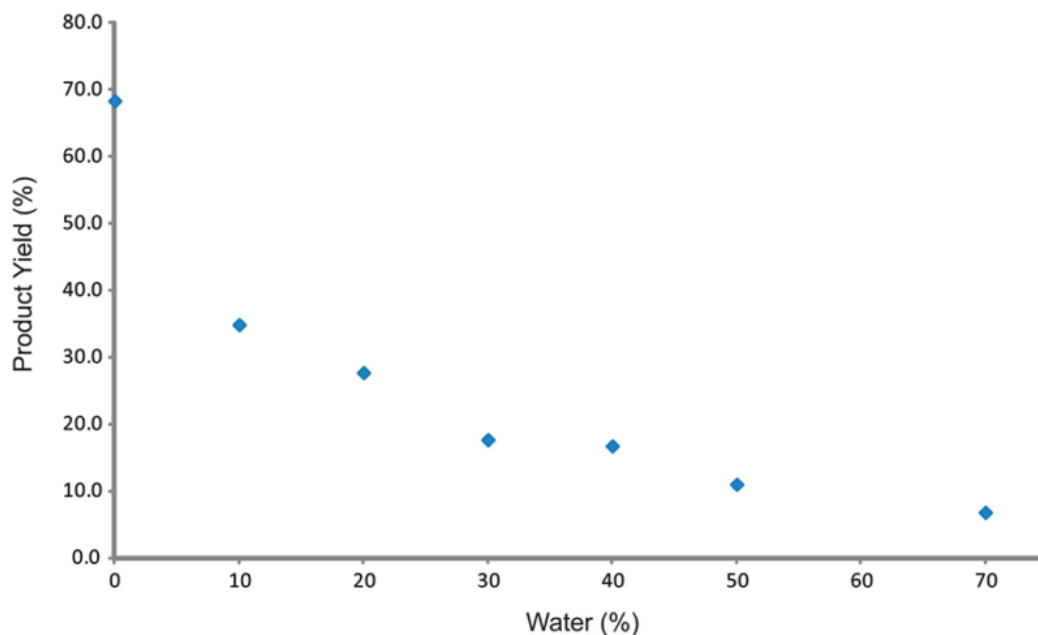
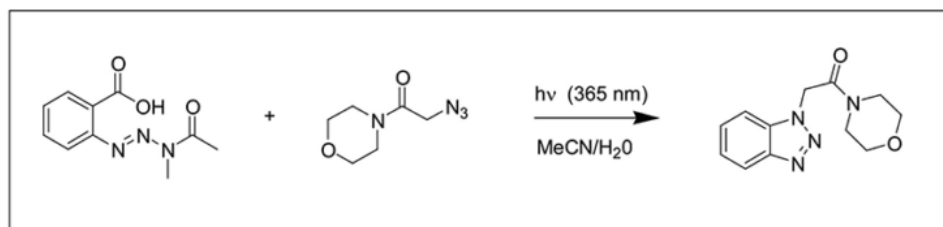


Figure 2.8: Water tolerance of our photoinduced, benzene click reaction. Benzotriazole yields were obtained as above in acetonitrile solution with increasing water percentage. Above 70% water, the starting materials were insoluble. All reactions were executed on 15 mM (0.75 μ M compound 1) scale at room temperature using an LED light source (3 min irradiation) and 1 equiv of azide.

Now equipped with a method to generate benzyne and trap azides which tolerates aqueous environments¹², efforts were turned towards functionalizing the aromatic ring of the *ortho*-triazenylbenzoic acid in order to conjugate to, and subsequently assess utility on a protein. To achieve this, we envisioned a electrophile-containing linker off of the aromatic ring of the TBA which could be attached a thiols or amines on the surface of the protein. Early attempts involved coupling a mono-BOC-protected diamine to 1-methyl-2-aminoterephthalate, followed by diazotization, amination, and hydrolysis to afford to a TBA which contained a linker

with a terminal BOC-protected amine. While the synthesis was straight forward, it was to our dismay that all attempts at BOC-deprotection failed, leaving behind triazene-protolysis products.

We considered a more modular approach could be achieved by installing an azide onto the the TBA, to which some terminal-alkyne functionalized attachment point could be easily installed. In order to avoid changing the electronics of the TBA, a benzyl azide seemed more appropriate introducing an azide through an amide coupling on a terephthalate. Also, we needed to consider that an appropriate intermediate had to contain the azide on an *ortho*-2-aminobenzyl alcohol motif in order to carry forth to the *N*-acetylated TBA. The benzyl azide intermediate, (2-amino-4-(azidomethyl)phenyl)methanol, was obtained in five steps, beginning with commercially available 1-methyl-2-nitroterephthalate. The free acid was selectively reduced with borane, followed by reduction of the nitro with iron powder in 97% and 94% yield, respectively, to afford a benzyl alcohol-modified methyl anthranilate. The benzyl alcohol was converted to the benzyl azide in two steps by treatment with thionyl chloride first, followed up sodium azide after a work-up in 87% yield for each step. Reduction of the ester proved tricky, as organic azides are susceptible to reduction by even mild reducing agents like sodium borohydride. However, use of neat diisobutylaluminum hydride gave the corresponding alcohol, (2-amino-4-(azidomethyl)phenyl)methanol, in 55% yield. With this key intermediate in hand, conversion the TBA was attempted using the diazotization-amination-acetylation-oxidation pathway, however, the oxidation step proved too harsh, and unwanted oxidation of the benzyl azide functionality was observed. To subvert undesirable oxidation, the triazenyl alcohol was first oxidized to the aldehyde with a Swern oxidation, followed by oxidation to the acid using sodium chlorite. From the (2-amino-4-(azidomethyl)phenyl)methanol intermediate, the benzyl azide *N*-acetyl TBA was obtained in a 25% yield over four steps. The azido *N*-acetyl TBA was then coupled with an alkyne-modified maleimide in 65% yield with a CuAAC reaction to afford a

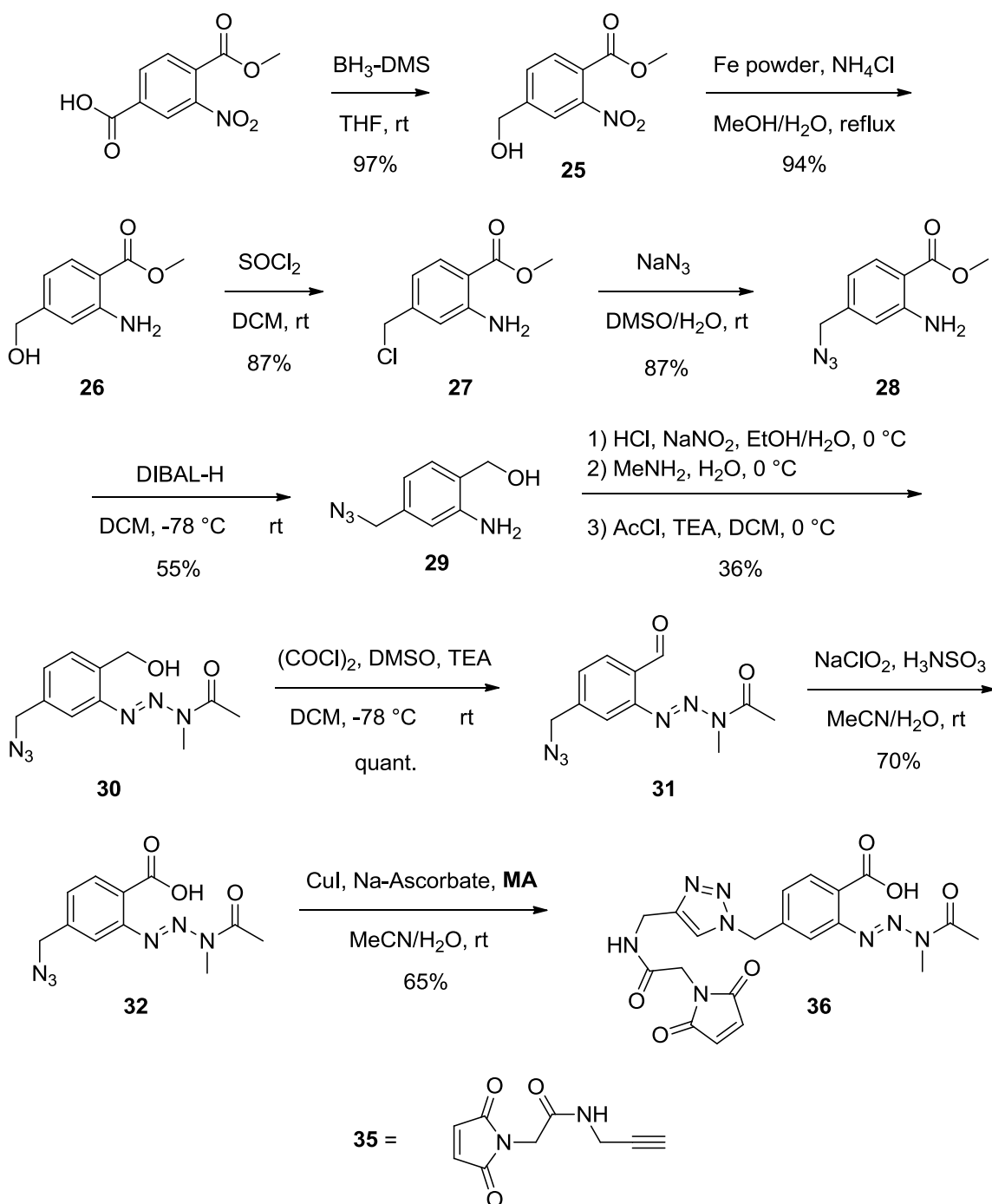


Figure 2.9: Synthesis of a maleimide linker-functionalized triazenylbenzoic acid. The maleimide would ideally label a thiol-containing protein for assessment of the photo-click reaction on a biomacromolecule.

maleimide-functionalized *N*-acetyl TBA. With a linker in place, we began to take a closer look at how the photo-induced click reaction performed in an aqueous environment.

Benzyne is inherently electrophilic; its highest occupied molecular orbital (HOMO) energy is almost the same as benzene itself, however the lowest unoccupied molecular orbital (LUMO) energy is far lower.¹³ Therefore, the most prominent side product we expect to see is that of benzyne being hydrated by the large excess of water surrounding it when generating benzyne in water. When the maleimide TBA was irradiated in a 9:1 water/acetonitrile solvent system (15 mM, 50 μ L), a majority of the TBA was consumed after 3 minutes. The LC-MS trace revealed a scatter of peaks which contained side products with m/z values consistent with the benzoic acid adduct, phenol (hydration product), and a number of other unidentified products (Figure 2.10). However, a major peak was generated which dwarfed all others that had two quite interesting m/z values associated with it, a parent ion peak for the loss of the terminal nitrogen

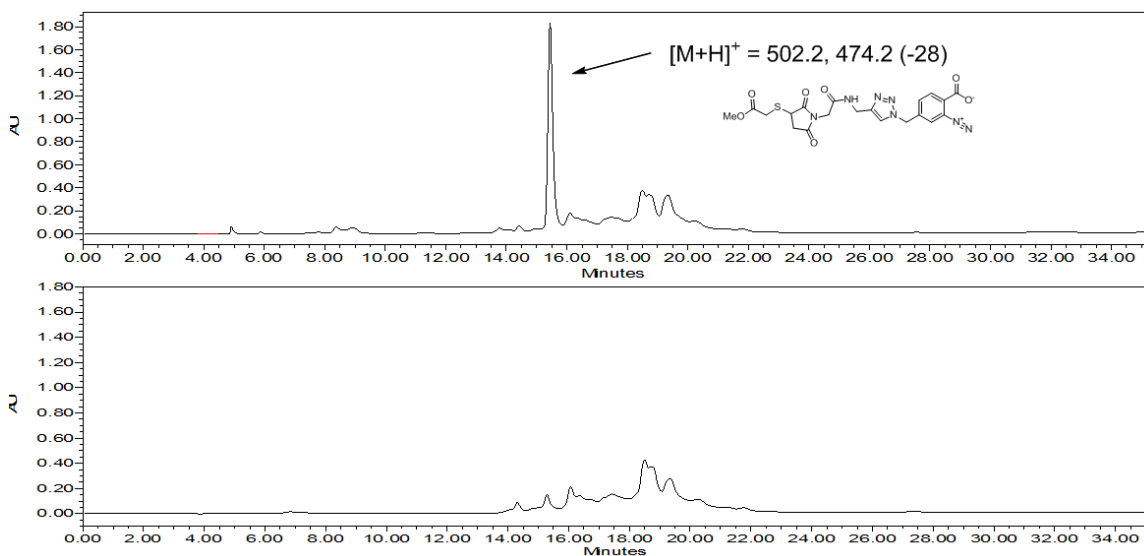


Figure 2.10: Irradiation of a 50 μ L solution of 15 mM maleimide triazenylbenzoic acid **36** (pre-conjugated to methyl thioglycolate). Top: 3 minutes of irradiation show presence of a peak corresponding to the diazonium adduct. Bottom: Further irradiation consumes the diazonium entirely.

species of the triazene (loss of acetamide), and a fragment that was 28 less than loss of acetamide (loss of diatomic nitrogen). The loss of acetamide peak is indicative of, barring the

impossible isolation, the suspected diazonium intermediate of photolysis. This is further supported by the -28 fragment, which would correspond to loss of nitrogen from diazonium. Furthermore, increasing irradiation time showed that the diazonium intermediate peak could be further reduced for a more complete reaction. Because three minutes of exposure to 365 nm light completely consumed TBA and any potential diazonium when the solvent was only acetonitrile, we surmised that water must decrease the rate of photolysis of the *ortho*-diazonium carboxylate.

To establish the degree of photolysis of TBA and diazonium carboxylate, a solvent system of 9:1 water/acetonitrile was chosen arbitrarily. 50 μL of a 2 mM solution of unfunctionalized TBA was irradiated for various time points (**Figure 2.11**). After only ten seconds, almost all of the TBA had been consumed, and a new peak had appeared that corresponded to the diazonium carboxylate. Complete disappearance of the diazonium carboxylate peak did not

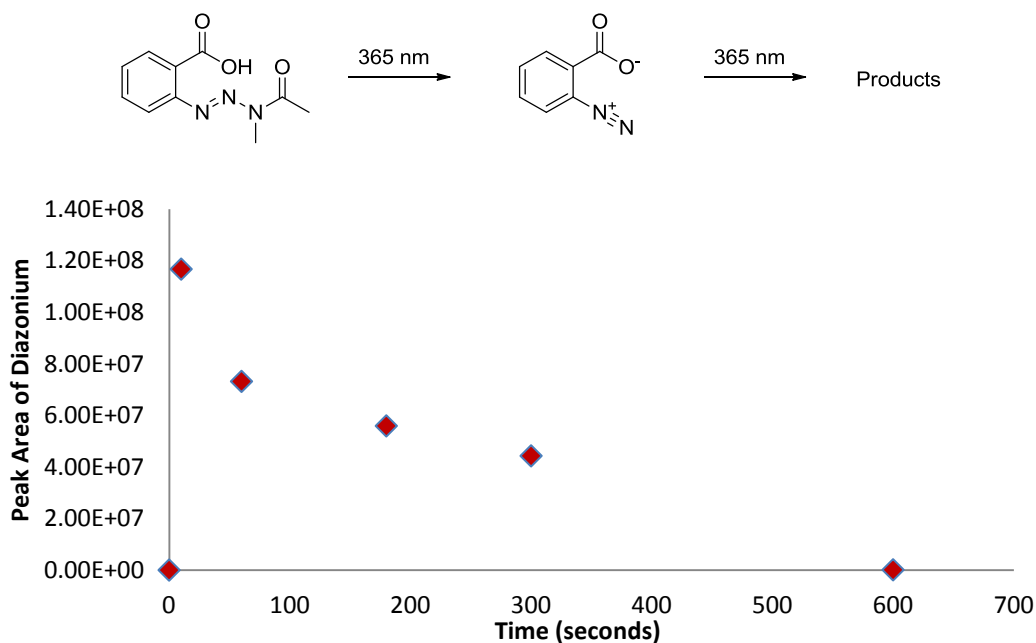


Figure 2.11: Irradiation of **1a** in 9:1 water/acetonitrile (2 mM, 50 μL). Peak area of the diazonium adduct was monitored versus irradiation time. Diazonium is noted form rapidly, but undergoes a very slow photolysis itself in an aqueous environment.

occur until about six minutes of irradiation, indicating that the photolytic conversion of TBA to diazonium was extremely rapid, but further photolysis of diazonium carboxylate to benzyne was extremely slow in an aqueous environment. Given that the observed yields of benzotriazole formation in water were only given three minutes of irradiation with one equivalent of azide, it should seem possible to drastically increase the yield by allowing for complete photolysis of the diazonium carboxylate intermediate and using a much higher molar fraction of coupling partner azide. However, one thing that needs to be taken into consideration is the concentration at which the reaction is carried out. In previous experiments done in the lab, concentrations of protein-labeling probes were 250 μM . The 15 mM concentrations used up to this point are not going to be very relevant, so concentrations of the reaction were lowered to 1 mM. Lower concentrations of benzyne, however, would be expected to result in a lower chance of benzyne molecules finding an azide to react with before hydrating. Therefore, the molar equivalents of azide to TBA was increased to 50 to help counter hydration rates and take advantage of the higher yields observed previously even in an acetonitrile solvent. Despite our best efforts, only a 4% yield of benzotriazole could be obtained at concentrations of 1 mM in 98% water. In order to achieve this, 50 equivalents of azide were required along with an irradiation time of 10 minutes. Such low yields requiring extensive irradiation times caused us to begin rethinking the possibility of using photolysis of TBAs to yield benzyne for biological applications.

C. Experimentals

1. General

Reagents and solvents for organic synthesis were used as received. Thin-layer chromatography (TLC) was conducted on glass-backed silica plates visualized with either UV illumination, basic permanganate stain, or bromocresol green stain. Flash chromatography was conducted on 60 Å silica gel. NMR spectra were recorded on a Bruker Advance 400, chemical shift values are

reported in ppm on the δ scale relative to TMS ($\delta = 0.00$) as an internal standard. Irradiation for photolysis was performed using an LED Engin LZ1-10U600 365 nm LED powered by a DC 12 V, 2 A source through a 700 mA FlexBlock Constant Current Driver. LC Separation was performed with a Waters 1525 system. The gradient employed was A = water + 0.1% formic acid, B = acetonitrile + 0.1% formic acid, 5–95% B over 60 min with a Waters XBridge C18 5u column (4.6 \times 150 mm). Mass spectra were acquired with a Waters Micromass ZQ mass detector in EI+ mode: Capillary voltage = 3.50 kV, cone voltage = 30 V, extractor = 3 V, RF lens = 0.0 V, source T = 100 $^{\circ}$ C, desolvation T = 200 $^{\circ}$ C, desolvation gas = 300 L h $^{-1}$, desolvation gas = 0.0 L h $^{-1}$ The system was operated by and spectra were processed using the Waters Empower software suite.

2. Synthetic Procedures

a. 2-(3-Acetyl-3-methyltriaz-1-en-1-yl)benzoic acid (1a)

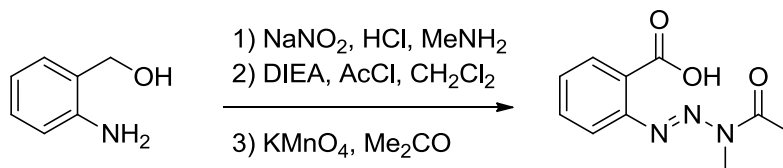


Figure 2.12: Synthesis of **1a**.

To a stirred suspension of 2-Aminobenzyl alcohol (1.85g, 15.0 mmol, 1.00 eq) in H₂O (12 mL) at 0 $^{\circ}$ C, was added conc. HCl (7.5 mL, 90 mmol, 6.00 eq). NaNO₂ (1.08g, 15.6 mmol, 1.03 eq) in H₂O (3 mL) was then added dropwise and the solution was allowed to stir for an additional 10 m. The resulting diazonium solution was then added dropwise to a stirred solution of 33% MeNH₂ in EtOH (36 mL, 288 mmol, 19.2 eq) at -25 $^{\circ}$ C. Immediately after addition, the reaction mixture was extracted with CHCl₃ (2 \times 60 mL). The combined organic layers were washed with NaHCO₃ (4 \times 60 mL), brine, dried over Na₂SO₄, and concentrated under reduced pressure to afford a red-orange oil that was used without further purification.

To a stirred solution of the red-orange oil in CH₂Cl₂ (100 mL) at 0 °C, was added DIEA (10.5 mL, 60.0 mmol, 4.0 eq) followed by careful addition of AcCl (1.07 mL, 15.0 mmol, 1.0 eq). After stirring for 2 h, the reaction mixture was carefully washed with dilute HCl several times until the aqueous layer achieved a pH of 5. The organic layer was washed with brine, dried over Na₂SO₄, and concentrated under reduced pressure to afford a yellow-orange solid that was used without further purification.

To a stirred solution of the yellow-orange solid in acetone (250 mL) was added KMnO₄ (3.34g, 21.1 mmol, 1.41 eq) and the reaction was allowed to stir for an additional 15 h. A saturated solution of Na₂SO₃ was then added until the purple color no longer persisted. The reaction was then diluted with EtOAc (200 mL), and carefully acidified with dilute HCl until the aqueous portion achieved a pH of 5. The organic layer was separated, washed with brine, dried over Na₂SO₄, and concentrated under reduced pressure to afford a brown solid, which was triturated in Et₂O and filtered to give 2-(3-Acetyl-3-methyltriaz-1-en-1-yl)benzoic acid (1.3 g, 5.9 mmol, 39%) as of a pale brown solid. ¹H NMR (400 MHz, CDCl₃) δ: 12.50 (br. s., 1 H), 8.41 (dd, *J* = 1.5, 7.8 Hz, 1 H), 7.85 - 7.78 (m, 1 H), 7.72 - 7.64 (m, 1 H), 7.62 - 7.55 (m, 1 H), 3.56 (s, 3 H), 2.68 (s, 3 H). ¹³C NMR (100 MHz, CDCl₃) δ: 172.41, 165.91, 164.34, 133.87, 133.20, 130.04, 125.12, 116.60, 28.51, 22.00. ESI-MS Calculated for C₁₀H₁₁N₃O₃ [M+H]⁺ = 222.09, found = 222.11

b. (E)-2-(morpholinodiazenyl)benzoic acid (1b)

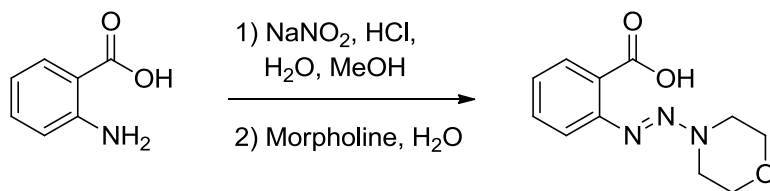


Figure 2.13: Synthesis of **1b**.

A solution of anthranilic acid (563 mg, 4.11 mmol, 1.0 eq) in 4 mL of H₂O and 4 mL of MeOH was acidified with 4 mL of 6M HCl and cooled to 0 °C. A solution of NaNO₂ (340 mg, 4.93

mmol, 1.20 eq) in 2 mL H₂O was added dropwise, and the reaction was allowed to stir another 30 min. The diazotized solution was then added dropwise to a solution of morpholine (3.58 mL, 41.1 mmol, 10.0 eq) in 50 mL H₂O at 0 °C and allowed to stir for 3 h. The reaction mixture was carefully acidified to pH 4-5 with 6M HCl and the precipitate was filtered, washed with water (2 × 50 mL), and allowed to dry in open air overnight to afford (E)-2-(morpholinodiazenyl)benzoic acid (707 mg, 3.01 mmol, 73%) as pale brown solid.

¹H NMR (400MHz, DMSO) δ = 7.77 (dd, *J* = 1.3, 7.7 Hz, 1 H), 7.57 - 7.45 (m, 2 H), 7.33 - 7.25 (m, 1 H), 3.80 (s, 9 H)

¹³C NMR (101MHz, DMSO) δ = 168.4, 148.6, 132.7, 130.4, 126.3, 125.9, 118.3

c. (Azidomethyl)benzene (15)

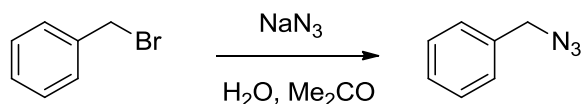


Figure 2.14: Synthesis of **15**.

To a stirred solution of Benzyl bromide (0.12 mL, 1.00 mmol, 1.0 eq) in 50 mL of 1:4 H₂O/Me₂CO (v/v) was added NaN₃ (96 mg, 1.50 mmol, 1.5 eq). After 24 h, the reaction was extracted with Et₂O (3 × 20 mL), washed with brine, dried over K₂CO₃, and concentrated under reduced pressure to give (Azidomethyl)benzene in quantitative yield as a pale yellow oil. ¹H NMR (400 MHz, CDCl₃) δ: 7.40 (m, 5 H), 4.37 (s, 2 H). ¹³C NMR (100 MHz, CDCl₃) δ: 135.54, 128.91, 128.37, 128.29, 54.85.

d. (E)-(3-Azidoprop-1-en-1-yl)benzene (16)

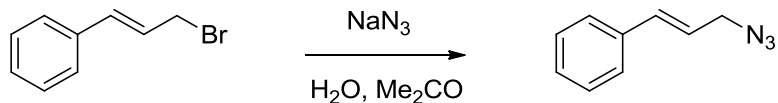


Figure 2.15: Synthesis of **16**.

To a stirred solution of NaN₃ (3.25 g, 50.0 mmol, 5.0 eq) in 100 mL of 4:1 Me₂CO/H₂O was added Cinnamyl bromide (1.97 g, 10.0 mmol, 1.0 eq). After stirring for 18 h, the reaction was diluted with EtOAc (50 mL), washed with brine (3 × 100 mL), dried over Na₂SO₄, and concentrated under reduced pressure to give (E)-(3-Azidoprop-1-en-1-yl)benzene (1.51g, 9.49 mmol, 95%) as a brown oil. ¹H NMR (400 MHz, CDCl₃) δ: 7.45 (m, 2 H), 7.38 (m, 2 H), 7.31 (m, 1 H), 6.69 (d, *J* = 15.7 Hz, 1 H), 6.28 (dt, *J* = 15.7, 6.7 Hz, 1 H). ¹³C NMR (100 MHz, CDCl₃) δ: 136.13, 134.56, 128.78, 128.29, 126.77, 122.53, 53.07.

e. Azidobenzene (17)

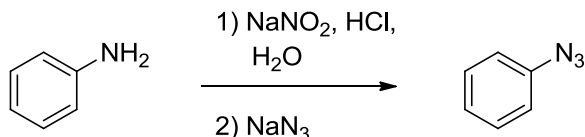


Figure 2.16: Synthesis of **17**.

To a stirred solution of Aniline (293 μL, 3.22 mmol, 1.0 eq) in H₂O (2 mL) and conc. HCl (1 mL) at 0 °C was added NaNO₂ (289 mg, 4.19 mmol, 1.3 eq) in H₂O (1 mL). After stirring for 15 m, a solution of NaN₃ (251 mg, 3.87 mmol, 1.2 eq) in H₂O (1 mL) was carefully added (CAUTION: vigorous release of N₂). The reaction was left to stir for 1 h, followed by extraction with Et₂O (3 × 20 mL). The combined organic layers were dried over K₂CO₃, and carefully concentrated under reduced pressure to give Azidobenzene (189 mg, 1.6 mmol, 50%) as an orange oil. ¹H NMR (400 MHz, CDCl₃) δ: 7.38 (m, 2 H), 7.17 (m, 1 H), 7.06 (m, 2 H). ¹³C NMR (100 MHz, CDCl₃) δ: 140.09, 129.79, 124.90, 119.09.

f. 1-Azido-4-methoxybenzene (18)

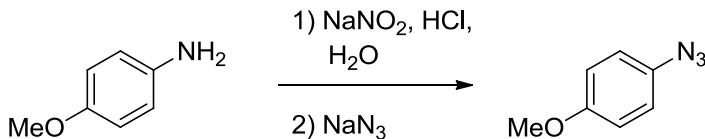


Figure 2.17: Synthesis of **18**.

To a stirred solution of p-Anisidine (396 mg, 3.21 mmol, 1.0 eq) in H₂O (2 mL) and conc. HCl (1 mL) at 0 °C was added NaNO₂ (289 mg, 4.19 mmol, 1.3 eq) in H₂O (1 mL). After stirring for 15 m, a solution of NaN₃ (251 mg, 3.87 mmol, 1.2 eq) in H₂O (1 mL) was carefully added (CAUTION: vigorous release of N₂). The reaction was left to stir for 1 h, followed by extraction with Et₂O (3 × 20 mL). The combined organic layers were dried over K₂CO₃, and carefully concentrated under reduced pressure to give 1-Azido-4-methoxybenzene (320 mg, 2.15 mmol, 67%) as a dark brown solid. ¹H NMR (400 MHz, CDCl₃) δ: 6.98 (m, 2 H), 6.92 (m, 2 H), 3.82 (s, 3 H). ¹³C NMR (100 MHz, CDCl₃) δ: 157.05, 132.38, 120.00, 115.16, 55.55.

g. 1-Azido-4-nitrobenzene (19)

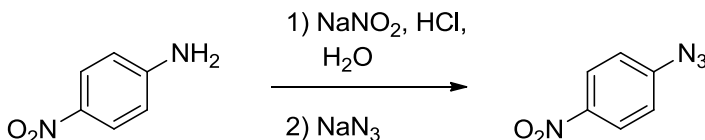


Figure 2.18: Synthesis of **19**.

To a stirred suspension of p-Nitroaniline (444 mg, 3.21 mmol, 1.0 eq) in H₂O (2 mL), MeOH (1 mL) and conc. HCl (1 mL) at 0 °C was added NaNO₂ (289 mg, 4.19 mmol, 1.3 eq) in H₂O (1 mL). After stirring for 15 m, a solution of NaN₃ (251 mg, 3.87 mmol, 1.2 eq) in H₂O (1 mL) was carefully added (CAUTION: vigorous release of N₂). The reaction was left to stir for 1 h, followed by extraction with Et₂O (3 × 50 mL). The combined organic layers were dried over K₂CO₃, and carefully concentrated under reduced pressure to give a solid yellow residue. The residue was purified over silica using flash column chromatography, eluting with 1:1 EtOAc/Hexanes to give

1-Azido-4-nitrobenzene (401 mg, 2.44 mmol, 76%) as a yellow solid. ^1H NMR (400 MHz, CDCl_3) δ : 8.27 (m, 2 H), 7.16 (m, 2 H). ^{13}C NMR (100 MHz, CDCl_3) δ : 146.88, 144.65, 125.58, 119.40.

h. 4-(*tert*-Butyl)benzyl 2-azidoacetate (20)

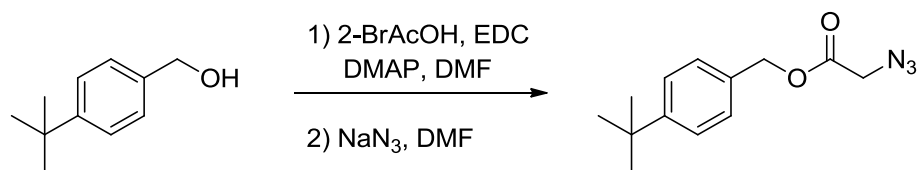


Figure 2.19: Synthesis of **20**.

To a stirred solution of 2-Bromoacetic acid (927 mg, 6.67 mmol, 1.33 eq) in DMF (50 mL) was added *N*-(3-Dimethylaminopropyl)-*N'*-ethylcarbodiimide hydrochloride (1.28 g, 6.67 mmol, 1.33 eq) and *N,N*-Dimethylamino pyridine (61 mg, 0.50 mmol, 0.10 eq). After stirring for 30 min, 4-*tert*-Butylbenzyl alcohol (885 μL , 5.00 mmol, 1.0 eq) was added, and the reaction was allowed to stir an additional 18 h. The reaction mixture was diluted with EtOAc (200 mL) and was washed with 0.1 M HCl (2 \times 50 mL), NaHCO_3 (2 \times 50 mL), and brine (2 \times 50 mL), dried over Na_2SO_4 , and concentrated under reduced pressure to give a orange residue.

The residue was taken up in DMF (10 mL), NaN_3 (1.30 g, 20.0 mmol, 4.0 eq) was added, and the reaction stirred for 18 h at 80 $^\circ\text{C}$. After cooling to room temperature, the reaction was diluted with EtOAc (50 mL) and was washed with H_2O (5 \times 50 mL), dried over Na_2SO_4 , and concentrated under reduced pressure to give a dark orange residue that was purified over silica using flash column chromatography, eluting with 70:30 (Hexanes:EtOAc) to give 4-(*tert*-Butyl)benzyl 2-azidoacetate (1.10 g, 4.45 mmol, 89%) as an orange oil. ^1H NMR (400 MHz, CDCl_3) δ : 7.44 (d, J = 8.3 Hz, 2 H), 7.35 (d, J = 8.6 Hz, 2 H), 5.22 (s, 2 H), 4.12 (s, 2 H), 1.35 (s, 9 H). ^{13}C NMR (100 MHz, CDCl_3) δ : 168.27, 151.83, 132.11, 128.56, 125.68, 67.38, 50.33, 34.68, 31.34.

i. Ethyl 2-azidoacetate (21)

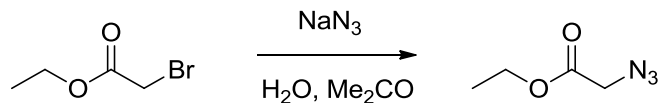


Figure 2.20: Synthesis of 21.

To a stirred solution of NaN_3 (3.25 g, 50.0 mmol, 5.0 eq) in 100 mL of 4:1 $\text{Me}_2\text{CO}/\text{H}_2\text{O}$ was added Ethyl 2-bromoacetate (1.1 mL, 10.0 mmol, 1.0 eq). After stirring for 18 h, the reaction was diluted with EtOAc (50 mL), washed with brine (3×100 mL), dried over Na_2SO_4 , and concentrated under reduced pressure to give Ethyl 2-azidoacetate (828 mg, 6.4 mmol, 64%) as a pale yellow oil. ^1H NMR (400 MHz, CDCl_3) δ : 4.28 (q, $J = 7.2$ Hz, 2 H), 3.88 (s, 2 H), 1.33 (t, $J = 7.2$ Hz, 3 H). ^{13}C NMR (100 MHz, CDCl_3) δ : 168.23, 61.58, 50.04, 13.81.

j. 2-Azido-1-morpholinoethanone (22)

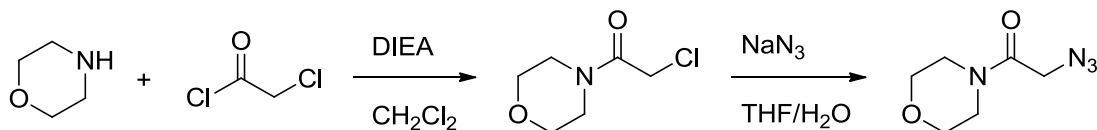


Figure 2.21: Synthesis of 22.

To a stirred solution of morpholine (0.88 mL, 10.0 mmol, 1.0 eq) and *N,N*-Diisopropylethylamine (2.1 mL, 12.5 mmol, 1.25 eq) in CH_2Cl_2 (50 mL) at 0 °C, was added chloroacetyl chloride (0.72 mL, 9.0 mmol, 0.9 eq) dropwise. The reaction was allowed to stir at 0 °C for 45 m, and for another 45 m at 25 °C. The reaction mixture was then diluted with EtOAc (250 mL), washed with 0.5 M HCl (4×25 mL), NaHCO_3 (4×25 mL), and brine. The organic layer was dried over Na_2SO_4 and concentrated under reduced pressure to yield 2-chloro-1-morpholinoethanone (979 mg, 5.99 mmol, 60%) as a brown oil that was used without further purification. To a stirring solution of NaN_3 (562 mg, 8.65 mmol, 1.5 eq) in H_2O (1.1 mL) was added a solution of 2-chloro-1-morpholinoethanone (943 mg, 5.76 mmol, 1.0 eq) in THF (223 μL) and was refluxed for 2 h. After cooling to room temperature, the reaction mixture was extracted

with EtOAc (3 × 25 mL), washed with brine, dried over Na₂SO₄, and concentrated under reduced pressure to give 2-azido-1-morpholinoethanone (559 mg, 3.28 mmol, 57%) as a light brown solid. ¹H NMR (400 MHz, CDCl₃) δ: 3.94 (s, 2 H), 3.74 - 3.68 (m, 4 H), 3.68 - 3.63 (m, 2 H), 3.40 (t, *J* = 4.8 Hz, 2 H). ¹³C NMR (100 MHz, CDCl₃) δ: 165.78, 66.63, 50.39, 45.37, 42.21.

k. N-(3-Azidopropyl)acetamide (23)

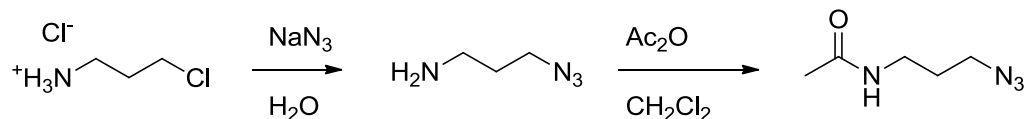


Figure 2.22: Synthesis of **23**.

To a stirred solution of 3-chloropropylamine hydrochloride (2.00 g, 15.4 mmol, 1.0 eq), in H₂O (20 mL) was added sodium azide (3.00 g, 46.1 mmol, 3.0 eq), and the mixture heated to 80 °C. After 18 h, the reaction was cooled and KOH pellets were added to basify the solution, followed by extraction with Et₂O (5 × 20 mL). The combined organic layers were dried over K₂CO₃ and carefully concentrated to give 3-azidopropyl amine (1.12 g, 11.2 mmol, 73%) as a colourless oil that was used without further purification. To a stirred solution of 3-azidopropyl amine (1.52 g, 15.2 mmol, 1.0 eq) in CH₂Cl₂ (15 mL) at 25 °C was added a solution of acetic anhydride (1.43 mL, 15.2 mmol, 1.0 eq) in CH₂Cl₂ (2.5 mL) dropwise over 5 minutes. After an additional 15 h of stirring, the reaction was washed with NaHCO₃ (2 × 40 ml), brine, dried over Na₂SO₄, and concentrated under reduced pressure to afford a yellow oil. Purification over silica using flash column chromatography, eluting with 95:5 (CH₂Cl₂:MeOH) to give *N*-(3-azidopropyl)acetamide (1.17 g, 8.23 mmol, 54%) as a pale yellow oil. ¹H NMR (400 MHz, CDCl₃) δ: 6.08 (br. s, 1 H), 3.34 (m, 4 H), 1.98 (s, 3 H), 1.79 (quin, *J* = 6.6 Hz, 2 H). ¹³C NMR (100 MHz, CDCl₃) δ: 170.80, 48.92, 36.66, 28.55, 22.70.

I. 3-Azidopropan-1-ol (24)

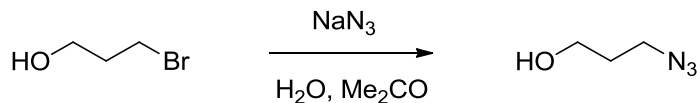


Figure 2.23: Synthesis of **24**.

To a stirred solution of 3-bromopropanol (0.44 mL, 5.00 mmol, 1.0 eq) in acetone (16 mL) was added a solution of NaN₃ (1.63g, 25.00 mmol, 5.0 eq) in H₂O (4 mL), followed by a small amount of KI. After 48 h, the reaction was extracted with Et₂O (3 × 50 mL), the combined organic layers were dried over K₂CO₃, and concentrated under reduced pressure to give 3-azidopropan-1-ol (481 mg, 4.76 mmol, 95%) as a yellow oil. ¹H NMR (400 MHz, CDCl₃) δ: 3.77 (m, 2 H), 3.47 (t, *J* = 6.7 Hz, 2 H), 1.85 (dt, *J* = 12.4, 6.4 Hz, 2 H), 1.73 (m, 1 H). ¹³C NMR (100 MHz, CDCl₃) δ: 59.60, 48.38, 31.40.

m. Synthesis of Benzotriazoles using Photolysis of Compound 1

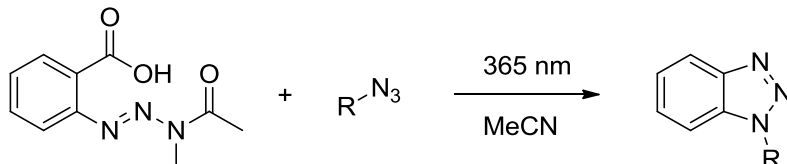


Figure 2.24: Synthesis of benzotriazoles using photolysis.

In a 20 mL scintillation vial was added MeCN (2 mL) followed by solutions of a corresponding azido compound (1.5 mL, 50 mM, 1.0 eq) and triazenylbenzoic acid (**1**) (1.5 mL, 50 mM, 1.0 eq) in MeCN. The vial was placed about 1 cm below the light source and irradiated for 15 m until complete consumption of **1** was observed. Reaction was repeated 10 times, samples were combined, and solvent was removed under reduced pressure. The reaction mixture was dissolved in CH₂Cl₂ (30 mL), washed with NaHCO₃, brine, dried over Na₂SO₄, concentrated under reduced pressure, and purified over silica using flash column chromatography to give the corresponding benzotriazole. Spectral data matched those obtained

from the Larock method. ESI-MS values of benzotriazole authentic standards obtained from Larock method are reported for comparison.

n. 1-Benzyl-1H-benzo[d][1,2,3]triazole (5)

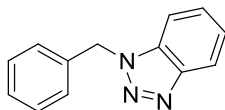


Figure 2.25: Synthesis of 5.

Pale brown solid (107 mg, 0.51 mmol, 68%). ^1H NMR (400 MHz, CDCl_3) δ : 8.08 (td, $J = 8.1, 1.0$ Hz, 1 H), 7.44 - 7.28 (m, 8 H), 5.86 (s, 2 H) ^{13}C NMR (100 MHz, CDCl_3) δ : 146.27, 134.74, 132.84, 129.01, 128.48, 127.59, 127.44, 123.97, 120.05, 109.74, 52.30. ESI-MS Calculated for $\text{C}_{13}\text{H}_{11}\text{N}_3$ $[\text{M}+\text{H}]^+ = 210.10$, found = 210.04, Authentic standard = 210.04.

o. 1-Cinnamyl-1H-benzo[d][1,2,3]triazole (6)

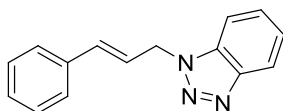


Figure 2.26: Synthesis of 6.

Pale yellow solid (102 mg, 0.43 mmol, 58%). ^1H NMR (400 MHz, CDCl_3) δ : 8.11 (d, $J = 8.3$ Hz, 1 H), 7.59 (d, $J = 8.3$ Hz, 1 H), 7.49 (td, $J = 7.6, 1.0$ Hz, 1 H), 7.44 - 7.26 (m, 6H), 6.71 (d, $J = 15.9$ Hz, 1 H), 6.43 (dt, $J = 15.9, 6.3$ Hz, 1 H), 5.48 (dd, $J = 6.3, 1.5$ Hz, 2 H). ^{13}C NMR (100 MHz, CDCl_3) δ : 146.30, 135.61, 134.43, 132.94, 128.72, 128.40, 127.41, 126.67, 124.00, 122.23, 120.05, 109.83, 50.57. ESI-MS Calculated for $\text{C}_{15}\text{H}_{13}\text{N}_3$ $[\text{M}+\text{H}]^+ = 236.12$, found = 236.08, Authentic standard = 236.08.

p. 1-Phenyl-1H-benzo[d][1,2,3]triazole (7)

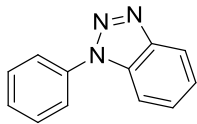


Figure 2.27: Synthesis of **7**.

Pale yellow solid (48 mg, 0.25 mmol, 33%). ^1H NMR (400MHz, CDCl_3) δ : 8.16 (dd, $J = 8.3, 1.0$ Hz, 1 H), 7.82 - 7.73 (m, 3 H), 7.66 - 7.59 (m, 2 H), 7.58 - 7.48 (m, 2 H), 7.47 - 7.42 (m, 1 H). ^{13}C NMR (100 MHz, CDCl_3) $\delta = 146.51, 137.01, 132.32, 129.88, 128.69, 128.26, 124.42, 122.88, 120.30, 110.39$. ESI-MS Calculated for $\text{C}_{12}\text{H}_9\text{N}_3$ $[\text{M}+\text{H}]^+ = 196.09$, found = 195.92, Authentic standard = 195.92.

q. 1-(4-Methoxyphenyl)-1H-benzo[d][1,2,3]triazole (8)

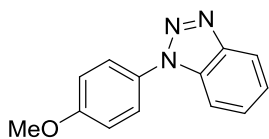


Figure 2.28: Synthesis of **8**.

Yellow Solid (67 mg, 0.30 mmol, 40%). ^1H NMR (400MHz, CDCl_3) δ : 8.13 (d, $J = 8.3$ Hz, 1 H), 7.69 - 7.62 (m, 3 H), 7.52 (td, $J = 7.7, 0.8$ Hz, 1 H), 7.45 - 7.38 (m, 1 H), 7.13 - 7.07 (m, 2 H), 3.89 (s, 3 H). ^{13}C NMR (100 MHz, CDCl_3) δ : 159.86, 146.20, 132.64, 129.95, 128.05, 124.57, 124.28, 120.10, 114.98, 110.28, 55.66. ESI-MS Calculated for $\text{C}_{13}\text{H}_{11}\text{N}_3\text{O}$ $[\text{M}+\text{H}]^+ = 226.10$, found = 226.15, Authentic standard = 226.02.

r. 1-(4-Nitrophenyl)-1H-benzo[d][1,2,3]triazole (9)

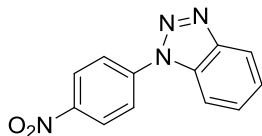


Figure 2.29: Synthesis of **9**.

Obtained via Larock procedure; no product could be isolated from photolysis. Yellow Solid (27 mg, 0.11 mmol, 37%). ^1H NMR (400 MHz, d_6 -DMSO) δ : 8.53 (m, 2 H), 8.27 (m, 3 H), 8.12 (dt, J = 8.4, 0.9 Hz, 1 H), 7.77 (ddd, J = 8.3, 7.1, 1.0 Hz, 1 H), 7.60 (ddd, J = 8.2, 7.1, 0.9 Hz, 1 H). ^{13}C NMR (100 MHz, d_6 -DMSO) δ : 147.03, 146.57, 141.71, 131.89, 129.96, 126.11, 125.83, 123.38, 120.57, 111.78. ESI-MS Calculated for $\text{C}_{12}\text{H}_8\text{N}_4\text{O}_2$ $[\text{M}+\text{H}]^+$ = 241.07, found = 241.05.

s. 4-(tert-Butyl)benzyl 2-(1H-benzo[d][1,2,3]triazol-1-yl)acetate (10)

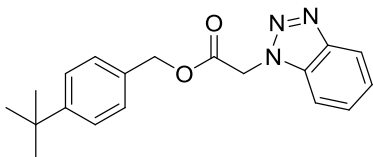


Figure 2.30: Synthesis of **10**.

Pale orange solid (87 mg, 0.27 mmol, 36%). ^1H NMR (400 MHz, CDCl_3) δ : 8.12 (dd, J = 8.3, 0.8 Hz, 1 H), 7.56 - 7.50 (m, 1 H), 7.49 - 7.38 (m, 4 H), 7.26 (d, J = 8.1 Hz, 2 H), 5.48 (s, 2 H), 5.22 (s, 2 H), 1.35 (s, 9 H). ^{13}C NMR (100 MHz, CDCl_3) δ : 166.32, 151.96, 146.07, 133.40, 131.63, 128.46, 127.92, 125.67, 124.14, 120.23, 109.29, 67.82, 49.11, 34.68, 31.30. ESI-MS Calculated for $\text{C}_{19}\text{H}_{21}\text{N}_3\text{O}_2$ $[\text{M}+\text{H}]^+$ = 324.17, found = 324.11, Authentic standard = 324.11.

t. Ethyl 2-(1H-benzo[d][1,2,3]triazol-1-yl)acetate (11)

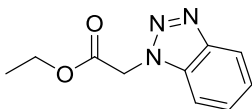


Figure 2.31: Synthesis of **11**.

Pale yellow solid (81 mg, 0.39 mmol, 53%). ^1H NMR (400 MHz, CDCl_3) δ : 8.04 (d, J = 8.3 Hz, 1 H), 7.52 - 7.43 (m, 2 H), 7.40 - 7.32 (m, 1 H), 5.40 (s, 2 H), 4.21 (q, J = 7.1 Hz, 2 H), 1.23 (t, J = 7.2 Hz, 3 H). ^{13}C NMR (100 MHz, CDCl_3) δ : 166.39, 145.96, 133.38, 127.88, 124.10, 120.06, 109.32, 62.28, 49.05, 14.02. ESI-MS Calculated for $\text{C}_{10}\text{H}_{11}\text{N}_3\text{O}_2$ $[\text{M}+\text{H}]^+$ = 206.09, found = 206.00, Authentic standard = 206.00.

u. 2-(1H-Benzo[d][1,2,3]triazol-1-yl)-1-morpholinoethanone (12)

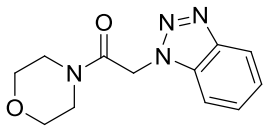


Figure 2.32: Synthesis of **12**.

White solid (108 mg, 0.44 mmol, 58%). ^1H NMR (400 MHz, d_6 -DMSO) δ : 8.02 (d, J = 8.3 Hz, 1 H), 7.74 (d, J = 8.3, 1 H), 7.52 (t, J = 7.5 Hz, 1 H), 7.39 (t, J = 7.5 Hz, 1 H), 5.83 (s, 2 H), 3.77 - 3.68 (m, 2 H), 3.68 - 3.58 (m, 4 H), 3.53 - 3.43 (m, 2 H). ^{13}C NMR (100 MHz, d_6 -DMSO) δ : 164.87, 145.54, 134.42, 127.58, 124.21, 119.44, 111.48, 66.44, 55.37, 49.24, 45.31, 42.38. ESI-MS Calculated for $\text{C}_{12}\text{H}_{14}\text{N}_4\text{O}_2$ $[\text{M}+\text{H}]^+$ = 247.12, found = 247.10, Authentic standard = 247.20.

v. N-(3-(1H-Benzo[d][1,2,3]triazol-1-yl)propyl)acetamide (13)

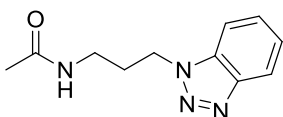


Figure 2.33: Synthesis of **13**.

Pale yellow solid (51 mg, 0.23 mmol, 31%). ^1H NMR (400 MHz, CDCl_3) δ : 8.01 (d, J = 8.3 Hz, 1 H), 7.55 - 7.51 (m, 1 H), 7.50 - 7.44 (m, 1 H), 7.39 - 7.32 (m, 1 H), 6.52 (br. s., 1 H), 4.69 (t, J = 6.8 Hz, 2 H), 3.26 (q, J = 6.3 Hz, 2 H), 2.22 (quin, J = 6.7 Hz, 2 H), 1.92 (s, 3 H). ^{13}C NMR (100 MHz, CDCl_3) δ : 170.74, 145.88, 132.87, 127.57, 124.16, 119.85, 109.39, 45.74, 36.80, 29.09, 23.13. ESI-MS Calculated for $\text{C}_{11}\text{H}_{14}\text{N}_4\text{O}$ $[\text{M}+\text{H}]^+$ = 219.12, found = 219.11, Authentic standard = 219.11.

w. 3-(1H-Benzo[d][1,2,3]triazol-1-yl)propan-1-ol (14)

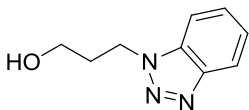


Figure 2.34: Synthesis of **14**.

Pale yellow oil (35 mg, 0.20 mmol, 26%). ^1H NMR (400 MHz, CDCl_3) δ : 8.02 (d, J = 8.3 Hz, 1 H), 7.60 (d, J = 8.3 Hz, 1 H), 7.46 (t, J = 7.7 Hz, 1 H), 7.35 (m, 1 H), 4.80 (t, J = 6.8 Hz, 2 H), 3.67 (t, J =

5.8 Hz, 2 H), 3.51 (br. s, 1 H), 2.25 (quin, $J = 6.3$ Hz, 2 H). ^{13}C NMR (100 MHz, CDCl_3) δ : 145.71, 133.17, 127.38, 124.05, 119.75, 109.55, 58.75, 44.69, 32.21. ESI-MS Calculated for $\text{C}_9\text{H}_{11}\text{N}_3\text{O}$ $[\text{M}+\text{H}]^+ = 178.10$, found = 178.11, Authentic standard = 178.02.

3. Functionalized Benzyne Precursor Synthesis

a. Methyl 4-(hydroxymethyl)-2-nitrobenzoate (25)

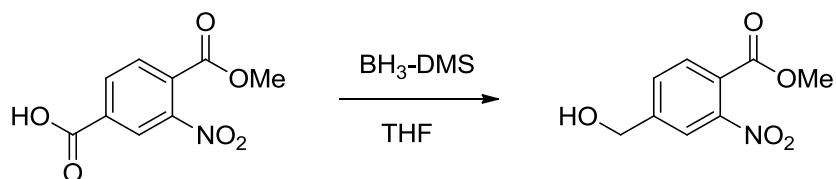


Figure 2.35: Synthesis of **25**.

To a stirred solution of 1-methyl-2-nitroterephthalate (8.39 g, 37.26 mmol, 1.0 eq) in 84 mL of THF under argon was added a solution of $\text{BH}_3\text{-DMS}$ (2M, 20.7 mL, 41.40 mmol, 1.11 eq). After stirring for 24 h, the reaction was quenched with 20 mL of H_2O and diluted with EtOAc (200 mL). The aqueous layer was removed, and the organic layer was washed with brine (2 \times 100 mL), dried over Na_2SO_4 , and concentrated under reduced pressure to give a crude yellow solid. The crude solid was dry-loaded and purified over silica (9:1 DCM/MeOH) to yield methyl 4-(hydroxymethyl)-2-nitrobenzoate (7.62 g, 36.1 mmol, 97%) as a white solid.

^1H NMR (400MHz, CDCl_3) $\delta = 7.85$ (s, 1 H), 7.69 (d, $J = 7.8$ Hz, 1 H), 7.61 (d, $J = 7.8$ Hz, 1 H), 4.80 (s, 2 H), 3.91 (s, 3 H), 2.61 (s, 1 H)

^{13}C NMR (101MHz, CDCl_3) $\delta = 165.9, 148.5, 146.3, 130.3, 130.0, 125.8, 121.5, 63.3, 53.3$

b. Methyl 2-amino-4-(hydroxymethyl)benzoate (26)

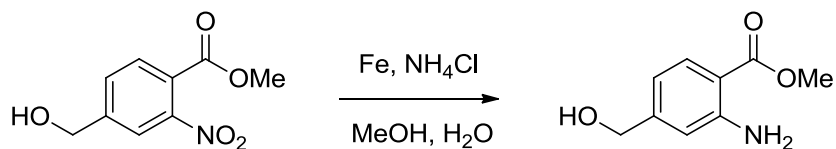


Figure 2.36: Synthesis of **26**.

A mechanically stirred solution of powdered iron (6.98 g, 124.97 mmol, 3.30 eq) and ammonium chloride (9.55 g, 178.53 mmol, 5.00 eq) in a 110 mL solution of 2:1 MeOH/H₂O was refluxed for 15 min. After cooling for 10 min, and a solution of methyl 4-(hydroxymethyl)-2-nitrobenzoate **25** (7.54 g, 35.71 mmol, 1.0 eq) in a 110 mL solution of 2:1 MeOH/H₂O was added, and the reaction was heated to reflux again until the starting material was consumed (monitored by TLC, 2 h). The reaction was allowed to cool, diluted with 100 mL of saturated NaHCO₃ and filtered. The solid was washed with DCM, and the filtrate was extracted with DCM (2 × 100 mL). The organic layer was separated and dried over Na₂SO₄, and concentrated under reduced pressure to give methyl 2-amino-4-(hydroxymethyl)benzoate (6.10 g, 33.67 mmol, 94%) as a white powder.

¹H NMR (400MHz, CDCl₃) δ = 7.76 (d, *J* = 8.3 Hz, 1 H), 6.73 (s, 1 H), 6.56 (d, *J* = 8.3 Hz, 1 H), 6.03 (br. s., 1 H), 4.53 (s, 2 H), 3.83 (s, 3 H)

¹³C NMR (101MHz, CDCl₃) δ = 167.3, 149.9, 147.6, 130.1, 130.0, 113.0, 107.8, 62.6, 50.3

c. Methyl 2-amino-4-(chloromethyl)benzoate (27)

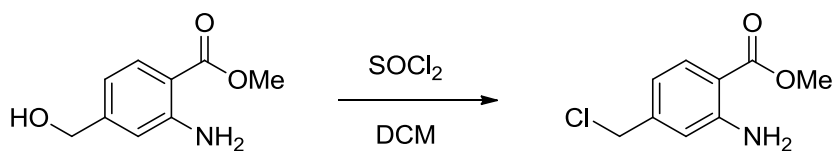


Figure 2.37: Synthesis of **27**.

To a stirred solution of methyl 2-amino-4-(hydroxymethyl)benzoate **26** (2.75 g, 15.18 mmol, 1.0 eq) in 200 mL of DCM was added SOCl₂ (3.30 mL, 45.53 mmol, 3.00 eq). After stirring for 48 h, a white solid was filtered and washed with DCM. The white solid was dissolved in 50 mL saturated NaHCO₃ and extracted with DCM (3 × 100 mL). The combined organic layers were dried over Na₂SO₄, and concentrated under reduced pressure to afford methyl 2-amino-4-

(chloromethyl)benzoate (2.62 g, 13.14 mmol, 87%) as an orange oil which solidified upon cooling to a pale brown solid.

$^1\text{H NMR}$ (400 MHz, CDCl_3) δ : 7.86 (d, 1 H), 6.71 (s, 1 H), 6.67 (d, 1 H), 5.77 (bs, 2 H), 4.49 (s, 2 H), 3.89 (s, 3 H).

d. Methyl 2-amino-4-(azidomethyl)benzoate (28)

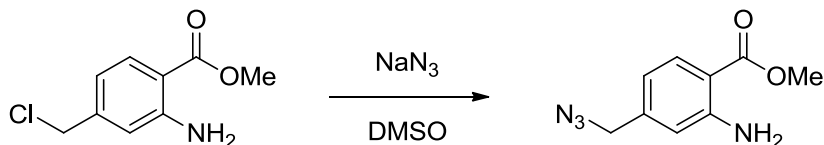


Figure 2.38: Synthesis of **28**.

To a stirred solution of methyl 2-amino-4-(chloromethyl)benzoate **27** (1.18 g, 5.91 mmol, 1.0 eq) in 40 mL of DMSO was added NaN₃ (576 mg, 8.86 mmol, 1.50 eq). After stirring for 24 h, the reaction was diluted with 100 mL of EtOAc and washed with H₂O (6 × 50 mL) and again with 100 mL of brine. The organic layer was separated and dried over Na₂SO₄, and concentrated under reduced pressure to afford methyl 2-amino-4-(azidomethyl)benzoate (1.06 g, 5.14 mmol, 87%) as an orange oil.

$^1\text{H NMR}$ (400 MHz, CDCl_3) δ : 7.87 (d, 1 H), 6.63 (s, 1 H), 6.60 (d, 1 H), 5.81 (bs, 2 H), 4.28 (s, 2 H), 3.89 (s, 3 H).

e. (2-Amino-4-(azidomethyl)phenyl)methanol (29)

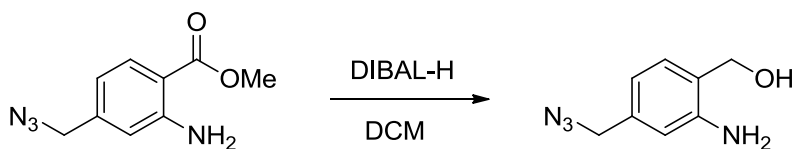


Figure 2.39: Synthesis of **29**.

A solution of methyl 2-amino-4-(azidomethyl)benzoate **28** (1.04 g, 5.03 mmol, 1.0 eq) in 50 mL of DCM under argon was cooled to -78 °C. A solution of DIBAL-H in hexanes (1M, 20.2 mL, 20.12 mmol, 4.00 eq) was added via addition funnel dropwise. After 2 h, the reaction was

allowed to warm to RT and was quenched with 10 mL H₂O, followed by addition of 5.8 g of Rochelle's salt and allowed to stir until the emulsion dispersed. The reaction mixture was extracted with DCM (3 × 50 mL), the combined organic layers were washed with brine (1 × 50 mL), dried over Na₂SO₄, and concentrated under reduced pressure. The crude material was dry loaded and purified over silica (60:40 Hexanes/EtOAc) to afford (2-amino-4-(azidomethyl)phenyl)methanol (493 mg, 2.77 mmol, 55%) as a yellow solid.

¹H NMR (400 MHz, CDCl₃) δ: 7.09 (d, 1 H), 6.67 (m, 2 H), 4.69 (s, 2 H), 4.26 (s, 2 H).

f. (E)-1-(3-(5-(azidomethyl)-2-(hydroxymethyl)phenyl)-1-methyltriazen-2-en-1-yl)ethanone (30)

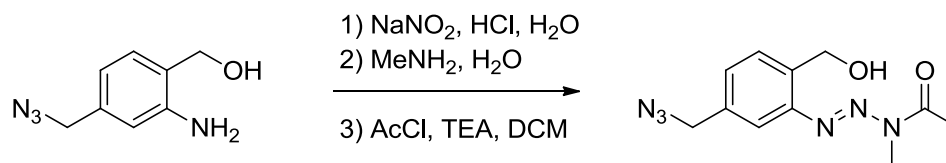


Figure 2.40: Synthesis of 30.

A suspension of (2-amino-4-(azidomethyl)phenyl)methanol **29** (546 mg, 3.06 mmol, 1.0 eq) in 2.5 mL of H₂O was acidified with 1.70 mL of 6M HCl and cooled to 0 °C. A solution of NaNO₂ (233 mg, 3.37 mmol, 1.10 eq) in 1 mL H₂O was added dropwise, and the reaction was allowed to stir another 30 min. The diazotized solution was then added dropwise to a solution of methylamine (40% in H₂O, 2.65 mL, 30.6 mmol, 10.0 eq) at 0 °C and allowed to stir for 10 minutes. The reaction mixture was extracted with DCM (2 × 50 mL). The combined organic layers were dried over Na₂SO₄, and concentrated under reduced pressure to afford a crude, orange residue. The crude material was dissolved in 50 mL of DCM and cooled to 0 °C. To the stirring solution was added triethylamine (513 μL, 3.68 mmol, 1.20 eq) followed by acetyl chloride (240 μL, 3.37 mmol, 1.10 eq) dropwise. The reaction was allowed to stir for 90 min while warming to RT. The reaction mixture was washed with 1M HCl (2 × 25 mL), and the organic layer was dried over Na₂SO₄, and concentrated under reduced pressure to afford a

crude, orange residue. The residue was dry loaded and purified over silica (95:5 DCM/MeOH) to afford (E)-1-(3-(5-(azidomethyl)-2-(hydroxymethyl)phenyl)-1-methyltriaz-2-en-1-yl)ethanone (286 mg, 1.09 mmol, 36%) as an orange, pasty solid.

^1H NMR (400 MHz, CDCl_3) δ : 7.54 (d, 1 H), 7.49 (s, 1 H), 7.35 (dd, 1 H), 4.99 (s, 2 H), 4.41 (s, 2 H), 3.46 (s, 3 H), 2.62 (s, 3 H), 2.50 (bs, 1 H).

g. (E)-2-(3-acetyl-3-methyltriaz-1-en-1-yl)-4-(azidomethyl)benzaldehyde (31)

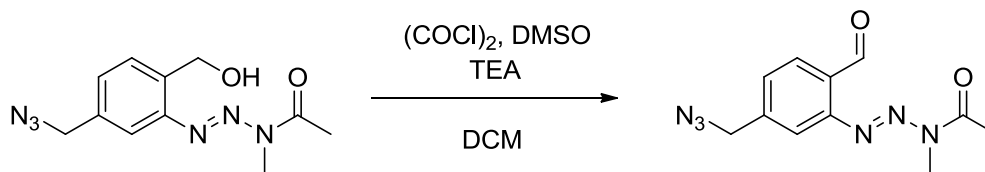


Figure 2.41: Synthesis of **31**.

To a solution of DMSO (767 μL , 10.80 mmol, 10.0 eq) in 5.8 mL of DCM cooled to $-78\text{ }^\circ\text{C}$ was added oxalyl chloride (183 μL , 2.16 mmol, 2.00 eq). After stirring for 30 min, a solution of (E)-1-(3-(5-(azidomethyl)-2-(hydroxymethyl)phenyl)-1-methyltriaz-2-en-1-yl)ethanone **30** (283 mg, 1.08 mmol, 1.0 eq) in 1.8 mL of DCM was added dropwise, and the reaction was allowed to stir another 30 min at $-78\text{ }^\circ\text{C}$. Triethylamine (753 μL , 5.40 mmol, 5.0 eq) was added dropwise at $-78\text{ }^\circ\text{C}$, then the reaction was removed from the cooling bath and allowed to stir until it warmed to RT. After warming, the reaction was quenched with 5 mL H_2O . The layers were separated, and the organic layer was washed with 1M HCl (1 \times 10 mL), dried over Na_2SO_4 , and concentrated under reduced pressure to afford (E)-2-(3-acetyl-3-methyltriaz-1-en-1-yl)-4-(azidomethyl)benzaldehyde (291 mg, 1.12 mmol, quantitative - crude) as a yellow orange solid that was used without further purification.

h. (E)-2-(3-acetyl-3-methyltriaz-1-en-1-yl)-4-(azidomethyl)benzoic acid (32)

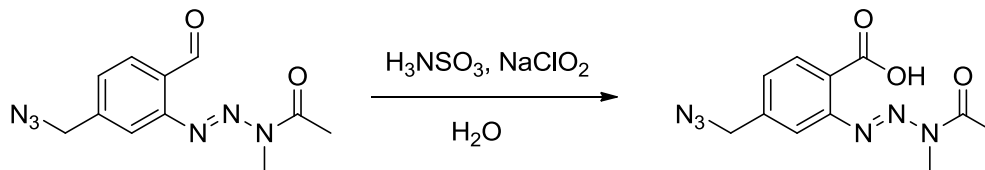


Figure 2.42: Synthesis of **32**.

To a stirred solution of crude (E)-2-(3-acetyl-3-methyltriaz-1-en-1-yl)-4-(azidomethyl)benzaldehyde **31** (291 μL , 1.12 mmol, 1.0 eq) in 16 mL of MeCN was added a solution of sulfamic acid (141 mg, 1.45 mmol, 1.30 eq) in 3 mL H_2O , followed by addition of a solution of sodium chlorite (152 mg, 1.68 mmol, 1.50 eq) in 3 mL H_2O . The reaction was allowed to stir at RT until completion (monitored by TLC, 60 min), after which it was diluted with 50 mL H_2O and extracted with DCM (3 \times 50 mL). The combined organic layers were extracted with saturated NaHCO_3 . The aqueous layer was carefully acidified with 1M HCl to pH = 4-5, and extracted with EtOAc (2 \times 50 mL). The combined organic layers were dried over Na_2SO_4 , and concentrated under reduced pressure to afford (E)-2-(3-acetyl-3-methyltriaz-1-en-1-yl)-4-(azidomethyl)benzoic acid (217 mg, 0.79 mmol, 70%) as a pale brown solid.

^1H NMR (400 MHz, CDCl_3) δ : 8.41 (d, 1 H), 7.74 (s, 1 H), 7.50 (d, 1 H), 4.53 (s, 2 H), 3.56 (s, 3 H), 2.70 (s, 3 H).

i. (E)-4-((carboxymethyl)amino)-4-oxobut-2-enoic acid (33)

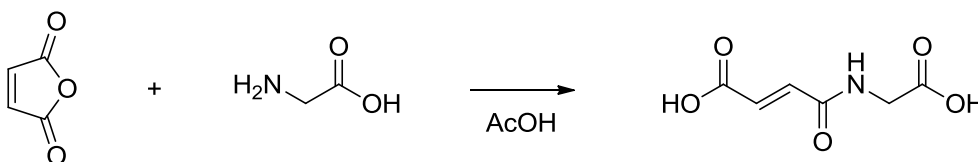


Figure 2.43: Synthesis of **33**.

To a solution of maleic anhydride (9.8 g, 100 mmol, 1.0 eq) in 100 mL of acetic acid was added glycine (7.5 g, 100 mmol, 1.0 eq). After vigorously stirring for 18 h, the suspension was

filtered and washed with water (3 × 100 mL). After being allowed to dry in open air overnight, (E)-4-((carboxymethyl)amino)-4-oxobut-2-enoic acid (14.7 g, 85 mmol, 85%) was obtained as a white solid.

^1H NMR (400MHz, DMSO) δ = 13.54 (br. s., 1 H), 9.20 (t, J = 5.6 Hz, 1 H), 6.43 (d, J = 12.5 Hz, 1 H), 6.30 (d, J = 12.5 Hz, 1 H), 3.91 (d, J = 5.9 Hz, 2 H)

^{13}C NMR (101MHz, DMSO) δ = 170.9, 166.5, 165.8, 133.5, 130.5, 41.4

j. 2-(2,5-dioxo-2,5-dihydro-1H-pyrrol-1-yl)acetic acid (34)

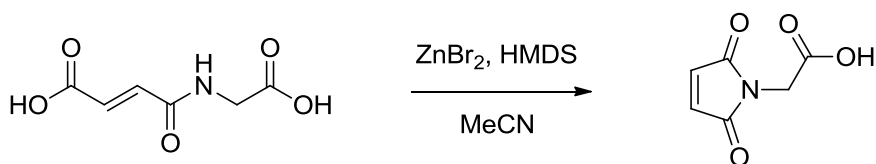


Figure 2.44: Synthesis of **34**.

A stirred solution of (E)-4-((carboxymethyl)amino)-4-oxobut-2-enoic acid **33** (3.98 g, 23 mmol, 1.0 eq), ZnBr₂ (5.18 g, 23 mmol, 1.0 eq), and hexamethyldisilazane (24.25 mL, 115 mmol, 5.0 eq) was refluxed for 60 min. The reaction mixture was concentrated under reduced pressure, acidified with 50 mL of 1M HCl, and extracted with EtOAc (3 × 50 mL). The combined organic layers were washed with brine (1 × 50 mL), dried over Na₂SO₄, and concentrated under reduced pressure to afford a crude solid which was recrystallized in DCM to yield 2-(2,5-dioxo-2,5-dihydro-1H-pyrrol-1-yl)acetic acid (2.30 g, 14.7 mmol, 64%) as off-white crystals.

^1H NMR (400MHz, DMSO) δ = 7.10 (s, 2 H), 4.14 (s, 2 H)

^{13}C NMR (101MHz, DMSO) δ = 170.8, 169.4, 135.3, 38.9

k. 2-(2,5-dioxo-2,5-dihydro-1H-pyrrol-1-yl)-N-(prop-2-yn-1-yl)acetamide (35)

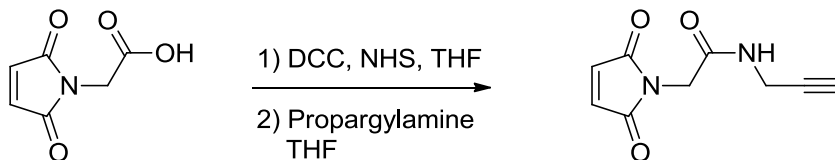


Figure 2.45: Synthesis of **35**.

To a stirred solution of 2-(2,5-dioxo-2,5-dihydro-1H-pyrrol-1-yl)acetic acid **34** (1.30g, 8.38 mmol, 1.0 eq) and *N*-hydroxysuccinamide (1.93 g, 16.76 mmol, 2.0 eq) in 180 mL of THF was added *N,N'*-dicyclohexylcarbodiimide (3.46 g, 16.76 mmol, 2.0 eq). After stirring for 24 h, the reaction was filtered and the solid washed with THF (2 × 50 mL). The filtrate was concentrated under reduced pressure to afford 1.0 g of a yellow solid which was dissolved in 75 mL of THF. To the stirring solution of yellow solid was added propargylamine (250 μ L, 3.9 mmol, 0.47 eq) and the reaction was allowed to stir another 18 h. The reaction was diluted in 100 mL of EtOAc and extracted with H₂O (3 × 50 mL), washed with brine (1 × 50 mL), dried over Na₂SO₄, and concentrated under reduced pressure to afford 2-(2,5-dioxo-2,5-dihydro-1H-pyrrol-1-yl)-*N*-(prop-2-yn-1-yl)acetamide (419 mg, 2.18 mmol, 26%) as a yellow powder.

¹H NMR (400MHz, DMSO) δ = 8.61 (t, *J* = 5.3 Hz, 1 H), 7.10 (s, 2 H), 4.04 (s, 2 H), 3.87 (dd, *J* = 2.6, 5.5 Hz, 2 H), 3.13 (t, *J* = 2.4 Hz, 1 H)

¹³C NMR (101MHz, DMSO) δ = 171.1, 166.5, 135.4, 81.1, 73.8, 28.5

l. (E)-2-(3-acetyl-3-methyltriaz-1-en-1-yl)-4-((2-(2,5-dioxo-2,5-dihydro-1H-pyrrol-1-yl)acetamido)methyl)-1H-1,2,3-triazol-1-yl)methyl)benzoic acid (36)

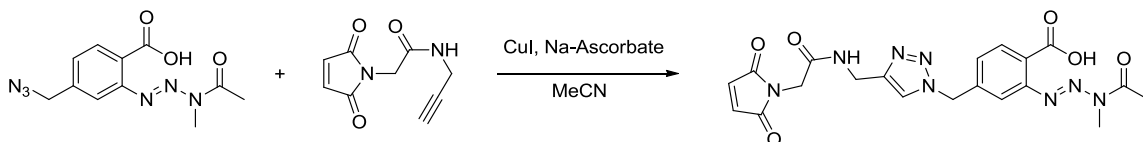


Figure 2.46: Synthesis of **36**.

To a stirred solution of (E)-2-(3-acetyl-3-methyltriaz-1-en-1-yl)-4-(azidomethyl)benzoic acid **32** (112 mg, 0.41 mmol, 1.00 eq) and 2-(2,5-dioxo-2,5-dihydro-1H-pyrrol-1-yl)-N-(prop-2-yn-1-yl)acetamide **35** (88 mg, 0.46 mmol, 1.11 eq) in 3 mL of MeCN and 300 μ L of H₂O was added copper(I) iodide (34 mg, 0.18 mmol, 0.45 eq) and sodium *L*-ascorbate (36 mg, 0.18 mmol, 0.45 eq). After 24 h, an additional 36 mg of **35** and 10 mg of copper(I) iodide was added, and the reaction was allowed to stir another 24 h. The reaction was diluted with 50 mL H₂O and extracted with DCM (3 \times 50 mL). The combined organic layers were then extracted with saturated NaHCO₃. The aqueous layer was carefully acidified with 1M HCl to pH = 4-5, and extracted with EtOAc (3 \times 50 mL). The combined organic layers were dried over Na₂SO₄, and concentrated under reduced pressure to afford (E)-2-(3-acetyl-3-methyltriaz-1-en-1-yl)-4-((4-(2-(2,5-dioxo-2,5-dihydro-1H-pyrrol-1-yl)acetamido)methyl)-1H-1,2,3-triazol-1-yl)methyl)benzoic acid (126 mg, 0.27 mmol, 66%) as a pale brown solid.

¹H NMR (400 MHz, DMSO-*d*₆) δ : 13.10 (bs, 1 H), 8.66 (t, 1 H), 8.04 (s, 1 H), 7.72 (d, 1 H), 7.41 (s, 1 H), 7.35 (dd, 1 H), 7.09 (s, 2 H), 5.71 (s, 2 H), 4.31 (d, 2 H), 4.03 (s, 2 H), 3.30 (s, 3 H), 2.44 (s, 3 H).

4. Spectroscopic Yield Determinations

a. General procedure for Benzotriazole Authentic Standard preparation using Larock Method

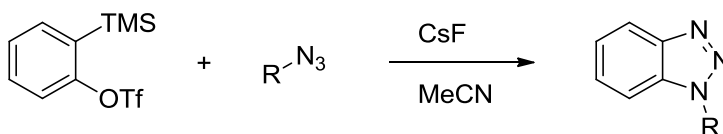
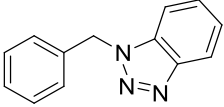


Figure 2.47: Synthesis of benzotriazoles via the Larock method.

To a stirred solution of 2-(trimethylsilyl)phenyl trifluoromethanesulfonate (85 μ L, 0.35 mmol, 1.2 eq) and the corresponding azido compound (0.30 mmol, 1.0 eq) in MeCN (10 mL) was added CsF (91 mg, 0.60 mmol, 2.0 eq). After stirring for 18 h, the reaction mixture was washed with NaHCO₃, brine, dried over Na₂SO₄, and purified over silica using flash column chromatography to give the corresponding Benzotriazole compound. Standard curves were

generated using pure benzotriazole prepared via the Larock procedure. Serial dilutions were done to prepare 500, 250, and 125 μM (MeCN) samples for a 3-point curve where peak area via HPLC was plotted against concentration.

Concentration of (5) (μM)	HPLC Peak Area
	
125	7811334
250	16224101
500	30114326

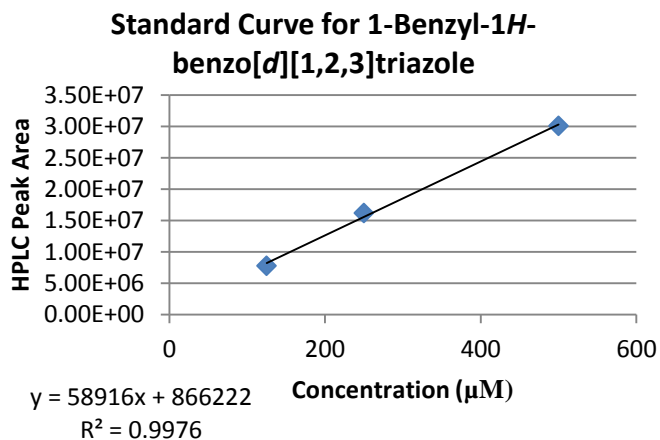


Figure 2.48: Example standard curve prep using 5.

b. Percent Conversion to Benzotriazole

In a 2 mL microcentrifuge tube was added MeCN (27.5 μL) followed by solutions of a corresponding azido compound (7.5 μL , 100 mM, 1.0 eq) and triazenylbenzoic acid (**1**) (15 μL , 50 mM, 1.0 eq) in MeCN. The tube was placed about 2 cm below the light source and irradiated for 3 m. 6.66 μL of the irradiated solution was diluted to 200 μL with MeCN and benzotriazole formation was monitored using HPLC-MS. 100% conversion would correlate to a 500 μM solution of benzotriazole.

	HPLC Peak Area	Percent Conversion
Run 1	24513945	83 %
Run 2	25272854	86 %
Run 3	23510758	80 %
Average		83 %
Standard Dev.		3 %

Table 2.2: Percent conversion to 5.

	HPLC Peak Area	Percent Conversion
Run 1	63090893	66 %
Run 2	63482716	67 %
Run 3	66055382	67 %
Average		67 %
Standard Dev.		1 %

Table 2.3: Percent conversion to **6**.

	HPLC Peak Area	Percent Conversion
Run 1	11650744	34 %
Run 2	11047481	32 %
Run 3	10971848	31 %
Average		32 %
Standard Dev.		2 %

Table 2.4: Percent conversion to **7**.

	HPLC Peak Area	Percent Conversion
Run 1	11983895	32 %
Run 2	11422097	30 %
Run 3	11840775	31 %
Average		31 %
Standard Dev.		1%

Table 2.5: Percent conversion to **8**.

	HPLC Peak Area	Percent Conversion
Run 1	1084017	3 %
Run 2	1097162	3 %
Run 3	965984	3 %
Average		3 %
Standard Dev.		0 %

Table 2.6: Percent conversion to **9**.

	HPLC Peak Area	Percent Conversion
Run 1	19635059	75 %
Run 2	18793702	72 %
Run 3	18942658	72 %
Average		73 %
Standard Dev.		2 %

Table 2.7: Percent conversion to **10**.

	HPLC Peak Area	Percent Conversion
Run 1	17649803	61 %
Run 2	16478454	57 %
Run 3	17646220	61 %
Average		60 %
Standard Dev.		2 %

Table 2.8: Percent conversion to **11**.

	HPLC Peak Area	Percent Conversion
Run 1	19211436	68 %
Run 2	20086228	71 %
Run 3	21737750	77 %
Average		72 %
Standard Dev.		5 %

Table 2.9: Percent conversion to **12**.

	HPLC Peak Area	Percent Conversion
Run 1	20679782	88 %
Run 2	20965516	90 %
Run 3	20479177	87 %
Average		88 %
Standard Dev.		2 %

Table 2.10: Percent conversion to **13**.

	HPLC Peak Area	Percent Conversion
Run 1	16930310	87 %
Run 2	16516603	85 %
Run 3	16410510	84 %
Average		85 %
Standard Dev.		2 %

Table 2.11: Percent conversion to **14**.

c. Molar Ratio, Irradiation Time, and Solvent Effect Experiments

In a 2 mL microcentrifuge tube was added the appropriate solvent, followed by solutions of (Azidomethyl)benzene (**15**) and triazenylbenzoic acid (**1**) in the appropriate solvent to achieve a 50 μ L solution of 15 mM triazenylbenzoic acid (**1**) and the corresponding concentration of (Azidomethyl)benzene (**15**) based on the appropriate molar ratio. The tube was

placed about 2 cm below the light source and irradiated for the appropriate time. 6.66 μL of the irradiated solution was diluted to 200 μL with MeCN and benzotriazole formation was monitored using HPLC-MS*. 100% conversion would correlate to a 500 μM solution of benzotriazole. *A new standard curve had to be prepared due to variations attributed to lamp performance after several weeks. Yield is based on new standard curve.

Entry	Solvent	Irradiation Time	Azide Equivalentents	HPLC Peak Area	Percent Conversion
1	THF	3 m	1	740864	3 %
2	THF	3 m	2	896018	3 %
3	THF	3 m	5	3296494	13 %
4	THF	3 m	10	5928268	23 %
5	CHCl_3	3 m	1	12268574	47 %
6	CHCl_3	3 m	2	14635806	56 %
7	CHCl_3	3 m	5	16913386	65 %
8	CHCl_3	3 m	10	15917112	61 %
9	Dioxane	3 m	1	6500111	25 %
10	Dioxane	3 m	2	7302813	28 %
11	Dioxane	3 m	5	10229420	39 %
12	Dioxane	3 m	10	11928272	46 %
13	MeCN	5 s	1	423307	2 %
14	MeCN	1 m	1	14588945	56 %
15	MeCN	3 m	1	21290649	82 %
16	MeCN	5 m	1	21616422	83 %
17	MeCN	3 m	2	23476480	90 %
18	MeCN	3 m	5	25305365	97 %
19	MeCN	3 m	10	25518267	98 %

Table 2.12: Solvent effects.

d. Water Tolerance Experiments

In a 2 mL microcentrifuge tube was added MeCN and the appropriate amount of H_2O followed by solutions of 2-Azido-1-morpholinoethanone (**22**) (7.5 μL , 100 mM, 1.0 eq)* and triazenylbenzoic acid (**1**) (15 μL , 50 mM, 1.0 eq) in MeCN. The tube was placed about 2 cm below the light source and irradiated for 3 m. 6.66 μL of the irradiated solution was diluted to

200 μL with MeCN and benzotriazole formation was monitored using HPLC-MS. 100% conversion would correlate to a 500 μM solution of benzotriazole. *Concentration was increased to achieve solutions >50% water.

% Water	Run 1		Run 2		Run 3*		Average	Standard Dev.
	Peak Area	Percent Conversion	Peak Area	Percent Conversion	Peak Area	Percent Conversion		
0	20472896	72 %	20533024	72 %	26118215	61 %	68 %	6 %
10	6207479	22 %	14891765	52 %	13190756	31 %	35 %	15 %
20	7349911	26 %	9894391	35 %	9792834	23 %	28 %	6 %
30	3092329	11 %	6562328	23 %	8368868	19 %	18 %	6 %
40	6096025	21 %	5027298	18 %	4940317	11 %	17 %	5 %
50	3535529	12 %	3308907	12 %	4034358	9 %	11 %	2 %
70	1662791	6 %	1474828	5 %	4262409	10 %	7 %	3 %

*A new standard curve had to be prepared due to variations attributed to lamp performance after several weeks. Yield is based on new standard curve.

Table 2.13: Water tolerance on conversion.

e. Photolysis of TBA and Diazonium with no azide partner

Reaction conditions: 50 μL solution of 2 mM **1**, varied irradiation (365 nm) times.

time (s)	peak area
0	0
10	1.17E+08
60	73197618
180	55932481
300	44308196
600	107941

Table 2.14: Monitoring consumption during photolysis.

D. References

1. Shi, F., Waldo, J. P., Chen, Y. & Larock, R. C. Benzyne click chemistry: synthesis of benzotriazoles from benzyne and azides. *Org. Lett.* **10**, 2409–2412 (2008).
2. Campbell-Verduyn, L., Elsinga, P. H., Mirfeizi, L., Dierckx, R. A. & Feringa, B. L. Copper-free 'click': 1,3-dipolar cycloaddition of azides and arynes. *Org. Biomol. Chem.* **6**, 3461 (2008).
3. Maki, Y., Takashi, F. & Suzuki, M. Photochemical Reactions. Part 10. Photolysis of o-

- Nitrobenzaldehyde N-Acylhydrazones leading to Benzyne and 5-Nitrophthalazines. *J. Chem. Soc. Perkins Trans. I* 553–557 (1979).
4. Nuyken, O., Stebani, J., Lipped, T., Wokaun, A. & Stasko, A. Photolysis, thermolysis, and protolytic decomposition of a triazene polymer in solution. *Macromol. Chem. Phys.* **761**, 751–761 (1995).
 5. Berry, R. S., Clardy, J. & Schafer, M. E. Benzyne. *J. Am. Chem. Soc.* **86**, 2738–2739 (1964).
 6. Ku, H. & Barrio, J. R. Convenient synthesis of aryl halides from arylamines via treatment of 1-aryl-3,3-dialkyltriazenes with trimethylsilyl halides. *J. Org. Chem.* **46**, 5239 (1981).
 7. van Heyningen, E. 1,2,3-Benzotriazines. *J. Am. Chem. Soc.* **77**, 6562–6564 (1955).
 8. Christopher Buxton, P. & Heaney, H. Aryne formation from 1-(3'-Carboxyaryl)-3,3-dimethyl triazenes. *Tetrahedron* **51**, 3929–3938 (1995).
 9. Schnapp, K. A. & Platz, M. S. A laser flash photolysis study of di-, tri- and tetrafluorinated phenylnitrenes; implications for photoaffinity labeling. *Bioconjug. Chem.* **4**, 178–83 (1993).
 10. Nakanishi, K. *et al.* Photoaffinity labeling of rhodopsin and bacteriorhodopsin. *Biophys Chem* **56**, 13–22. (1995).
 11. Liu, L.-H. & Yan, M. Perfluorophenyl Azides : New Applications in. *Acc. Chem. Res.* **43**, 1434–43 (2010).
 12. Gann, A. W. *et al.* A photoinduced, benzyne click reaction. *Org. Lett.* **16**, 2003–2005 (2014).
 13. Gilchrist, T. L. in *Triple-Bonded Functional Groups (1983)* 383–419 (John Wiley & Sons, Ltd., 2010).

CHAPTER III

PHOTOLYSIS OF *ORTHO*-TRIAZENYLBENZOIC ACIDS TO YIELD *ORTHO*-DIAZONIUM

CARBOXYLATE

A. Introduction

The failure to synthesize benzotriazoles from photoinduced benzyne in sufficient yields at biologically relevant concentrations in sufficient yields was undoubtedly very disappointing. We did learn, however, that the *ortho*-diazonium carboxylate intermediate was rapidly produced. This is quite surprising due to most photolysis of triazenes reported involve a radical mechanism with no apparent diazonium intermediate.¹ Because aryl diazonium species typically require harsh conditions such as highly acidic and/or oxidizing reagents to synthesize, we were interested in using *ortho*-triazenylbenzoic acids as a photo-caged diazonium. Aryl diazonium salts are common reagents which are highly reactive species themselves, albeit not as reactive as an aryne. The diazonium moiety itself is commonly employed as a leaving group for nucleophilic aromatic substitution reactions. The N_2^+ can be displaced by halides using iodide salts for aryl iodides², fluoroboric acid for aryl fluorides³, and the appropriate cuprous chloride or bromide for aryl chlorides or aryl bromides, respectively^{4,5}. This type of reaction falls under a class of named reactions called Sandmeyer reactions. Other transformations of aryl diazonium to aryl azides⁶, cyanides⁷, borates⁸, and even aryl-aryl couplings are possible through the displacement of nitrogen gas⁹. The diazo functionality can be retained if the diazonium is treated with an amine or electron-rich aromatic compound, which act as nucleophiles towards the terminal nitrogen of diazonium to afford triazenes¹⁰ or azobenzenes¹¹, respectively.

Seeing this as a potential opportunity, efforts were quickly turned into finding ways to utilize diazonium rather than benzyne. Initial inspirations were drawn from a simple test we

had used when testing solutions for the presence of diazonium. During the synthesis of triazenes, an aryl amine was first converted into a diazonium salt, then aminated with a secondary amine. To visualize if there was any significant amount of diazonium remaining

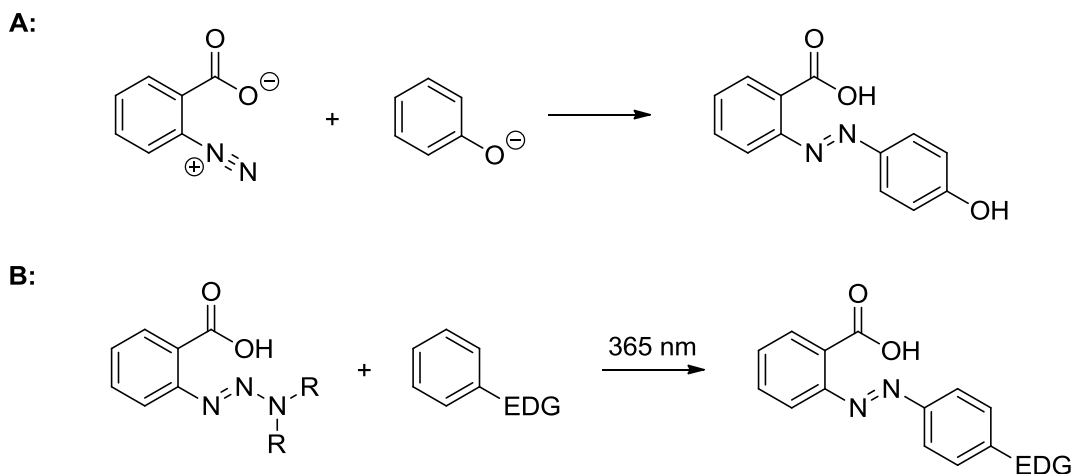


Figure 3.1: Making use of the rapidly photo-generated diazonium carboxylate. A) Simple test for presence of diazonium carboxylate in solution using basic phenol. Rapid formation of the azobenzene turns the solution yellow. B) New photo-click method: photogenerate diazonium carboxylate which will rapidly couple to an electron-rich aromatic partner.

during the amination step, a small aliquot of the reaction mixture was treated with a basic solution of phenol. If diazonium was present, the phenol would rapidly react to form an azobenzene, and in the case of our synthesis, the azobenzene formed was 2-(4-Hydroxyphenylazo)benzoic acid (HABA) (**Figure 3.1 A**). Upon formation, the solution would become yellow due to the presence of HABA. Such a rapid reaction prompted us to explore the possibility of using the photo-generated diazonium as a rapid coupling agent for a new, click-type reaction (**Figure 3.1 B**).

Synthesis of azobenzenes from a diazotized aniline is not a novel concept, and this method is, in fact, how the majority of azobenzenes are synthesized¹¹. Aryl diazoniums are nucleophilic at the terminal nitrogen, and will react with a nucleophilic aromatic ring, provided

there is sufficient amount of electron density in the ring from electron-donating substituents. The difficulty in using this reaction is obtaining fast kinetics under neutral conditions. Typically, the pH of the coupling stage is raised when using hydroxy-based aromatic nucleophiles due to low nucleophilicity of phenols while uncharged, and pH is lowered when using primary or secondary aniline-based aromatic nucleophiles to limit triazene formation. Tertiary anilines couple to diazonium under acidic conditions, but much faster under basic conditions. Thus, we deemed it necessary that an appropriate aromatic nucleophile would be sufficiently nucleophilic on its own without relying on pH to drive the reaction to completion on a seconds to minutes time-scale.

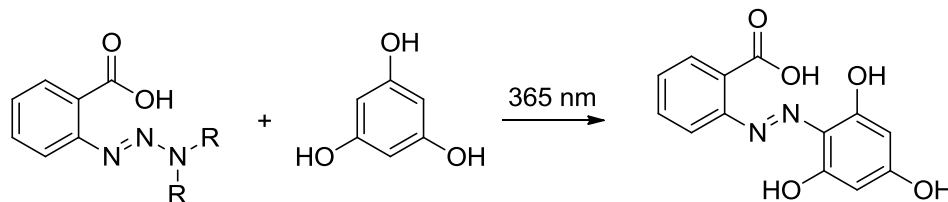


Figure 3.2: Proposed diazonium click reaction core. A triazenylenecarboxylic acid will be irradiated to generate diazonium carboxylate which will rapidly couple with the highly electron-dense phloroglucinol reaction partner.

To achieve this, we turned to the cheap, commercially available polyphenol 1,3,5-trihydroxybenzene, also known by its common name, phloroglucinol (**Figure 3.2**). Phloroglucinol exists as two tautomeric forms in equilibrium with each other, and an intermediate anion formed during tautomerization can be used to explain its high nucleophilic character without assistance from high pH levels. Investigations centered around characterizing the kinetics and efficiency of *ortho*-triazenylenecarboxylic acid photolysis and of resulting diazonium coupling to phloroglucinol.

B. Results and Discussion

A requirement for a good photo-induced click reaction is that it has a very fast photo-activation step and also a very fast coupling step. In our previous attempt with benzyne, the rate of photo-activation was prohibitively slow. However, the rate of photolysis of the TBA to yield diazonium was much faster, which prompted us to measure the quantum yield. Quantum yield is a measurement which measures the efficiency of a photo reaction by directly comparing the number of photons absorbed by a compound and how many of those photons actually promote the desired reaction or transformation.¹² Values of quantum yields typically range from $\phi = 0$, indicated no reaction, to $\phi = 1$, indicating a perfectly efficient photo reaction. Quantum yields can exceed $\phi = 1$, but this is usually associated with photo-induced chain reactions. In order to measure quantum yield, a compound is irradiated in the presence of another compound with a known quantum yield, typically referred to as a chemical actinometer. Upon correcting for absorbance values at the irradiation wavelength, quantum yield can be obtained by directly comparing how much of the compound was consumed versus the actinometer reference compound.¹³ For our experiment, we chose 2-nitrobenzyl alcohol as an actinometer since it has a defined quantum yield of $\phi = 0.5$ at 365 nm irradiation across a wide variety of solvents and is not pH dependent.¹⁴ It was decided that both derivatives of TBA, *N*-acetyl and *N*-dialkyl, would be tested to see if the results matched what was previously observed in acetonitrile.

To our surprise, both TBA derivatives had remarkably similar quantum yields in a phosphate-buffered saline (PBS) solution at pH 7.4, $\phi = 0.36$ for the *N*-acetyl and $\phi = 0.35$ for the *N*-dialkyl. This is indicative of a large solvent dependence for each reaction. Since treatment of diazonium with *N*-methylacetamide yielded no TBA product, we can consider the

photolysis of the *N*-acetyl TBA to diazonium and *N*-methylacetamide essentially irreversible in both acetonitrile and aqueous systems. In the case of the *N*-dialkyl TBA, the resulting amine after initial photo-induced triazene cleavage is expected to have different reactivities in each solvent system. In acetonitrile, the amine is neutral and is very nucleophilic which allows for potentially easy recombination with diazonium to reform the triazene functionality. Because the photo-cleavage reaction is in competition with recombination in this case, the photolysis of the *N*-dialkyl TBA appeared to be much slower than the *N*-acetyl TBA in acetonitrile. However, in an aqueous solvent, the amine is in an equilibrium with its protonated state, reducing its nucleophilicity relative to that in acetonitrile. Reduced nucleophilicity would lead to reduced competition with the recombination reaction, leading to an apparently faster rate of photolysis in an aqueous solvent versus acetonitrile.

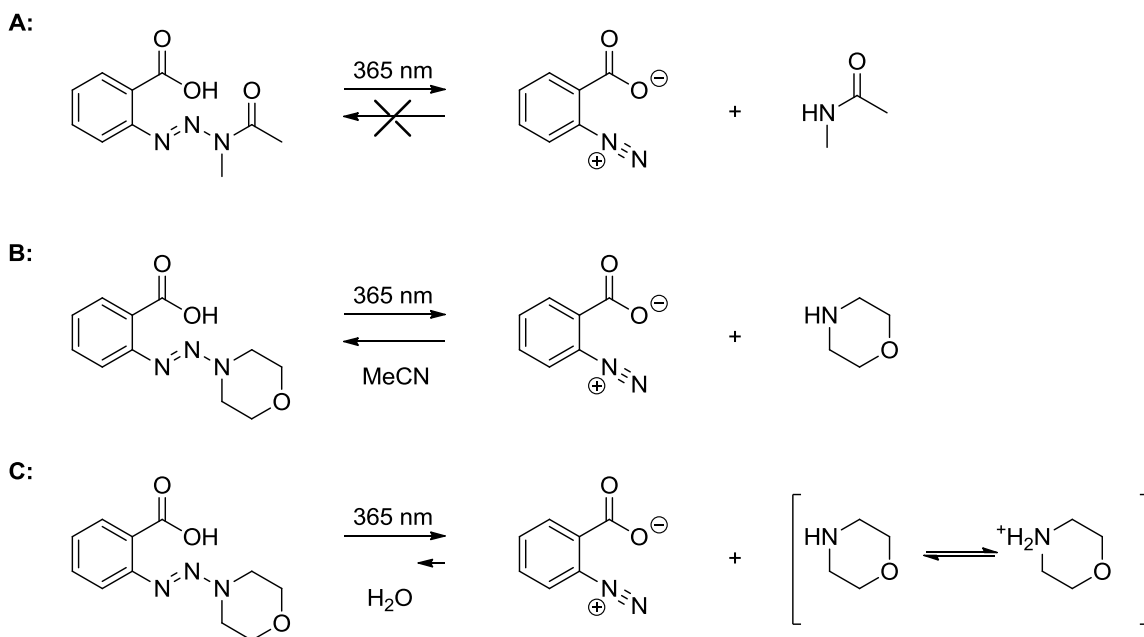


Figure 3.3: Proposed explanation for slower photolysis of **1b** in acetonitrile than in water. A) Amide recombination with diazonium does not occur regardless of solvent, giving way to rapid apparent photolysis. B) Secondary amine in acetonitrile is nucleophilic enough to promote recombination, giving a slower apparent photolysis. C) Secondary amine is mostly protonated in aqueous solution, allowing for a much slower rate of recombination.

The mechanism of diazonium formation by expulsion of the terminal nitrogenous species of the triazene was supported by an experiment where a solution of the *N*-dialkyl TBA was irradiated in PBS for 20 seconds, followed by HPLC-MS analysis immediately after and again 3 hours after (**Figure 3.4**). Analysis immediately after irradiation showed 98% consumption of the TBA, while the postponed analysis showed only 80% consumption, indicating that the TBA had been moderately regenerated by recombination of diazonium with the secondary amine.

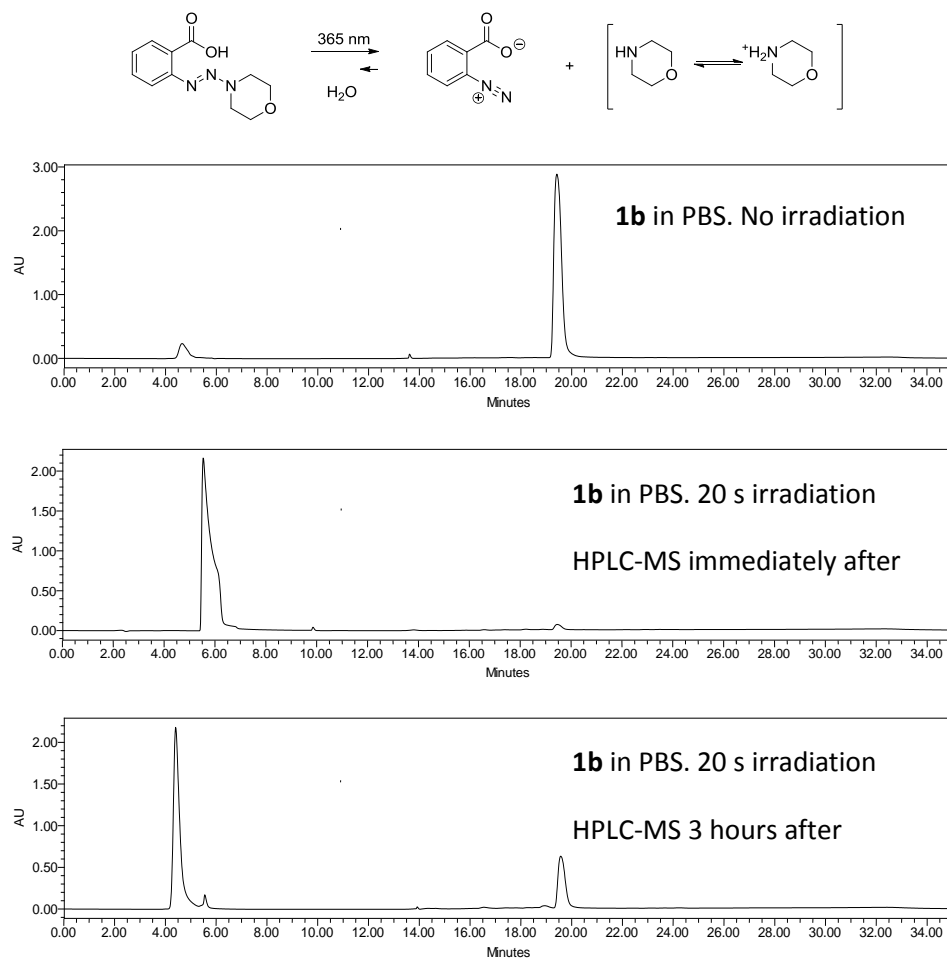


Figure 3.4: Support for recombination. After allowing the irradiated triazeryl benzoic acid to incubate with no added reaction partner, reformation was observed, confirming that the terminal nitrogen group is able to recombine.

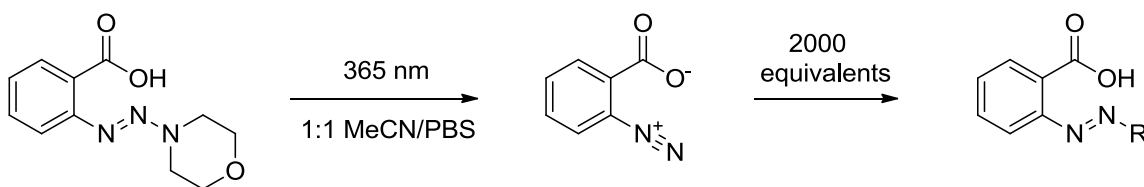
While the quantum yield represents how well the absorbed photons are at initiating photochemistry, the TBA derivatives studied had rather low absorbance values at 365 nm.

Theoretically, rate of photolysis could be further increased by red-shifting the TBAs' λ_{max} to allow more photons to be absorbed at 365 nm for potential chemistry. Regardless, the discovery of near identical quantum yields between derivatives proved incredibly valuable since the synthesis of the *N*-dialkyl TBA is much simpler and straightforward.

With the efficiency of the photolysis measured, our attention turned towards examining the efficiency of the nucleophilic addition to the diazonium carboxylate. Mechanistic studies of azobenzene formation from the coupling of diazonium salt and electron-rich aromatic have previously established that reactions of this type are classified as electrophilic aromatic substitutions.¹⁵ The coupling reactions are second order in nature and can be studied using pseudo-first order conditions in which one of the reagents is used in a large excess. An observed first order rate constant can be converted to a second-order rate constant by factoring out the concentration of the excess reagent. Phloroglucinol was chosen as the reagent to be used in excess as to limit the use of large quantities of unstable diazonium and, since larger amounts of diazonium require longer irradiation times, to keep irradiation times as low as possible. To monitor kinetics, we took advantage of azobenzene-containing compounds having large absorbance bands in the visible spectrum, and monitored azobenzene formation using stopped-flow UV-Vis spectroscopy. A solution of the *N*-dialkyl TBA at 100 μM was irradiated until no more TBA could be observed by HPLC-MS to generate a solution of diazonium. Another solution containing 100 molar equivalents of phloroglucinol was combined with the diazonium solution. The products were compared to a synthetic standard of the expected azobenzene product prepared from diazotization of anthranilic acid, followed by treatment with phloroglucinol.

Unfortunately, we did not observe the desired distribution of products we expected, which was a single addition of a diazonium to phloroglucinol. While this was the major product

at 66%, we also observed double addition at 34%. We found this multiaddition problematic, as the synthetic standard only contained about 5% double addition. The most likely reason the



Azobenzene and Triazene Formation

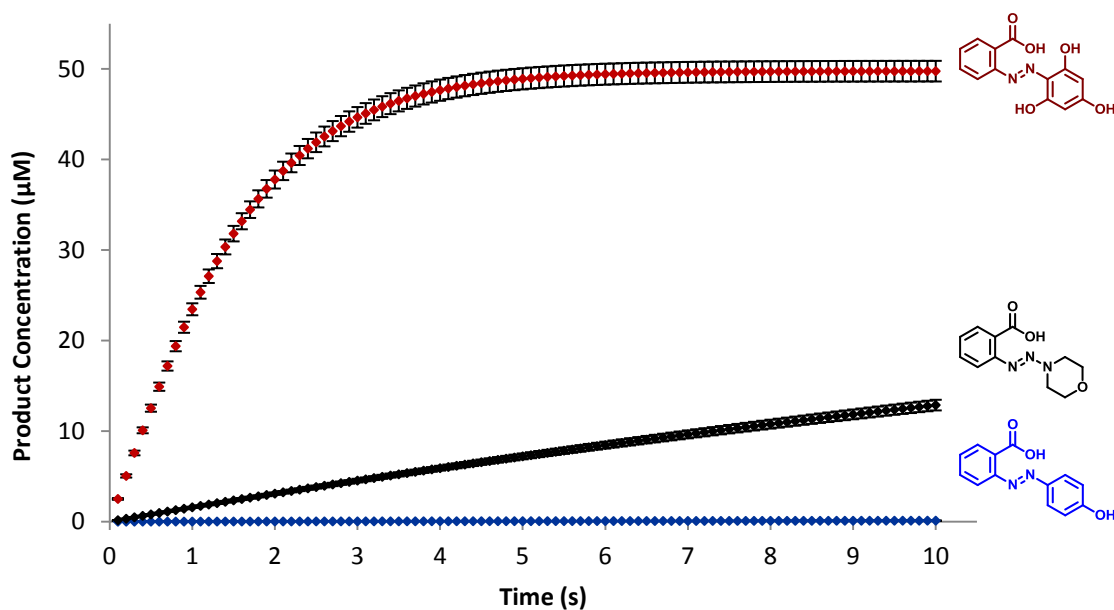


Figure 3.5: Kinetic analysis of photogenerated diazonium carboxylate's coupling. Partners are 2000x phenol (blue), morpholine (black), or phloroglucinol (red). The product formed from each reaction is shown on the right. Reactions were carried out on a 50 μM scale in 1:1 MeCN/1X PBS.

synthetic standard did not suffer from the multiaddition problem was that once a single addition had occurred, the product became insoluble and crashed out of solution, greatly reducing the likelihood of undergoing further addition to another diazonium. By increasing the molar equivalents of phloroglucinol to 2000, the amount of double addition product decreased to

levels observed in the synthetic standard, allowing us to directly compare the spectrum of the photo-induced diazonium addition reaction to the synthetic standard. When the addition was controlled by a stopped-flow system, the reaction between 50 μM irradiated TBA and 2000 equivalents of phloroglucinol reached completion in less than 10 seconds (**Figure 3.5**). Astonishingly, using the absorbance values obtained from the standard, the reaction turned out to be quantitative. This meant that not only was the addition of phloroglucinol to diazonium quantitative, but the initial photolysis of TBA to diazonium was clean, and the resulting diazonium was stable enough during the time it took to load into the stopped-flow system. Recombination during that time would be expected, but since the concentration and rate are both low, little to no recombination was observed. Further analysis¹⁶ using a double exponential fitting gave a second order rate constant of k_2 of $7.53 \text{ M}^{-1}\text{s}^{-1}$.

Comparison of phenol addition and morpholine addition were also done. Addition of phenol to afford HABA proceeded incredibly slow, only to give trace product, most likely because of phenol's low nucleophilicity under the neutral conditions. Addition to morpholine to afford the original TBA back proceeded much faster than phenol, but was still only about 20% complete after 10 seconds. These observations lead us to believe that phloroglucinol could have extremely high selectivity over other potential reactive partners in a biological setting. Addition of diazonium ions to protein residues¹⁷ like tryptophan, histidine, lysine, and tyrosine is known, but requires reaction times of up to an hour at elevated pHs, further strengthening the idea of using phloroglucinol as a highly competitive target for a photo-generated diazonium species. With this in mind, we began to set our eyes on modifying biological systems with a TBA to investigate its practical use.

C. Experimentals

1. General

Reagents and solvents for organic synthesis were used as received. Thin-layer chromatography (TLC) was conducted on glass-backed silica plates visualized with either UV illumination, basic permanganate stain, or bromocresol green stain. Flash chromatography was conducted on 60 Å silica gel. NMR spectra were recorded on a Bruker Advance 400, chemical shift values are reported in ppm on the δ scale relative to TMS ($\delta = 0.00$) as an internal standard. Irradiation for photolysis was performed using an LED Engin LZ1-10U600 365 nm LED powered by a DC 12 V, 2 A source through a 700 mA FlexBlock Constant Current Driver. UV-Vis experiments were carried out on a NanoDrop 2000 spectrometer (NanoDrop, Wilmington, DE, USA). LC Separation was performed with a Waters 1525 system. The gradient employed was A = water + 0.1% formic acid, B = acetonitrile + 0.1% formic acid, 5–95% B over 60 min with a Waters XBridge C18 5 μ column (4.6 \times 150 mm). Mass spectra were acquired with a Waters Micromass ZQ mass detector in EI+ mode: Capillary voltage = 3.50 kV, cone voltage = 30 V, extractor = 3 V, RF lens = 0.0 V, source T = 100 °C, desolvation T = 200 °C, desolvation gas = 300 L h⁻¹, desolvation gas = 0.0 L h⁻¹. The system was operated by and spectra were processed using the Waters Empower software suite.

2. Synthetic Procedures

a. (E)-2-((2,4,6-trihydroxyphenyl)diazenyl)benzoic acid (**37**)

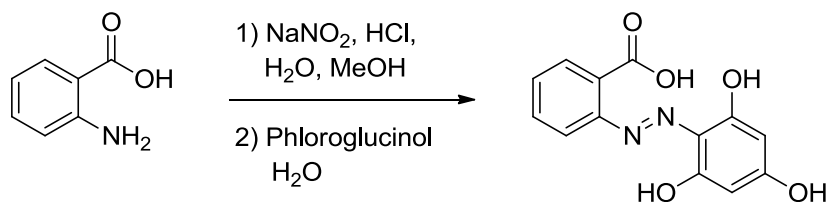


Figure 3.6: Synthesis of **37**.

A solution of anthranilic acid (563 mg, 4.11 mmol, 1.0 eq) in 4 mL of H₂O and 4 mL of MeOH was acidified with 4 mL of 6M HCl and cooled to 0 °C. A solution of NaNO₂ (340 mg, 4.93 mmol, 1.20 eq) in 2 mL H₂O was added dropwise, and the reaction was allowed to stir another 30 min. The diazotized solution was then added dropwise to a solution of phloroglucinol (1.55 g, 12.3 mmol, 3.00 eq) in 150 mL H₂O at 0 °C and allowed to stir for 3 h. The precipitate was filtered, washed with water (3 × 50 mL), and allowed to dry in open air overnight to afford (E)-2-((2,4,6-trihydroxyphenyl)diazenyl)benzoic acid (986 mg, 3.58 mmol, 87%) as dark red solid.

¹H NMR (400MHz, DMSO) δ = 8.30 (d, *J* = 8.3 Hz, 1 H), 7.95 (d, *J* = 7.6 Hz, 1 H), 7.67 (t, *J* = 7.6 Hz, 1 H), 7.39 (t, *J* = 7.5 Hz, 1 H), 5.78 (s, 2 H)

¹³C NMR (101MHz, DMSO) δ = 168.8, 168.1, 147.1, 133.6, 131.4, 127.5, 125.9, 123.7, 117.2, 96.2

3. Quantum Yield Determination

Relative quantum yields were determined using a procedure as previously described. *o*-Nitrobenzyl alcohol was used as the secondary actinometer since it does not strongly absorb at the irradiation wavelength, nor does its photolysis byproducts, and has a quantum yield of $\phi = 0.5$ across a variety of solvent conditions, including neutral aqueous buffers. A 100 μ L solution of 1X PBS at pH 7.4 containing 1 mM *o*-nitrobenzyl alcohol and 1 mM of either **1** or **37** in was

irradiated for 10 s. Analysis by HPLC-MS was carried out and compared to a non-irradiated sample to determine extent of photolysis for each compound in solution.

	Time (s)	Peak Area 1	Peak Area 2	Average	% Completion
o-Nitrobenzyl alcohol	0	50972376	50691399	5083188	
	5	37471548	37735803	37603676	26%
37 (di-alkyl)	0	62076028	63012588	62544308	
	5	28075478	37684910	32880194	47%
o-Nitrobenzyl alcohol	0	47721130	49708993	48715062	
	5	36055317	37232028	36643673	25%
1 (acetyl)	0	73072763	74019208	73545986	
	5	38273446	37686806	37980126	48%

Table 3.1: Reaction completions for quantum yield determination.

$$\frac{\phi_{oNBA}}{\% \text{ Completion}_{oNBA}} = \frac{\text{Apparent } \phi_{TBA}}{\% \text{ Completion}_{TBA}} \quad \text{Actual } \phi_{TBA} = \text{Apparent } \phi_{TBA} \left(\frac{\epsilon_{oNBA}}{\epsilon_{TBA}} \right)$$

Figure 3.7: Equation for converting reaction completion to relative quantum yield.

Compound	ϵ @ 365 nm	Apparent ϕ	Actual ϕ
o-Nitrobenzyl alcohol	3.26		
37	8.40	0.91	0.35
1	8.80	0.98	0.36

Table 3.2: Extinction coefficients and subsequent relative quantum yields.

4. Kinetics

Solutions of diazonium were prepared by irradiating 500 μ L solutions of 100 μ M **37** for 45 seconds (no TBA remaining, confirmed by HPLC-MS, not shown) in 1:1 acetonitrile/1X PBS pH 7.4. Solutions of coupling partner were prepared to 2000 equivalents (200 mM) partner (phloroglucinol, phenol, or morpholine) in 1:1 acetonitrile/1X PBS pH 7.4. Subsequent analysis was done using an SF-61 DX2 Double Mixing Stopped-Flow spectrometer (TgK Scientific, Bradford-on-Avon, UK), monitoring formation of product at the indicated wavelength under pseudo-first order conditions. Analysis and fitting was done using Kinetic Studio software. Standard curves for the resulting products (**37**, **38**, and HABA) were obtained on the

spectrometer as to quantify the reaction. A concentration vs. time plot was extrapolated from the fits using the molar absorbances for every 0.1 s (frequency of measurement made by instrument) and normalized.

a. Addition of Diazonium to Phloroglucinol (420nm)

Fit to a double exponential of $Y = -A_1e^{(-R_1x)} - A_2e^{(-R_2x)} + C$

	Experiment 1	Experiment 2	Experiment 3
A1	-0.67814	-1.70049	-2.09108
A2	1.95367	3.0726	3.17594
C	1.29752	1.39035	1.10663
R1	1.56878	1.31598	1.32382
R2	0.86119	0.95428	1.04405

Table 3.3: Double exponential constants for phloroglucinol kinetics.

After fit analysis, reaction proved quantitative, meaning the concentration of diazonium $[N_2^+]$ is equal to concentration of triazenylbenzoic acid [TBA], allowing us to utilize an analysis demonstrated for the cycloaddition of nitrile-imines with alkenes. Therefore the first order rate law for the addition of reaction partner to diazonium is as follows:

$$rate = \frac{d[N_2^+]}{dt} = -k_{obs}[N_2^+] = \frac{d[TBA]}{dt} = -k_{obs}[TBA]$$

Integrated:

$$\ln\left(\frac{[TBA]_t}{[TBA]_0}\right) = -k_{obs}t$$

The concentration of [TBA] at time t can be inferred from measuring azobenzene $[AB]_t$ formation:

$$[TBA]_t = [TBA]_0 - [AB]_t$$

Therefore:

$$\ln\left(\frac{[TBA]_0 - [AB]_t}{[TBA]_0}\right) = -k_{obs}t$$

Plotting $\ln\left(\frac{[TBA]_0 - [AB]_t}{[TBA]_0}\right)$ vs $-k_{obs}t$ allows to solve for the slope, k_{obs} , and converting to second order by factoring in the concentration of reaction partner allows for determination of k_2 :

$$k_2 = \frac{k_{obs}}{[Phloroglucinol]}$$

b. Addition of Diazonium to Morpholine (305 nm)

Fit to a double single of $Y = -Ae^{(-Rx)} + C$

	Experiment 1	Experiment 2	Experiment 3
A	0.31254	0.28712	0.25693
C	0.04806	0.04818	0.04885
R	0.49359	0.46072	0.42096

Table 3.4: Linear constants for morpholine kinetics.

Reaction did not go to completion after 10s, rate was not determined.

c. Addition of Diazonium to Phenol (347 nm)

Fit to a linear equaton of $Y = Mx + C$

	Experiment 1	Experiment 2	Experiment 3
M	0.00021	0.0002	0.00019
C	-0.02038	-0.02029	-0.01938

Table 3.5: Linear constants for phenol kinetics.

Reaction did not go to completion after 10s, rate was not determined.

D. References

1. Julliard, M., Scelles, M., Guillemonat, A., Vernin, G. & Metzger, J. The photochemical behavior of bis aryl-1,3 triazenes. *Tetrahedron Lett.* 375–378 (1977).

2. Krasnokutskaya, E. A., Semenischeva, N. I., Filimonov, V. D. & Knochel, P. A New, One-Step, Effective Protocol for the Iodination of Aromatic and Heterocyclic Compounds via Aprotic Diazotization of Amines. *Synthesis (Stuttg)*. **2007**, 81–84 (2007).
3. Laali, K. K. & Gettwert, V. J. Fluorodiazonation in ionic liquid solvents: New life for the Balz-Schiemann reaction. *J. Fluor. Chem.* **107**, 31–34 (2001).
4. Sandmeyer, T. Ueber die Ersetzung der Amidgruppe durch Chlor in den aromatischen Substanzen. *Berichte der Dtsch. Chem. Gesellschaft* **17**, 1633–1635 (1884).
5. Beletskaya, I. P., Sigeev, A. S., Peregudov, A. S. & Petrovskii, P. V. Catalytic Sandmeyer Bromination. *Synthesis (Stuttg)*. **2007**, 2534–2538 (2007).
6. Kutonova, K. V., Trusova, M. E., Postnikov, P. S., Filimonov, V. D. & Parello, J. A Simple and Effective Synthesis of Aryl Azides via Arenediazonium Tosylates. *Synthesis (Stuttg)*. **45**, 2706–2710 (2013).
7. Sandmeyer, T. Ueber die Ersetzung der Amid-gruppe durch Chlor, Brom und Cyan in den aromatischen Substanzen. *Berichte der Dtsch. Chem. Gesellschaft* **17**, 2650–2653 (1884).
8. Zhao, C.-J., Xue, D., Jia, Z.-H., Wang, C. & Xiao, J. Methanol-Promoted Borylation of Arylamines: A Simple and Green Synthetic Method to Arylboronic Acids and Arylboronates. *Synlett* **25**, 1577–1584 (2014).
9. Roglans, A., Pla-Quintana, A. & Moreno-Mañas, M. Diazonium salts as substrates in palladium-catalyzed cross-coupling reactions. *Chem. Rev.* **106**, 4622–43 (2006).
10. Ku, H. & Barrio, J. R. Convenient synthesis of aryl halides from arylamines via treatment of 1-aryl-3,3-dialkyltriazenes with trimethylsilyl halides. *J. Org. Chem.* **46**, 5239 (1981).

11. Wang, M., Funabiki, K. & Matsui, M. Synthesis and properties of bis(hetaryl)azo dyes. *Dye. Pigment.* **57**, 77–86 (2003).
12. Valenzeno, D. P., Pottier, R. H., Mathis, P. & Douglas, R. H. Photobiological Techniques. (1991). at <<http://dx.doi.org/10.1007/978-1-4615-3840-0>>
13. Papageorgiou, G., Ogden, D., Kelly, G. & Corrie, J. E. T. Synthetic and photochemical studies of substituted 1-acyl-7-nitroindolines. *Photochem. Photobiol. Sci.* **4**, 887–96 (2005).
14. Gaplovsky, M. *et al.* Photochemical reaction mechanisms of 2-nitrobenzyl compounds: 2-nitrobenzyl alcohols form 2-nitroso hydrates by dual proton transfer. *Photochem. Photobiol. Sci.* **4**, 33–42 (2005).
15. Albar, H. A., Shawali, A. S. & Abdaliah, M. A. Substituent effects on azo coupling of indoles. *Can. J. Chem.* **71**, 2144–2149 (1993).
16. Wang, Y., Song, W., Hu, W. J. & Lin, Q. Fast alkene functionalization in vivo by photoclick chemistry: HOMO lifting of nitrile imine dipoles. *Angew. Chemie - Int. Ed.* **48**, 5330–5333 (2009).
17. Riordan, J. F. & Vallee, B. L. Diazonium Salts as Specific Reagents and Probes of Protein Conformation. *Methods Enzymol.* 521–531 (1971).

CHAPTER IV

BIOLOGICAL APPLICATIONS AND FUTURE DIRECTIONS OF PHOTO-GENERATED *ORTHO*- DIAZONIUM CARBOXYLATE

A. Introduction

The primary goal of developing a photo-click reaction was to establish a new bioorthogonal conjugation reaction that is also fast, highly targetable, and relies on cheap easily synthesized partners.¹ In the highly dynamic environment of the cell, important changes take less than a second, therefore reactions that require minutes to go to completion cannot be used to study such changes. The nitrile-imine photo-click methods have shown application on live cells, but up to this point, requires harmful 302 nm irradiation and reactions on the minute time-scale.² Using a synthetically demanding spiro-alkene drastically improved the reaction speed, however it has not yet been demonstrated in a biological setting.³ The quantitative photo-generation of *ortho*-diazonium carboxylate at 365 nm and subsequent coupling with phloroglucinol introduced in the previous chapter set up a new scaffold that could be a competitor in the field of photo-click with some further development and demonstration of application (**Figure 4.1**).

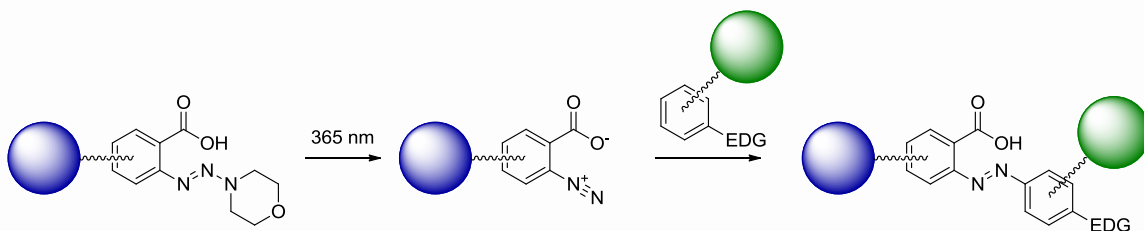


Figure 4.1: Design of click reaction using photo-generated diazonium carboxylate. The triazene, coupled to a biomacromolecule, would be irradiated in the presence of a reporter-functionalized phloroglucinol. The phloroglucinol would couple to the diazonium in a selective fashion, attaching the reporter to the biomacromolecule of choice.

With a potentially bioorthogonal photo-click reaction in hand, we were interested in labeling biological systems. As highlighted by a click chemistry review by Bertozzi, a sequential process should be considered when demonstrating a new bioorthogonal reaction.⁴ Following characterization of the reaction, demonstration of the reaction on biological systems should be done first on proteins, then on cells, and eventually followed up by live animals such as mice or zebrafish. We envisioned a functionalizing our reactive partners, the *N*-dialkyl TBA and phloroglucinol, so that the TBA could be conjugated to a desired biological system and essentially "clicked" to a phloroglucinol moiety upon irradiation. Ideally, the phloroglucinol would be modified with some function that would make attachment easy to detect, such as a fluorophore.

B. Results and Discussion

While a functionalized derivative of the *N*-acetyl TBA had been synthesized, we decided that the 10-step synthesis which contained several low yielding steps in the later stages was not going to be very attractive to future researchers. Thankfully, the quantum yield experiments discussed in the previous chapter indicated that there was no disadvantage to using the much easier to synthesize *N*-dialkyl TBA instead. The goal of using a benzyl azide TBA derivative remained the same, as to not deviate the electronics of the ring from the original, unfunctionalized TBA. Because the key 2-aminobenzyl alcohol intermediate was not necessary, the synthesis became more streamlined. Starting with 1-methyl-2-nitroterephthalate, a borane reduction followed by and iron powder reduction yielded the benzyl alcohol modified methyl anthrinilate, mirroring the first two steps of *N*-acetyl TBA functionalization. From there, the anthrinilate was diazotized and converted to the triazene by treatment with morpholine in 92% yield after purification. The benzyl alcohol was cleanly converted to the benzyl azide using

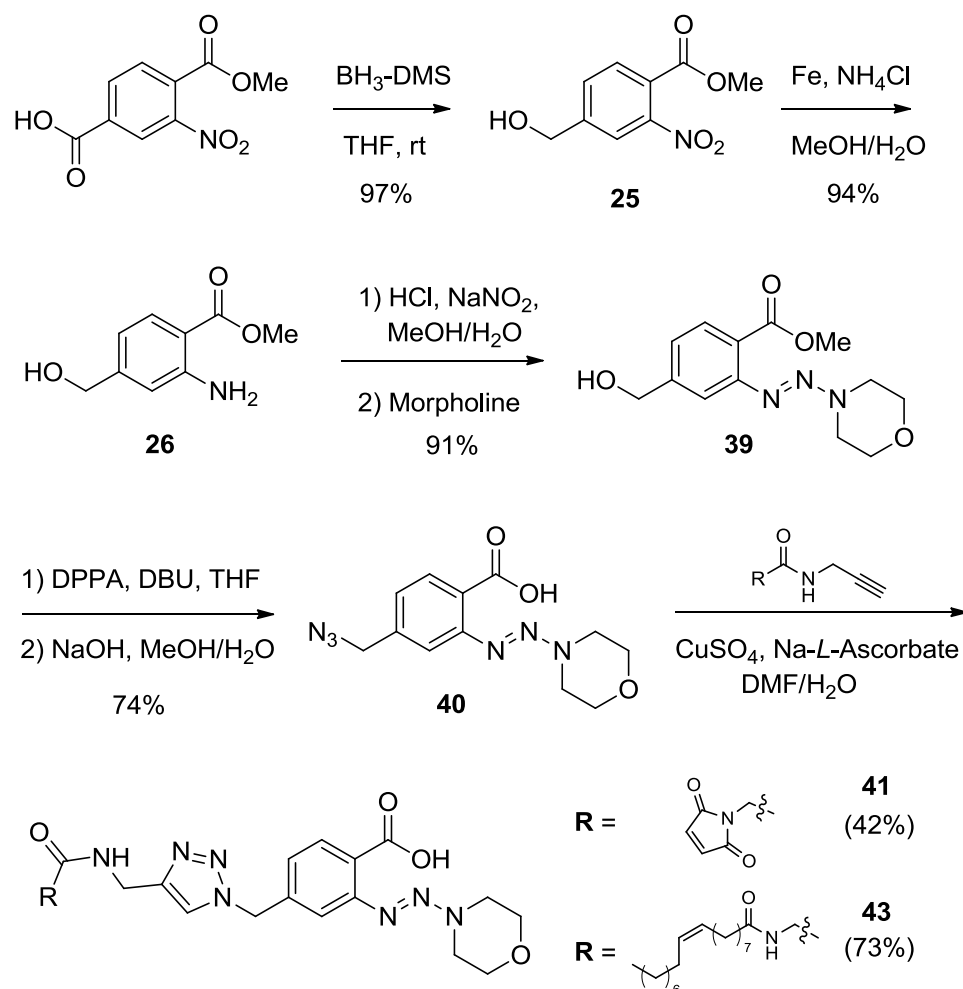


Figure 4.2: Synthesis of functionalized triazenylbenzoic acids. With alkyne tags in hand, functionalized diazonium precursors can be obtained in as little as 5 moderate to high yielding steps.

diphenylphosphoryl azide (DPPA) and base, and after a work up, the crude material was hydrolyzed in methanolic sodium hydroxide to both cleave the ester to yield the benzyl azido *N*-dialkyl TBA in 76% yield over two steps and destroy any remaining excess DPPA. With a benzyl azide modified TBA in hand, we attached a maleimide electrophile using a traditional CuAAC method with an alkyne-functionalize maleimide in 49% yield. Functionalization of phloroglucinol was achieved by substitution at one of the hydroxyl groups rather than an alkylation of an aromatic carbons. A mono-alkylation on the carbons is typically very difficult and has only recently been shown to proceed in good yields with certain electron deficient

electrophiles.⁵ However, substitution of a hydroxyl with a secondary amine takes full advantage of phloroglucinol's rapid tautomerization between keto and hydroxy states (**Figure 4.3**). In the keto state, an amine can condense to form an imine, and then tautomerize to yield the aryl

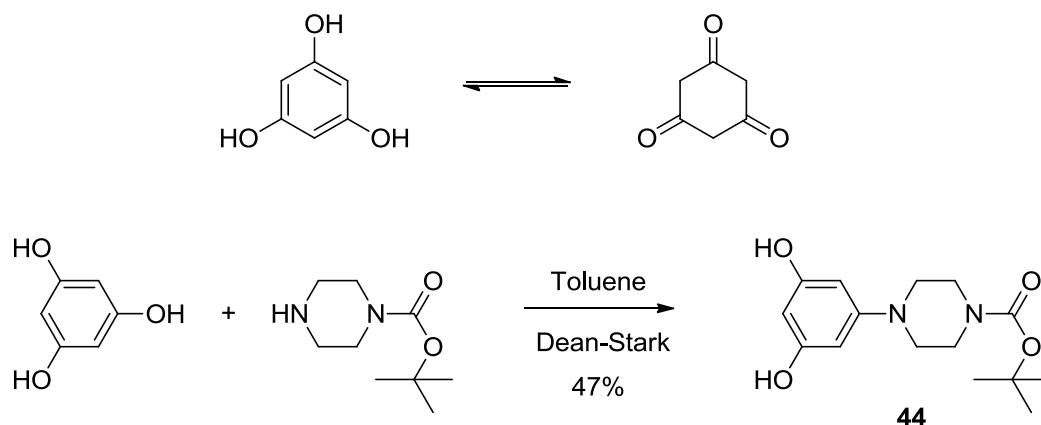


Figure 4.3: Phloroglucinol tautomerization. The keto state allows for rapid condensation with primary and secondary amines. 1-Boc-piperazine condenses with phloroglucinol readily to give an easily functionalized dihydroxyphenyl piperazine.

amine. Phloroglucinol was successfully condensed with 1-Boc-piperazine (**Figure 4.3**) to afford dihydroxyphenyl-N-Boc-piperazine (BocDHPP) in 47% yield. The Boc group can be easily deprotected to yield an amine which can be coupled to an acid-functionalized reporter group. A deprotected BocDHPP was coupled with a Cyanine 3 dye to yield Cy3-DHPP in 64% yield using simple amide coupling conditions (**Figure 4.4**).

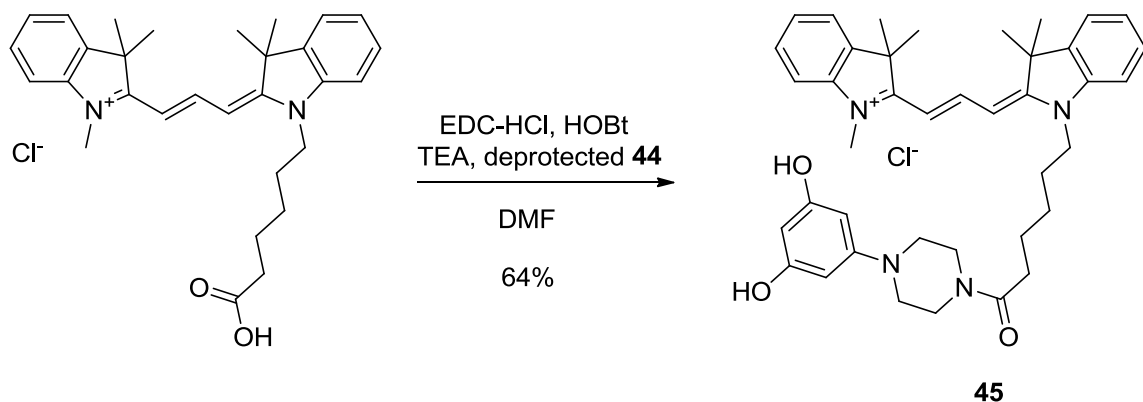
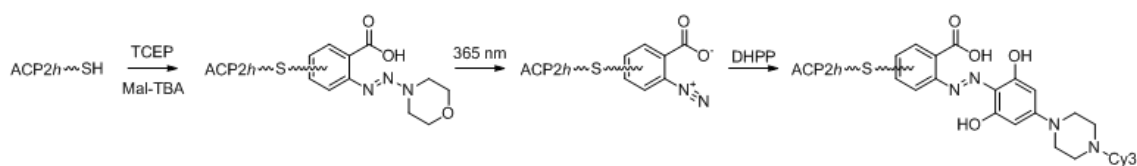


Figure 4.4: Deprotected Boc-DHPP coupling with Cyanine-3

The new maleimide-functionalized *N*-dialkyl TBA was used to conjugate our system to proteins in order to assess viability on a complex biomacromolecule. Our previous kinetic analysis along with studies done previously gave us confidence that the photogenerated diazonium would not react to a large extent with any functional groups present on the protein, and would react very quickly with an appropriately functionalized phloroglucinol. In order to visualize protein labeling, we chose to use in-gel fluorescence to monitor Cy3-labeled proteins. Protein labeled with 10x maleimide TBA via TCEP-reduced cysteines was irradiated in the



25 μ M ACP2h + 100 eq TCEP	X	X	X	X	X	X	X	X
10 eq Mal-TBA			X	X			X	X
10 eq Cy3-DHPP					X	X	X	X
365 nm @ 15 s		X		X		X		X

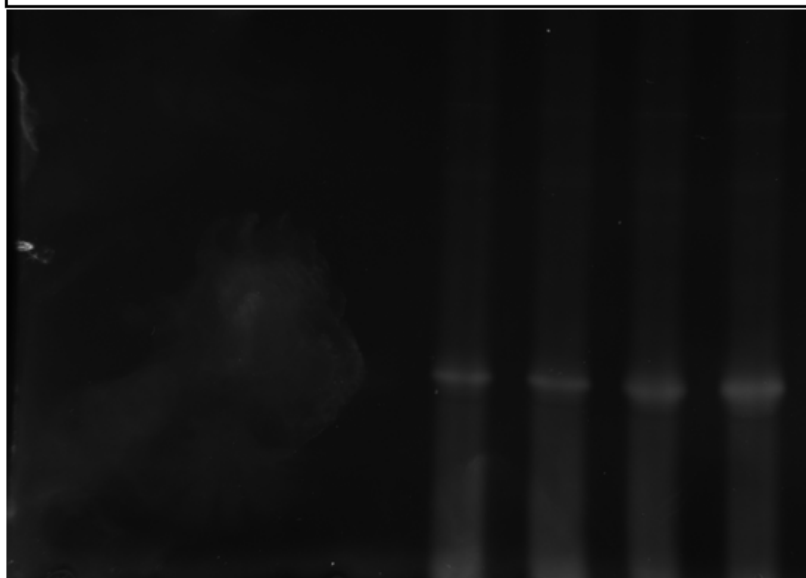
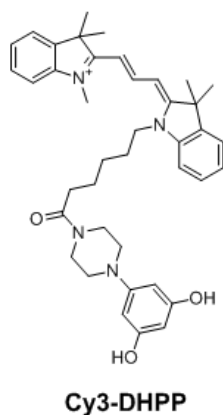


Figure 4.5: Labeling *h*ACP2 with 10x Mal-TBA **41** followed by irradiation in the presence of 10x Cy3-DHPP **45**. No specific labeling observed. The culprit is most likely reduction of the diazonium by TCEP in solution.

presence of 10x Cy3-DHPP for 15 seconds, and, with no added incubation time aside from the time it took to prepare samples for gel-loading. Using the *holo* acyl carrier protein from module

2 (*hACP2*) of the 6-DEBS polyketide synthase⁶ (single available thiol for loading) to establish reaction conditions, Cy3 labeling was initially poor (**Figure 4.5**). Upon further consideration of the high potential for aryl diazoniums to be reduced, it was determined that the disulfide reducing agent must be removed after the reduction step. Once the TCEP had been removed,

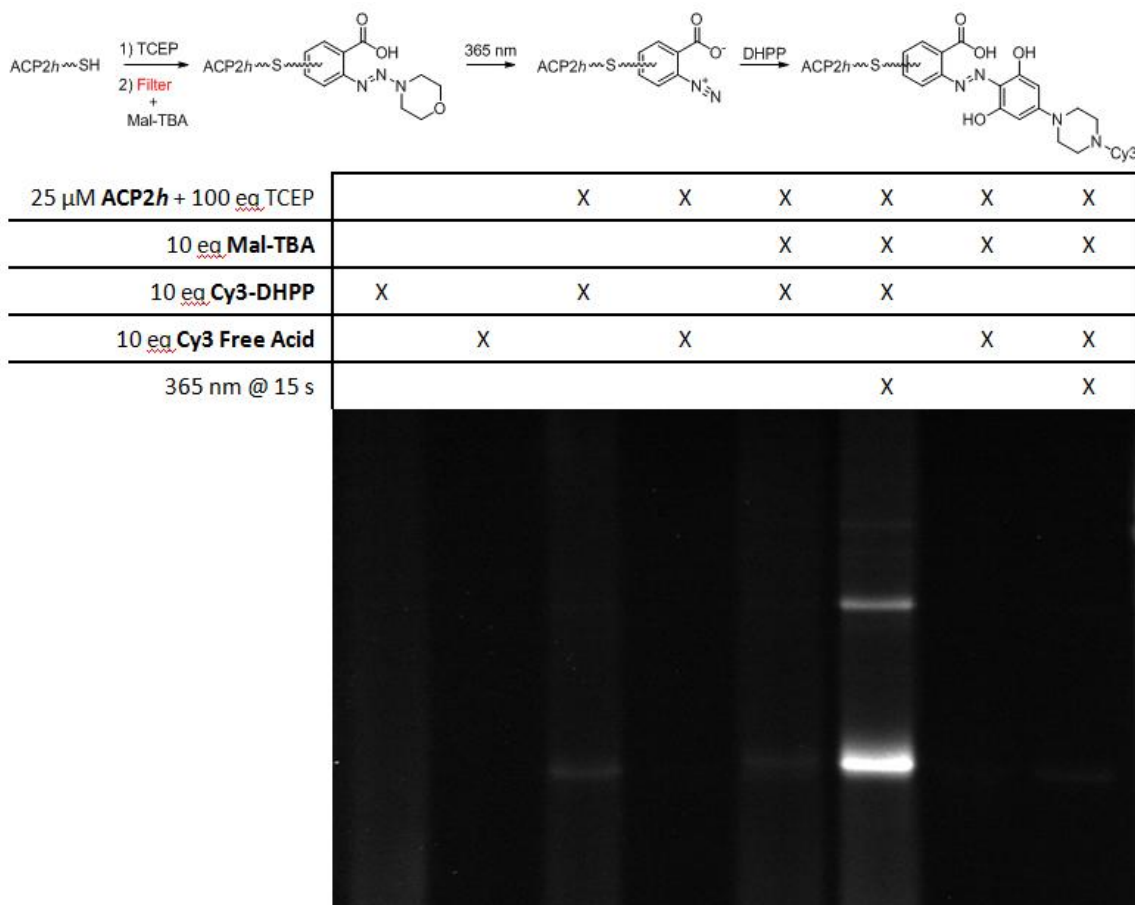


Figure 4.6: Removing TCEP prior to labeling *hACP2* with 10x Mal-TBA **41** followed by irradiation in the presence of 10x Cy3-DHPP **45**. Removal of TCEP allowed for much more efficient photo-induced labeling since the diazonium was not being reduced.

Cy3 labeling of *hACP2* proved a remarkable success, showing strong fluorescence only in the lane containing labeled protein that had been irradiated in the presence of Cy3-DHPP (**Figure 4.6**). Some small amount of non-specific labeling is seen in lanes containing Cy3-DHPP, the nature of which has not yet been identified. A band appears around the expected mass of

dimer, which could be attributed to a few things: photo-induced dimerization of the protein, multiple additions of diazonium to an already azobenzene-modified Cy3-DHPP protein (2 additional reactions potentially possible), or labeling of residual non-reduced protein.

With conditions established using *hACP2*, we turned our eyes to more interesting and useful proteins with exposed cysteines that could be potentially labeled with our maleimide TBA. Prolyl hydroxylase domain-containing protein 2 (PHD2) is an enzyme which assists in regulation of oxygen homeostasis⁷ which has three surface exposed cysteines. Using the same procedure as *hACP2*, the labeling experiment was conducted with a full set of controls (**Figure 4.7**). The lane which contains protein, maleimide TBA, Cy3-DHPP, and irradiation shows much

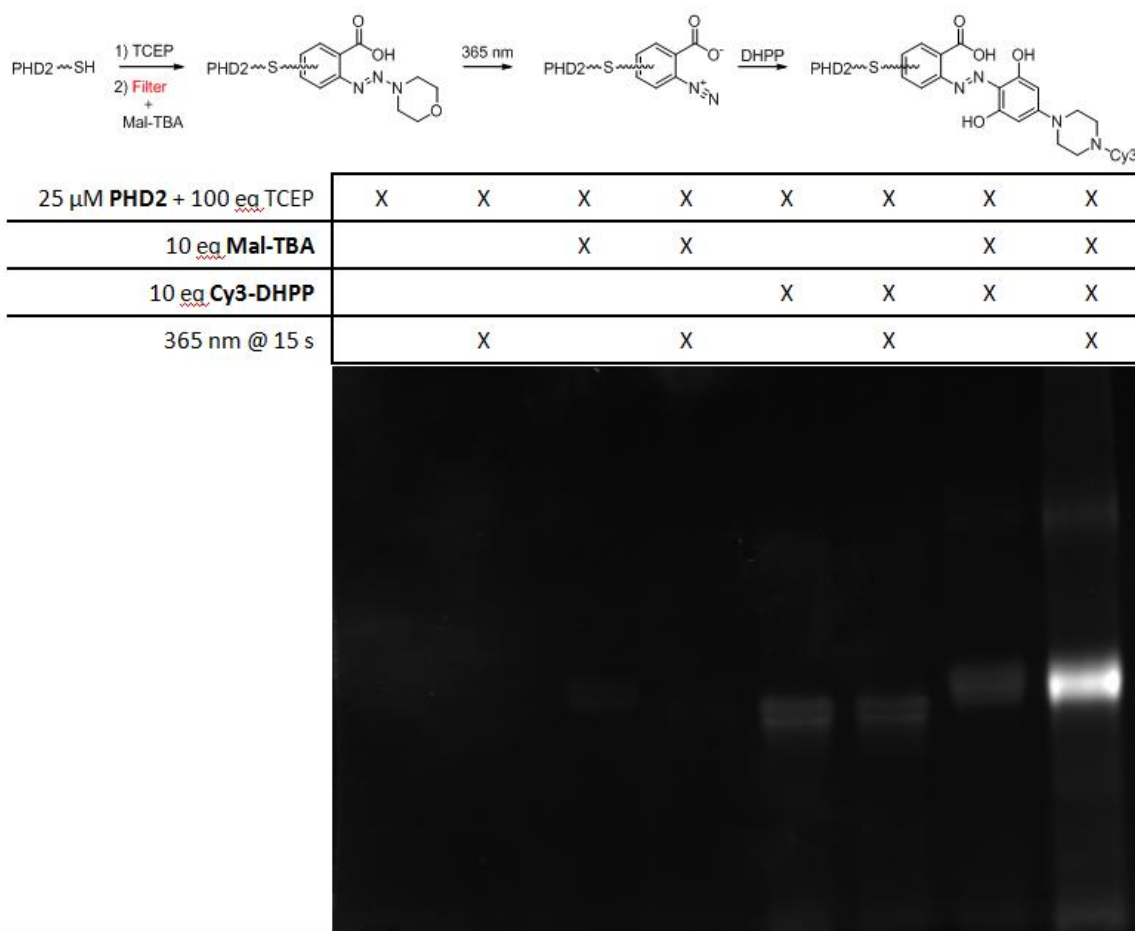


Figure 4.7: Labeling of PHD2. Photoinduced labeling visible, along with small side reaction.

stronger signal than all lanes, but the side reaction in lanes containing Cy3-DHPP is still present. An array of additional proteins was examined for labeling potential, including the kinase PAK2, lysozyme, and factor-inhibiting HIF-1 (FIH), and all showed selectivity for Cy3-DHPP labeling only when the maleimide-treated proteins were irradiated (**Figure 4.8**). We were excited to see that

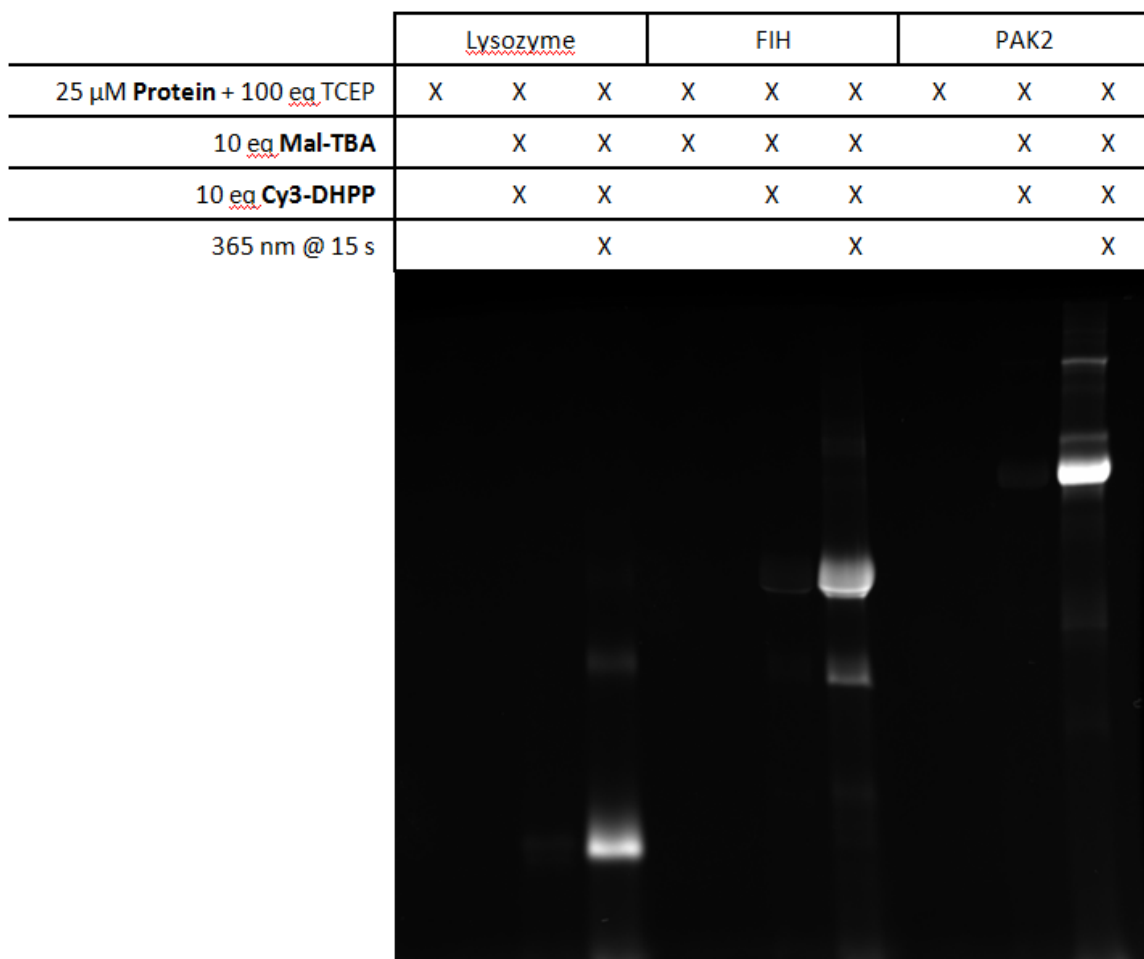


Figure 4.8: Labeling array of proteins. Again, only lanes containing protein labeled with **41** and irradiated in the presence of **45** show significant fluorescence.

our photo-induced labeling method utilizing a photogenerated diazonium coupling to a modified phloroglucinol moiety showed remarkable selectivity considering how reactive diazonium ions can be. However, proteins only represent a single biomacromolecule, and the labeling technique needed to be demonstrated in a more complex environment.

In order to label cells, we decided to use a scaffold previously described which involves using a fatty acid-modified probe being incorporated into a cellular membrane.^{8,9} We envisioned a fatty acid functionalization on the TBA core would allow for incorporation into the membrane of a cell, and irradiation would yield membrane-bound diazonium reactive sites where a DHPP-functionalized reporter could stick to. The reporter we decided to use was biotin-based, and avidin-bound FITC could be used to visualize membrane labeling (**Figure 4.9**).

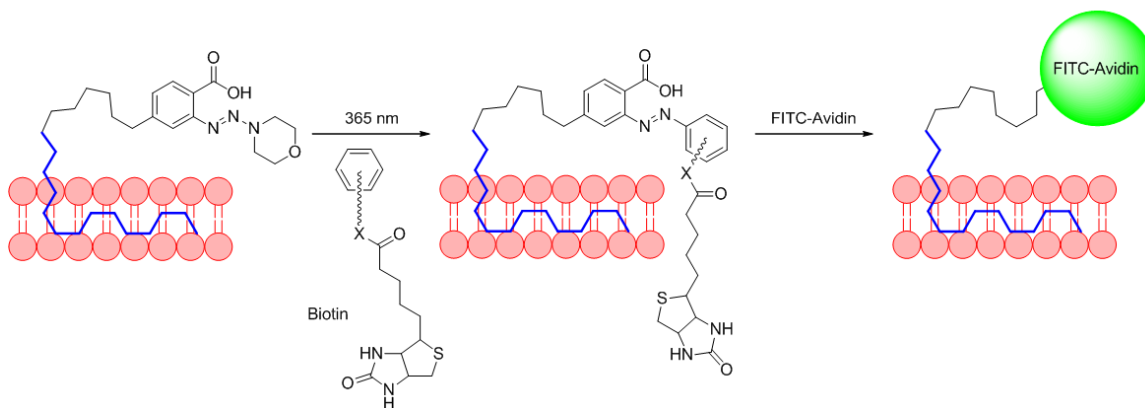


Figure 4.9: Proposed experiment for labeling cellular membranes. A fatty acid-labeled triazenybenzoic acid would incorporate into the membrane, and, upon irradiation, would attach to a biotin analog that had been functionalized with an electron-rich aromatic ring. With a biotin moiety attached to the membrane, visualization could be done with FITC-avidin.

Cy3-DHPP could theoretically be used, however because the Cy3 core is inherently very non-polar, diffusion into the cell would be problematic in generating too much background signal by accumulating in the cytosol.^{10,11}

A fatty acid TBA was synthesized by first functionalizing oleic acid with an alkyne using an amide coupling and propargylamine in 97% yield. Using a similar CuAAC procedure that was used for the maleimide TBA synthesis, the alkyne-functionalized oleic acid was coupled to benzyl azide TBA to give an oleic acid modified TBA core in 74% yield (**Figure 4.2**). Two derivatives of biotin were synthesized, one containing a phenylpiperazine with a meta dimethylamino group

(Biotin-dimethylaminophenyl piperazine - Biotin-DMAPP), and another phenylpiperazine with two meta hydroxyl groups (Biotin-DHPP) (**Figure 4.10**). The DMAPP derivative was synthesized

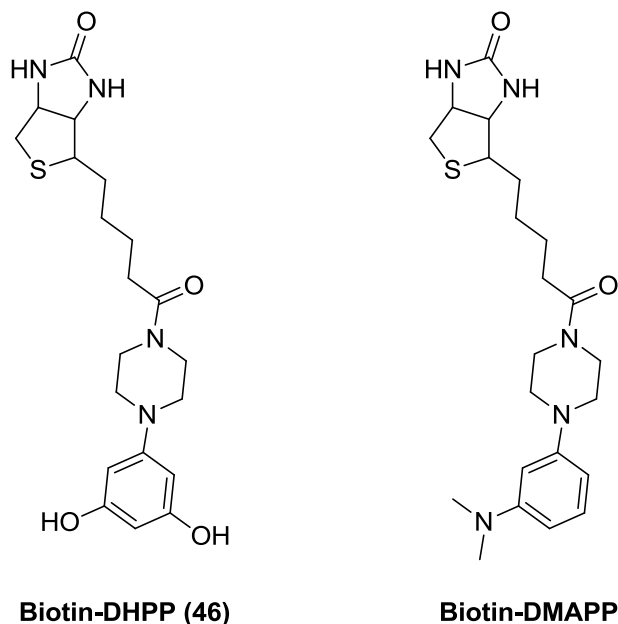


Figure 4.10: Two biotin analogs functionalized with different electron-rich aromatic rings. Biotin-DHPP was synthesized in a moderate yield, but biotin-DMAPP was only synthesized once in only enough quantity to utilize for cell work, and could not be synthesized again.

from the tin(II) chloride promoted reduction of *N,N*-dimethylamino-3-nitroaniline, followed by piperazine ring formation by refluxing with bis(2-chloroethyl)amine hydrochloride in butanol to presumably give *N,N*-dimethyl-3-(piperazin-1-yl)aniline (DMAPP). Due to the high polarity and basicity of the intermediates, no purification was possible. The crude DMAPP was coupled to biotin using EDC-promoted amide coupling, but the yield was not sufficient for characterization other than HPLC-MS. Repeated attempts at synthesis all resulted in failure, and the potential use of DMAPP as a coupling partner for diazonium was largely ignored for the remainder of the project, aside from preliminary cellular membrane labeling.

Chinese hamster ovarian cancer cells (CHO cells) were incubated with the oleic acid modified TBA and irradiated for 10 seconds in the presence of the biotin-DMAPP reporter. After

removal of excess biotin-DMAPP, the cells were treated with FITC-labeled avidin to visualize where the biotin was located. As designed, the technique afforded fluorescence in the form of halos around the cells, which is what is expected when cellular membranes are labeled (**Figure 4.11**).¹² No fluorescence was observed when the sample did not include even one of the

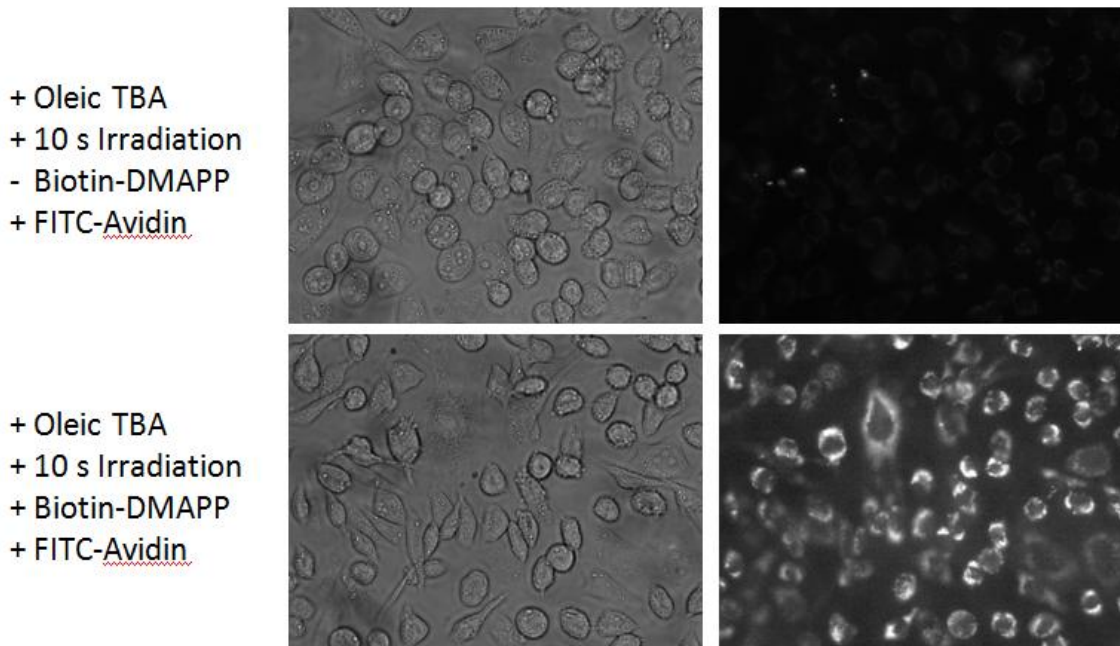


Figure 4.11: Labeling of CHO cells. Cells were incubated with a fatty acid-modified triazenyl benzoic acid and irradiated in the presence of Biotin-DMAPP in order to label the membrane with biotin. Imaging was then done after treatment with FITC-avidin.

following; oleic-TBA, Biotin-DMAPP, or irradiation. Even more promising was that this method proved capable of labeling cells with a photo-induced click reaction with only 10 seconds of irradiation, as opposed to previous methods using nitrile-imines requiring up to 2 minutes of irradiation.² With a method in place, and the irreproducible synthesis of the biotin-DMAPP reporter, we set out to use our more established reporter tag, DHPP. Biotin-DHPP was synthesized from using an EDC-promoted amide coupling with deprotected Boc-DHPP, similar to how Cy3-DHPP was synthesized, in a 42% yield. Having a much more reliable syntheses towards a biotinylated reaction partner was initially promising, however no success was achieved when

cellular membranes were again targeted for labeling. The same procedures used when biotin-DMAPP was utilized failed to show any significant labeling using both CHO and HeLa cell lines. It should be noted that even though membrane labeling was achieved with biotin-DMAPP, several attempts were required and only the best image is shown. There are many unknowns within the cell work thus far. It is not clear whether or not the oleic acid is appropriately incorporating into the membrane, if at all. It is also unknown how efficient the photolysis is if the probe in these conditions, or if the diazonium is reacting with some unknown reagent. If the diazonium is being formed, it could be that the coupling partner cannot efficiently access the diazonium for a reaction.

C. Future Directions

As it currently stands, development of this new photogenerated diazonium click reaction is very much in the beginning stages. We can use development of the nitrile imine-alkene photo-click technique as a guideline to gauge our progress. Initially, the photo-click reaction was described and characterized in the flask¹³, similar to what was put forth in the third chapter of this work. Second, the reaction was incorporated within a protein environment followed by a cellular environment^{14,15}, both showing success. Third, realizing the reaction may not yet be fully optimized, the kinetics were gradually improved by modifications to the tetrazole core¹⁶ and the alkene.² The nitrile imine-alkene photo-click reaction is currently at a stage where an incredibly fast reaction has been demonstrated with spiro-based cyclopropenes, but has not been demonstrated *in vivo*.³ The work described herein is about halfway through the second stage, having shown ability to label proteins, but only marginally able to label cells. Future work would be based around proving cellular viability and improving reaction kinetics even further.

1. Bioorthogonal Development

As demonstrated by the bioorthogonal cyclooctyne, tetrazine-TCO, and nitrile imine-alkene reactions done on cells, at least one of the reaction partners must be pre-incorporated into the system using genetic or metabolic modification. Metabolic inclusion of azides¹⁷ as targets for cyclooctyne is relatively simple due to the stability of organic azides, however the targets or reactive probes of tetrazine-TCO or nitrile imine-alkene reactions required the incorporation of unnatural amino acids using genetic modification. For tetrazine-TCO reactions, the a tetrazine amino acid was introduced¹⁸; for the nitrile imine-alkene reactions, *O*-allyl tyrosine¹⁵ or a cyclopropene-modified lysine² was introduced. Azo compounds have been demonstrated as capable unnatural amino acids¹⁹, so it is within reason to think that triazene

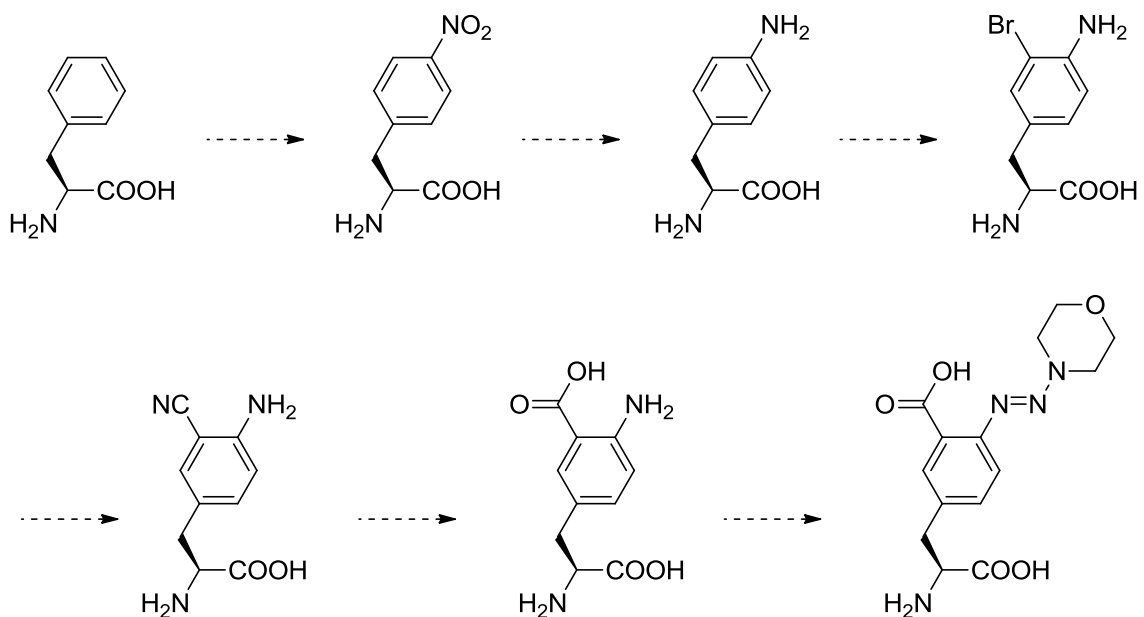


Figure 4.12: Proposed synthetic pathway to a triazenylbenzoic acid unnatural amino acid.

functionalities can be as well, given the analogous structure. A proposed synthetic scheme to an unnatural triazenylbenzoic as begins with the nitration of phenylalanine, followed by reduction

to afford *p*-aminophenylalanine. Alpha bromination followed by cyanide substitution and hydrolysis would afford an anthranilic acid functionalized unnatural amino acid. Simple conversion to the triazene using methods established throughout this work should yield a triazenylbenzoic acid unnatural amino acid (**Figure 4.12**). It may be worth considering a phloroglucinol unnatural amino acid, however given the tendency for phloroglucinol to undergo amine substitutions, having a free amine only 4 or 5 carbons away may prove problematic. Also, a self-condensation between the acid and a hydroxyl on the phloroglucinol core may be of issue. With a genetically introduced triazenylbenzoic acid rather than a fatty acid-membrane incorporation, we can be sure that the probe is in place and verify the capability of photochemistry on the genetically modified protein of choice.

2. Improving Kinetics

Although the kinetics appear to be rather quickly, requiring no incubation time for protein labeling, future experiments where small amounts of probe are necessary may require even faster kinetics to observe desirable labeling. To do so, modifications to the TBA core, TBA terminal nitrogenous species, and reactive partner should be considered since only a few variations have been evaluated. Looking at the reaction step-by-step, the first step is photolysis to yield the diazonium. Both probes that were evaluated (1 and 37) have very low absorbance values at the irradiation wavelength, although moderate quantum yields. The λ_{max} for around 280 nm for 1 and 305 nm for 37. At first glance, the lower electronic density on the terminal nitrogenous species, the lower the absorption λ_{max} appears to be. With only two data points, it is difficult to say what varying the functionality on the terminal triazene nitrogen would do, but it follows that a more electron-dense species may have an even more red-shifted absorbance. If so, a higher absorption at 365 nm could be expected, possibly speeding the photochemical

reaction and requiring less irradiation time. A triazene made with N,O-dimethylhydroxylamine in place of morpholine may be worth investigating.

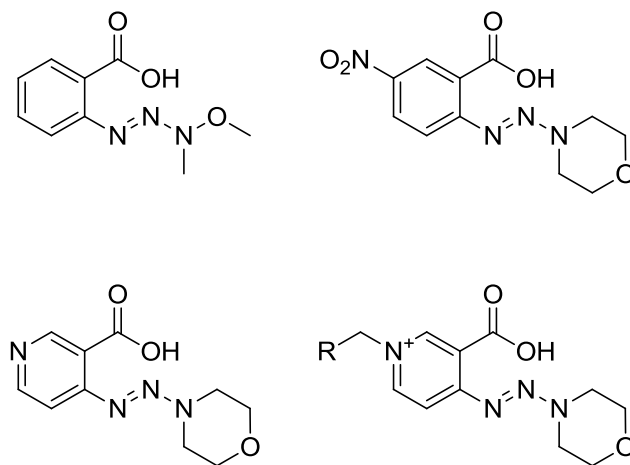


Figure 4.13: Variations of the triazenyloxybenzoic acid core that could improve rates of photolysis and/or rates of electron-rich aromatic ring addition.

The next step in the reaction is addition of a reaction to the diazonium. It has been shown that electron withdrawing groups on aryl diazoniums can dramatically increase the kinetics of azobenzene formation by increasing the electrophilicity of the terminal azo nitrogen. Addition of a nitro group *para* to the triazenyloxy group would afford a *para*-nitro diazonium upon photolysis that should have much faster kinetics than what we observed in the previous chapter. Looking away from benzene as the core ring, more electron deficient rings could also be considered, such as a pyridine or other nitrogen-containing heterocycles. An added bonus to a pyridine derivative is potentially easy functionalization by alkylation of the aromatic nitrogen, which would further decrease the electron density for faster kinetics.

D. Experimentals

1. General

Reagents and solvents for organic synthesis were used as received. Thin-layer chromatography (TLC) was conducted on glass-backed silica plates visualized with either UV illumination, basic permanganate stain, or bromocresol green stain. Flash chromatography was conducted on 60 Å silica gel. NMR spectra were recorded on a Bruker Advance 400, chemical shift values are reported in ppm on the δ scale relative to TMS ($\delta = 0.00$) as an internal standard. Irradiation for photolysis was performed using an LED Engin LZ1-10U600 365 nm LED powered by a DC 12 V, 2 A source through a 700 mA FlexBlock Constant Current Driver. LC Separation was performed with a Waters 1525 system. The gradient employed was A = water + 0.1% formic acid, B = acetonitrile + 0.1% formic acid, 5–95% B over 60 min with a Waters XBridge C18 5u column (4.6 \times 150 mm). Mass spectra were acquired with a Waters Micromass ZQ mass detector in EI+ mode: Capillary voltage = 3.50 kV, cone voltage = 30 V, extractor = 3 V, RF lens = 0.0 V, source T = 100 °C, desolvation T = 200 °C, desolvation gas = 300 L h⁻¹, desolvation gas = 0.0 L h⁻¹ The system was operated by and spectra were processed using the Waters Empower software suite.

2. Synthetic Procedures

a. (E)-methyl 4-(hydroxymethyl)-2-(morpholinodiazenyl)benzoate (39)

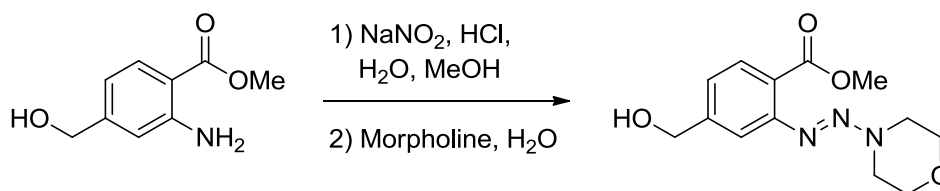


Figure 4.14: Synthesis of **39**.

A solution of methyl 2-amino-4-(hydroxymethyl)benzoate **26** (3.30 g, 18.21 mmol, 1.0 eq) in 20 mL of MeOH was acidified with 20 mL of 6M HCl and cooled to 0 °C. A solution of NaNO₂ (1.51 g, 21.85 mmol, 1.20 eq) in 8 mL H₂O was added dropwise, and the reaction was allowed to stir another 30 min. The diazotized solution was then added dropwise to a 100 mL solution of 16g NaHCO₃ and morpholine (4.78 mL, 54.63 mmol, 3.00 eq) in H₂O at 0 °C and allowed to stir for 1.5 h. The reaction mixture was extracted with EtOAc (3 × 100 mL), the combined organic layers washed with H₂O (3 × 100 mL) and 100 mL brine, and dried over Na₂SO₄ and concentrated under reduced pressure to afford a crude orange oil which was purified over silica (95:5 DCM/MeOH) to yield (E)-methyl 4-(hydroxymethyl)-2-(morpholinodiazenyl)benzoate (4.62 g, 16.54 mmol, 91%) as an orange oil.

¹H NMR (400MHz, CDCl₃) δ = 7.65 (d, *J* = 8.1 Hz, 1 H), 7.33 (s, 1 H), 7.19 - 7.13 (m, 1 H), 4.66 (s, 2 H), 3.86 - 3.77 (m, 11 H), 2.80 (br. s., 1 H)

¹³C NMR (101MHz, CDCl₃) δ = 168.2, 149.6, 145.5, 130.1, 124.9, 123.7, 117.2, 66.3, 64.4, 52.1

b. (E)-4-(azidomethyl)-2-(morpholinodiazenyl)benzoic acid (40)

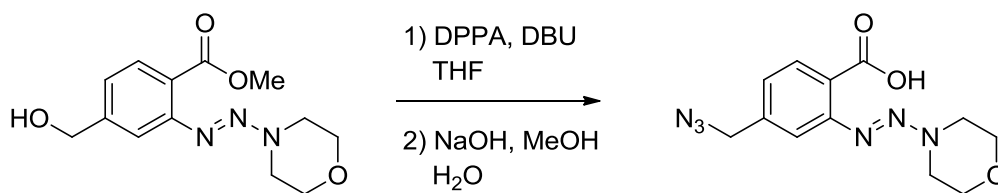


Figure 4.15: Synthesis of **40**.

To a solution of methyl (E)-methyl 4-(hydroxymethyl)-2-(morpholinodiazenyl)benzoate **39** (4.50 g, 16.11 mmol, 1.0 eq) in 80 mL of THF was added diphenylphosphoryl azide (4.51 mL, 20.95 mmol, 1.30 eq) and 1,8-Diazabicyclo[5.4.0]undec-7-ene (3.13 mL, 20.95 mmol, 1.30 eq), and the reaction was allowed to stir for 36 h at 50 °C. The reaction mixture was diluted with 100

mL EtOAc, washed with 1M HCl (1 × 50 mL), H₂O (2 × 100 mL) and 100 mL of brine). The organic layer was dried over Na₂SO₄ and concentrated under reduced pressure to yield a crude orange oil. The crude material was dissolved in 40 mL MeOH and 10 mL of 5M NaOH was added while stirring at 50 °C. After complete consumption of ester was observed by HPLC-MS, the reaction was cooled to 0 °C and carefully acidified with 6M HCl to pH 4-5. The precipitate was filtered, washed with water, and allowed to dry open to air overnight to yield (E)-4-(azidomethyl)-2-(morpholinodiazenyl)benzoic acid (3.46 g, 11.92 mmol, 74%) as white solid.

¹H NMR (400MHz, DMSO) δ = 13.09 (br. s., 1 H), 7.78 (d, *J* = 8.1 Hz, 1 H), 7.47 (s, 1 H), 7.31 - 7.24 (m, 1 H), 4.55 (s, 2 H), 3.86 - 3.77 (m, 8 H)

¹³C NMR (101MHz, DMSO) δ = 168.2, 148.8, 140.5, 130.9, 125.9, 125.6, 117.8, 53.5

c. (E)-4-((4-((2-(2,5-dioxo-2,5-dihydro-1H-pyrrol-1-yl)acetamido)methyl)-1H-1,2,3-triazol-1-yl)methyl)-2-(morpholinodiazenyl)benzoic acid (41)

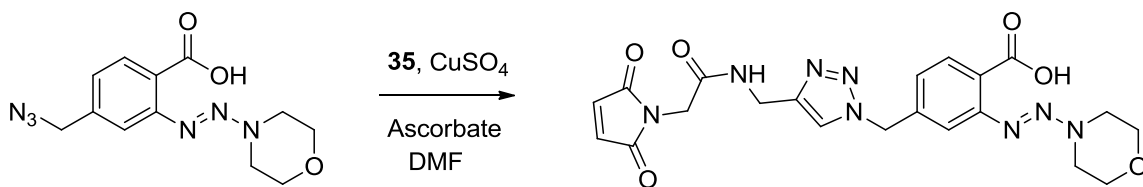


Figure 4.16: Synthesis of **41**.

To a solution of methyl (E)-4-(azidomethyl)-2-(morpholinodiazenyl)benzoic acid **41** (349 mg, 1.20 mmol, 1.0 eq) and 2-(2,5-dioxo-2,5-dihydro-1H-pyrrol-1-yl)-N-(prop-2-yn-1-yl)acetamide **35** (231 mg, 1.20 mmol, 1.0 eq) in 15 mL of DMF was added copper(II) sulfate pentahydrate (30 mg, 0.12 mmol, 0.1 eq) and sodium *L*-ascorbate (48 mg, 0.24 mmol, 0.2 eq). After stirring for 24 h, the reaction mixture was diluted with 50 mL EtOAc, washed with H₂O (5 × 50 mL), then with saturated NaHCO₃ (2 × 50 mL). The basic aqueous layers were combined and

carefully acidified with 6M HCl to pH 4-5. The precipitate was filtered, washed with water, and allowed to dry open to air overnight to yield (E)-4-((4-((2-(2,5-dioxo-2,5-dihydro-1H-pyrrol-1-yl)acetamido)methyl)-1H-1,2,3-triazol-1-yl)methyl)-2-(morpholinodiazenyl)-benzoic acid (283 mg, 0.59 mmol, 49%) as a brown solid.

^1H NMR (400MHz, DMSO) δ = 13.06 (br. s., 1 H), 8.68 (br. s., 1 H), 8.01 (s, 1 H), 7.74 (d, J = 8.1 Hz, 1 H), 7.43 (s, 1 H), 7.19 (d, J = 7.8 Hz, 1 H), 7.09 (s, 2 H), 5.65 (s, 2 H), 4.32 (d, J = 5.1 Hz, 2 H), 4.05 (s, 2 H), 3.80 (br. s., 8 H)

^{13}C NMR (101MHz, DMSO) δ = 171.1, 168.2, 166.6, 148.8, 145.2, 140.6, 135.3, 130.9, 125.8, 125.6, 123.7, 117.9, 52.8, 40.1, 34.8

d. (Z)-N-(prop-2-yn-1-yl)heptadec-9-enamide (42)

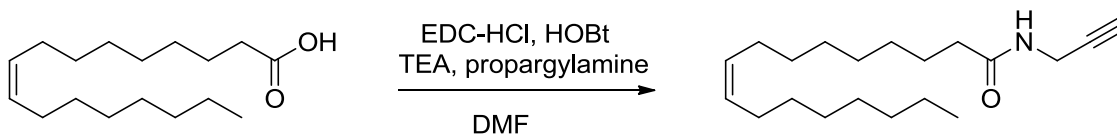


Figure 4.17: Synthesis of 42.

To a solution of oleic acid (2.08 g, 7.36 mmol, 1.0 eq) in 50 mL DMF was added *N*-(3-dimethylaminopropyl)-*N'*-ethylcarbodiimide hydrochloride (2.12 g, 11.05 mmol, 1.50 eq), 1-Hydroxybenzotriazole hydrate (1.69 g, 11.05 mmol, 1.50 eq), and triethylamine (1.37 mL, 9.80 mmol, 1.33 eq), and the reaction was stirred for 30 m. To the stirred solution of activated ester was added propargylamine (0.71 mL, 11.05 mmol, 1.50 eq) and the reaction was allowed to stir for an additional 24 h. The reaction was diluted with 100 mL EtOAc, washed with H₂O (5 × 50 mL), then with saturated NaHCO₃ (2 × 50 mL), and 1M HCl (2 × 50 mL). The organic layer was

dried over Na₂SO₄ and concentrated under reduced pressure to yield (Z)-N-(prop-2-yn-1-yl)heptadec-9-enamide (283 mg, 0.59 mmol, 49%) as a white solid.

¹H NMR (400MHz, CDCl₃) δ = 5.95 (br. s., 1 H), 5.41 - 5.28 (m, 2 H), 4.05 (dd, *J* = 2.6, 5.3 Hz, 2 H), 2.25 - 2.16 (m, 3 H), 2.07 - 1.95 (m, 4 H), 1.69 - 1.59 (m, 2 H), 1.27 (s, 10 H), 1.30 (s, 11 H), 0.92 - 0.83 (m, 3 H)

¹³C NMR (101MHz, CDCl₃) δ = 172.9, 130.0, 129.7, 79.7, 71.4, 36.4, 31.9, 29.8, 29.7, 29.5, 29.3, 29.3, 29.1, 29.1, 27.2, 27.2, 25.6, 22.7, 14.1

e. 4-((4-((Z)-heptadec-9-enamidomethyl)-1H-1,2,3-triazol-1-yl)methyl)-2-((E)-morpholinodiazenyl)benzoic acid (43)

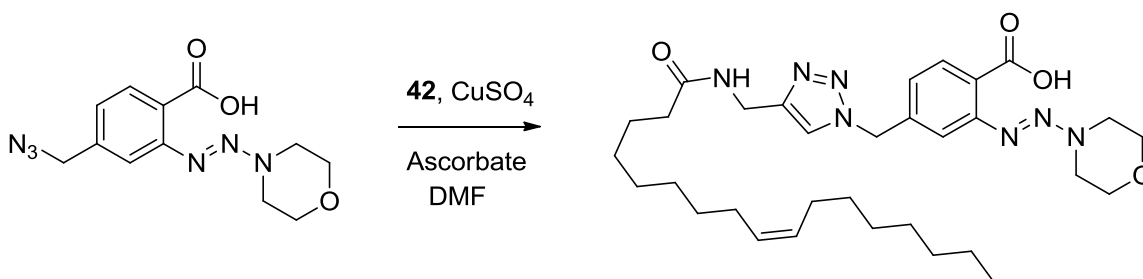


Figure 4.18: Synthesis of **43**.

To a solution of methyl (E)-4-(azidomethyl)-2-(morpholinodiazenyl)benzoic acid **41** (500 mg, 1.72 mmol, 1.0 eq) and (Z)-N-(prop-2-yn-1-yl)heptadec-9-enamide **42** (525 mg, 1.72 mmol, 1.0 eq) in 20 mL of DMF was added copper(II) sulfate pentahydrate (43 mg, 0.17 mmol, 0.1 eq) and sodium *L*-ascorbate (68 mg, 0.34 mmol, 0.2 eq). After stirring for 24 h, the reaction mixture was diluted with 50 mL EtOAc, washed with H₂O (5 × 50 mL), then with saturated NaHCO₃ (2 × 50 mL). The basic aqueous layers were combined and carefully acidified with 6M HCl to pH 4-5. The precipitate was filtered, washed with water, and allowed to dry open to air overnight to

yield 4-((4-((Z)-heptadec-9-enamidomethyl)-1H-1,2,3-triazol-1-yl)methyl)-2-((E)-morpholinodiazenyl)benzoic acid (758 mg, 1.27 mmol, 74%) as an off-white solid.

^1H NMR (400MHz, CDCl_3) δ = 8.20 (d, J = 8.1 Hz, 1 H), 7.62 (d, J = 1.2 Hz, 1 H), 7.59 (s, 1 H), 7.16 (dd, J = 1.5, 8.1 Hz, 1 H), 6.65 (s, 1 H), 5.52 (s, 2 H), 5.40 - 5.28 (m, 2 H), 4.47 (d, J = 5.9 Hz, 2 H), 3.99 (br. s., 4 H), 3.91 (br. s., 2 H), 3.88 - 3.82 (m, 2 H), 3.71 (q, J = 6.9 Hz, 3 H), 2.21 - 2.14 (m, 2 H), 2.03 - 1.96 (m, 4 H), 1.64 - 1.55 (m, 2 H), 1.36 - 1.20 (m, 26 H), 0.91 - 0.84 (m, 3 H)

^{13}C NMR (101MHz, CDCl_3) δ = 173.5, 166.5, 148.4, 145.6, 140.3, 133.5, 130.0, 129.7, 125.9, 122.6, 122.2, 115.7, 77.3, 58.2, 53.6, 36.4, 34.8, 31.9, 29.7, 29.7, 29.5, 29.3, 29.2, 29.1, 27.2, 27.2, 25.6, 22.7, 18.4, 14.1

f. tert-butyl 4-(3,5-dihydroxyphenyl)piperazine-1-carboxylate (44)

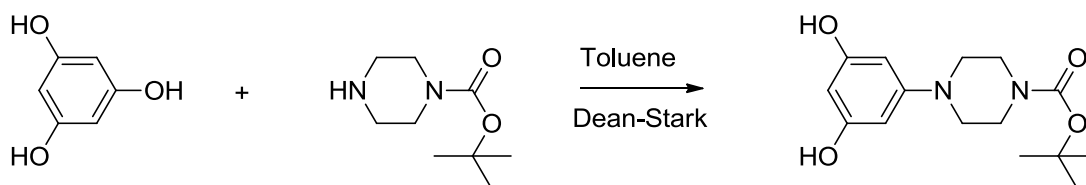


Figure 4.19: Synthesis of **44**.

To a mechanically stirred solution of 1-boc-piperazine (6.0 g, 32.2 mmol, 1.0 eq) in 100 mL of toluene was added phloroglucinol (4.06 g, 32.2 mmol, 1.0 eq). The suspension was refluxed for 4 h using a Dean-Stark apparatus to facilitate removal of water. The reaction mixture was cooled, and then concentrated under reduced pressure to yield a dark red foam. Addition of 100 mL DCM initially dissolved the crude material, but a precipitate formed within a few seconds or upon sonicated in a cool water bath. The precipitate was filtered and washed with DCM to afford a red powder. The red powder was decolorized by dissolving it in 250 mL of a 1:1 DCM/diethyl ether system and swirling in 15 g of activated charcoal for 5 min, and filtering.

Concentration of the decolorized solution under reduced pressure yielded tert-butyl 4-(3,5-dihydroxyphenyl)piperazine-1-carboxylate (4.45 g, 15.1 mmol, 47%) as a pale pink solid.

^1H NMR (400MHz, DMSO) δ = 8.97 (s, 2 H), 5.80 (d, J = 1.7 Hz, 2 H), 5.77 - 5.71 (m, 1 H), 3.41 (dd, J = 4.4, 9.8 Hz, 4 H), 3.02 - 2.94 (m, 4 H), 1.42 (s, 9 H)

^{13}C NMR (101MHz, DMSO) δ = 159.2, 154.3, 153.3, 95.1, 79.4, 48.8, 28.5

g. 2-((1E,3E)-3-(1-(6-(4-(3,5-dihydroxyphenyl)piperazin-1-yl)-6-oxohexyl)-3,3-dimethylindolin-2-ylidene)prop-1-en-1-yl)-1,3,3-trimethyl-3H-indol-1-ium chloride (45)

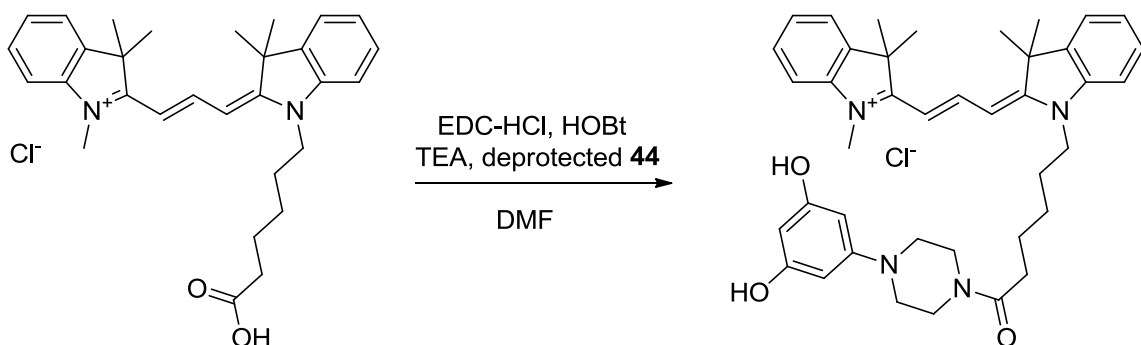


Figure 4.20: Synthesis of 45.

To a solution of 2-((1E,3E)-3-(1-(5-carboxypentyl)-3,3-dimethylindolin-2-ylidene)prop-1-en-1-yl)-1,3,3-trimethyl-3H-indol-1-ium chloride²⁰ (492 mg, 1.00 mmol, 1.0 eq) in 10 mL DMF was added *N*-(3-dimethylaminopropyl)-*N'*-ethylcarbodiimide hydrochloride (288 mg, 1.50 mmol, 1.50 eq), 1-Hydroxybenzotriazole hydrate (230 mg, 1.50 mmol, 1.50 eq), and triethylamine (209 μL , 1.33 mmol, 1.33 eq), and the reaction was stirred for 30 m. To the stirred solution of activated ester was added the trifluoroacetic acid-deprotected 44 (617 mg, 2.00 mmol, 2.00 eq) in 5 mL DMF and the reaction was allowed to stir for an additional 24 h. The reaction was diluted with 50 mL DCM, washed with H_2O (5 \times 50 mL), then with saturated NaHCO_3 (2 \times 50 mL) and 50 mL brine. The organic layer was dried over Na_2SO_4 and concentrated under reduced

pressure to afford a crude pink residue which was dry loaded and purified over silica (9:1 DCM/MeOH) to yield 2-((1E,3E)-3-(1-(6-(4-(3,5-dihydroxyphenyl)piperazin-1-yl)-6-oxohexyl)-3,3-dimethylindolin-2-ylidene)prop-1-en-1-yl)-1,3,3-trimethyl-3H-indol-1-ium chloride (428 mg, 0.59 mmol, 64%) as a pink/metallic green solid.

h. 4-(5-(4-(3,5-dihydroxyphenyl)piperazin-1-yl)-5-oxopentyl)tetrahydro-1H-thieno[3,4-d]imidazol-2(3H)-one (46)

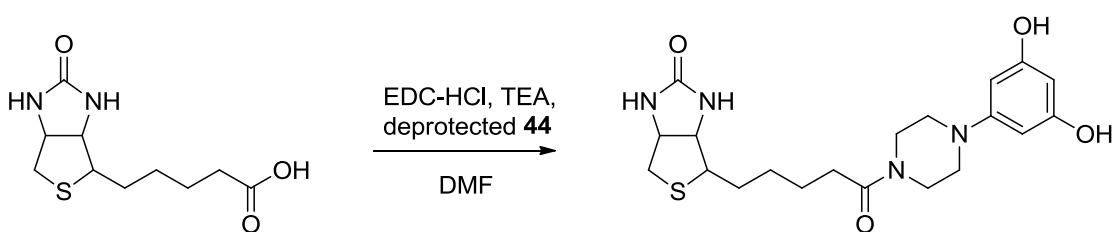


Figure 4.21: Synthesis of 46.

To a solution of *D*-biotin (244 mg, 1.00 mmol, 1.0 eq) in 10 mL DMF was added *N*-(3-dimethylaminopropyl)-*N'*-ethylcarbodiimide hydrochloride (288 mg, 1.50 mmol, 1.50 eq), triethylamine (181 μ L, 1.30 mmol, 1.30 eq), and the reaction was stirred for 30 m. To the stirred solution of activated ester was added the anhydrous HCl-deprotected 44 (254 mg, 1.10 mmol, 1.10 eq) and additional triethylamine (153 μ L, 1.10 mmol, 1.10 eq) in 10 mL DMF and the reaction was allowed to stir for an additional 24 h. The reaction was concentrated under reduced pressure to afford a crude residue which was dry loaded and purified over silica (85:15 Acetone/MeOH - Note, will probably clog fritted columns) to yield 4-(5-(4-(3,5-dihydroxyphenyl)piperazin-1-yl)-5-oxopentyl)tetrahydro-1H-thieno[3,4-d]imidazol-2(3H)-one (180 mg, 0.43 mmol, 43%) as an off-white solid.

^1H NMR (400MHz, DMSO) δ = 9.10 (s, 2 H), 6.47 (s, 1 H), 6.40 (s, 1 H), 5.86 - 5.76 (m, 3 H), 4.35 - 4.22 (m, 1 H), 4.22 - 4.10 (m, 1 H), 3.54 (br. s., 4 H), 3.40 (s, 2 H), 3.14 - 3.07 (m, 1 H), 3.01 (br. s.,

2 H), 2.96 (br. s., 2 H), 2.82 (dd, $J = 5.0, 12.3$ Hz, 1 H), 2.59 (d, $J = 12.5$ Hz, 1 H), 2.33 (t, $J = 7.3$ Hz, 2 H), 1.70 - 1.58 (m, 1 H), 1.57 - 1.45 (m, 3 H), 1.36 (br. s., 2 H)

^{13}C NMR (101MHz, DMSO) $\delta = 171.1, 163.3, 159.3, 153.1, 95.2, 95.0, 61.5, 59.7, 55.9, 49.3, 48.8, 45.2, 41.3, 32.6, 31.2, 30.1, 28.8, 28.6, 25.3$

3. Protein Labeling

Protein labeling reactions were done at volumes of 30 μL . 1X PBS buffer solution at pH 7.4, tris(2-carboxyethyl)phosphine (TCEP) at 2.5 mM, and protein were reacted at ambient temperature for 20 min. After reduction, the TCEP was removed using Amicon Ultra-0.5 mL 3K centrifugal filter devices. Reduced protein solutions were diluted to 500 μL and spun at 14,000 $\times g$ for 30 min on an Eppendorf 5148 centrifuge. This process was repeated once more, followed by recovery of concentrated protein by spinning at 2000 $\times g$ for 3 min to give roughly 50 μL of reduced protein, which was diluted up to 60 μL . 10 equivalents of **41** were incubated with reduced protein for 2 h at ambient temperature, and split into 30 μL reactions. 10 equivalents of **45** were added to the reaction, and the samples were irradiated for 15 s. Labeled protein samples were diluted to 35 μL with gel-loading buffer, treated with 1 μL of 1M DTT, and separation was performed on 12% SDS-PAGE with 5% stacking gel ran at 120 V, 50 mA, 90 min. In-gel fluorescence was visualized using a BioRad imager using a Rhodamine blot method. Total protein was stained using Coomassie stain.

4. Cell Labeling

CHO (or HeLa) cells were incubated with 1 μM **43** for 15 minutes in their home media and washed via perfusion. Cells were then irradiated for 10 s with incubated with Biotin-DMAPP or

44. Cells were then washed for 2 minutes, incubated with 1:100 avidin-FITC washed for another 2 minutes, and imaged using an appropriate FITC filter.

E. References

1. Kolb, H. C., Finn, M. G. & Sharpless, K. B. Click Chemistry: Diverse Chemical Function from a Few Good Reactions. *Angew. Chemie - Int. Ed.* **40**, 2004–2021 (2001).
2. Yu, Z., Pan, Y., Wang, Z., Wang, J. & Lin, Q. Genetically encoded cyclopropene directs rapid, photoclick-chemistry-mediated protein labeling in mammalian cells. *Angew. Chemie - Int. Ed.* **51**, 10600–4 (2012).
3. Yu, Z. & Lin, Q. Design of spiro[2.3]hex-1-ene, a genetically encodable double-strained alkene for superfast photoclick chemistry. *J. Am. Chem. Soc.* **136**, 4153–4156 (2014).
4. Sletten, E. M. & Bertozzi, C. R. From Mechanism to Mouse: A Tale of Two Bioorthogonal Reactions. *Acc. Chem. Res.* **44**, 666–676 (2011).
5. Gissot, A., Wagner, A. & Mioskowski, C. Buffer-induced, selective mono-C-alkylation of phloroglucinol: application to the synthesis of an advanced intermediate of catechin. *Tetrahedron* **60**, 6807–6812 (2004).
6. Khosla, C., Tang, Y., Chen, A. Y., Schnarr, N. a & Cane, D. E. Structure and mechanism of the 6-deoxyerythronolide B synthase. *Annu. Rev. Biochem.* **76**, 195–221 (2007).
7. Fong, G.-H. & Takeda, K. Role and regulation of prolyl hydroxylase domain proteins. *Cell Death Differ.* **15**, 635–641 (2008).
8. Sklar, L. a, Hudson, B. S. & Simoni, R. D. Conjugated polyene fatty acids as fluorescent probes: binding to bovine serum albumin. *Biochemistry* **16**, 5100–5108 (1977).

9. Wilton, D. C. The fatty acid analogue 11-(dansylamino)undecanoic acid is a fluorescent probe for the bilirubin-binding sites of albumin and not for the high-affinity fatty acid-binding sites. *Biochem. J.* **270**, 163–6 (1990).
10. Baumgart, T., Hunt, G., Farkas, E. R., Webb, W. W. & Feigenson, G. W. Fluorescence probe partitioning between Lo/Ld phases in lipid membranes. *Biochim. Biophys. Acta - Biomembr.* **1768**, 2182–2194 (2007).
11. Cunningham, C. W. *et al.* Uptake, Distribution and Diffusivity of Reactive Fluorophores in Cells: Implications toward Target Identification. *Mol. Pharm.* **7**, 1301–1310 (2010).
12. Poloukhtine, A. a., Mbua, N. E., Wolfert, M. a., Boons, G. J. & Popik, V. V. Selective labeling of living cells by a photo-triggered click reaction. *J. Am. Chem. Soc.* **131**, 15769–15776 (2009).
13. Wang, Y., Rivera Vera, C. I. & Lin, Q. Convenient synthesis of highly functionalized pyrazolines via mild, photoactivated 1,3-dipolar cycloaddition. *Org. Lett.* **9**, 4155–4158 (2007).
14. Song, W., Wang, Y., Qu, J., Madden, M. M. & Lin, Q. A Photoinducible 1,3-Dipolar Cycloaddition Reaction for Rapid, Selective Modification of Tetrazole-Containing Proteins. *Angew. Chemie Int. Ed.* **47**, 2832–2835 (2008).
15. Song, W., Wang, Y., Qu, J. & Lin, Q. Selective functionalization of a genetically encoded alkene-containing protein via ‘photoclick chemistry’ in bacterial cells. *J. Am. Chem. Soc.* **130**, 9654–9655 (2008).
16. Wang, Y., Song, W., Hu, W. J. & Lin, Q. Fast alkene functionalization in vivo by photoclick chemistry: HOMO lifting of nitrile imine dipoles. *Angew. Chemie - Int. Ed.* **48**, 5330–5333

(2009).

17. Laughlin, S. T. & Bertozzi, C. R. Metabolic labeling of glycans with azido sugars and subsequent glycan-profiling and visualization via Staudinger ligation. *Nat. Protoc.* **2**, 2930–2944 (2007).
18. Blizzard, R. J. *et al.* Ideal Bioorthogonal Reactions Using A Site-Specifically Encoded Tetrazine Amino Acid. *J. Am. Chem. Soc.* **137**, 10044–10047 (2015).
19. Bose, M., Groff, D., Xie, J., Brustad, E. & Schultz, P. G. The Incorporation of a Photoisomerizable Amino Acid into Proteins in *E. coli* The Incorporation of a Photoisomerizable Amino Acid into Proteins in *E. coli*. *J. Am. Chem. Soc. Commun.* **128**, 388–389 (2006).
20. Kvach, M. V. *et al.* A convenient synthesis of cyanine dyes: Reagents for the labeling of biomolecules. *European J. Org. Chem.* 2107–2117 (2008). doi:10.1002/ejoc.200701190

BIBLIOGRAPHY

- Agard, N. J., Prescher, J. a & Bertozzi, C. R. A Strain-Promoted [3 + 2] Azide - Alkyne Cycloaddition for Covalent Modification of Biomolecules in Living Systems. *J. Am. Chem. Soc.* **126**, 15046–15047 (2004).
- Agard, N. J., Baskin, J. M., Prescher, J. A., Lo, A. & Bertozzi, C. R. A Comparative Study of Bioorthogonal Reactions with Azides. *ACS Chem. Biol.* **1**, 644–648 (2006).
- Albar, H. A., Shawali, A. S. & Abdaliah, M. A. Substituent effects on azo coupling of indoles. *Can. J. Chem.* **71**, 2144–2149 (1993).
- Amoroso, J. W., Borketey, L. S., Prasad, G. & Schnarr, N. A. Direct Acylation of Carrier Proteins with Functionalized β -Lactones. *Org. Lett.* **12**, 2330–2333 (2010).
- Arumugam, S. & Popik, V. V. Light-Induced Hetero-Diels À Alder Cycloaddition : A Facile and Selective Photoclick Reaction. *J. Am. Chem. Soc.* 5573–5579 (2011).
- Brown, W. E., Green, A. H., Cedel, T. E. & Cairns, J. Biochemistry of Protein-Isocyanate Interactions: A comparison of the Effects of Aryl vs. Alkyl Isocyanates. *Environ. Health Perspect.* **72**, 5–11 (1987).
- Baskin, J. M. *et al.* Copper-free click chemistry for dynamic in vivo imaging. *Proc. Natl. Acad. Sci. U. S. A.* **104**, 16793–16797 (2007).
- Baumgart, T., Hunt, G., Farkas, E. R., Webb, W. W. & Feigenson, G. W. Fluorescence probe partitioning between Lo/Ld phases in lipid membranes. *Biochim. Biophys. Acta - Biomembr.* **1768**, 2182–2194 (2007).
- Beletskaya, I. P., Sigeev, A. S., Peregudov, A. S. & Petrovskii, P. V. Catalytic Sandmeyer Bromination. *Synthesis (Stuttg).* **2007**, 2534–2538 (2007).
- Bergstrom, F. W. & Horning, C. H. The Action of Bases on Organic Halogen Compounds. V. The Action of Potassium Amide on Some Aromatic Halides. *J. Org. Chem.* **11**, 334–340 (1946).
- Berry, R. S., Clardy, J. & Schafer, M. E. Benzyne. *J. Am. Chem. Soc.* **86**, 2738–2739 (1964).
- Blackman, M. L., Royzen, M. & Fox, J. M. Tetrazine ligation: fast bioconjugation based on inverse-electron-demand Diels-Alder reactivity. *J. Am. Chem. Soc.* **130**, 13518–9 (2008).
- Blizzard, R. J. *et al.* Ideal Bioorthogonal Reactions Using A Site-Specifically Encoded Tetrazine Amino Acid. *J. Am. Chem. Soc.* **137**, 10044–10047 (2015).
- Boren, B. C. *et al.* Ruthenium-catalyzed azide– alkyne cycloaddition: scope and mechanism. *J. Am. Chem. Soc.* **130**, 8923–8930 (2008).
- Bose, M., Groff, D., Xie, J., Brustad, E. & Schultz, P. G. The Incorporation of a Photoisomerizable Amino Acid into Proteins in *E. coli* The Incorporation of a Photoisomerizable Amino Acid into Proteins in *E. coli*. *J. Am. Chem. Soc. Commun.* **128**, 388–389 (2006).

- Buxton, C. P.; Heaney, H. Aryne formation from 1-(3'-Carboxyaryl)-3,3-dimethyl triazines. *Tetrahedron* **51**, 3929–3938 (1995).
- Campbell-Verduyn, L., Elsinga, P. H., Mirfeizi, L., Dierckx, R. A. & Feringa, B. L. Copper-free 'click': 1,3-dipolar cycloaddition of azides and arynes. *Org. Biomol. Chem.* **6**, 3461 (2008).
- Cunningham, C. W. *et al.* Uptake, Distribution and Diffusivity of Reactive Fluorophores in Cells: Implications toward Target Identification. *Mol. Pharm.* **7**, 1301–1310 (2010).
- Darko, A. *et al.* Conformationally strained trans-cyclooctene with improved stability and excellent reactivity in tetrazine ligation. *Chem. Sci.* **5**, 3770 (2014).
- Fong, G.-H. & Takeda, K. Role and regulation of prolyl hydroxylase domain proteins. *Cell Death Differ.* **15**, 635–641 (2008).
- Gann, A. W. *et al.* A photoinduced, benzyne click reaction. *Org. Lett.* **16**, 2003–2005 (2014).
- Gaplovsky, M. *et al.* Photochemical reaction mechanisms of 2-nitrobenzyl compounds: 2-nitrobenzyl alcohols form 2-nitroso hydrates by dual proton transfer. *Photochem. Photobiol. Sci.* **4**, 33–42 (2005).
- Gilchrist, T. L. in *Triple-Bonded Functional Groups (1983)* 383–419 (John Wiley & Sons, Ltd., 2010).
- Gilman, H. & Avakian, S. Dibenzofuran. XXIII. Rearrangement of Halogen Compounds in Amination by Sodamide. *J. Am. Chem. Soc.* **67**, 349–351 (1945).
- Gissot, A., Wagner, A. & Mioskowski, C. Buffer-induced, selective mono-C-alkylation of phloroglucinol: application to the synthesis of an advanced intermediate of catechin. *Tetrahedron* **60**, 6807–6812 (2004).
- Green, J. R. (Cycloheptyne)dicobalt Complexes in Organic Synthesis. *European J. Org. Chem.* **2008**, 6053–6062 (2008).
- Griffin, C. W., Carski, T. R. & Warner, G. S. Labeling Procedures Employing Crystalline Fluorescein Isothiocyanate. *J. Bacteriol.* 534–537 (1961).
- Himeshima, Y., Sonoda, T. & Kobayashi, H. Fluoride-induced 1,2-elimination of *o*-trimethylsilylphenyl triflate to benzyne under mild conditions. *Chem. Lett.* 1211–1214 (1983).
- Huisgen, R. 1,3-Dipolar Cycloadditions. *Proc. Chem. Soc.* 357–369 (1961).
- Jewett, J. C., Sletten, E. M. & Bertozzi, C. R. Rapid Cu-free click chemistry with readily synthesized biarylazacyclooctynones. *J. Am. Chem. Soc.* **132**, 3688–3690 (2010).
- Julliard, M., Scelles, M., Guillemonat, A., Vernin, G. & Metzger, J. The photochemical behavior of bis aryl-1,3 triazines. *Tetrahedron Lett.* 375–378 (1977).
- Karver, M., Weissleder, R. & Hilderbrand, S. A. Synthesis and Evaluation of a Series of 1,2,4,5-Tetrazines for Bioorthogonal Conjugation Conjugation Center for Systems Biology. *Bioconjug. Chem.* 2263–2270 (2011). doi:10.1021/bc200295y

- Khosla, C., Tang, Y., Chen, A. Y., Schnarr, N. a & Cane, D. E. Structure and mechanism of the 6-deoxyerythronolide B synthase. *Annu. Rev. Biochem.* **76**, 195–221 (2007).
- Klán, P. *et al.* Photoremovable protecting groups in chemistry and biology: Reaction mechanisms and efficacy. *Chem. Rev.* **113**, 119–191 (2013).
- Kolb, H. C., Finn, M. G. & Sharpless, K. B. Click Chemistry: Diverse Chemical Function from a Few Good Reactions. *Angew. Chemie - Int. Ed.* **40**, 2004–2021 (2001).
- Krasnokutskaya, E. A., Semenischeva, N. I., Filimonov, V. D. & Knochel, P. A New, One-Step, Effective Protocol for the Iodination of Aromatic and Heterocyclic Compounds via Aprotic Diazotization of Amines. *Synthesis (Stuttg.)* **2007**, 81–84 (2007).
- Ku, H. & Barrio, J. R. Convenient synthesis of aryl halides from arylamines via treatment of 1-aryl-3,3-dialkyltriazenes with trimethylsilyl halides. *J. Org. Chem.* **46**, 5239 (1981).
- Kutonova, K. V, Trusova, M. E., Postnikov, P. S., Filimonov, V. D. & Parello, J. A Simple and Effective Synthesis of Aryl Azides via Arenediazonium Tosylates. *Synthesis (Stuttg.)* **45**, 2706–2710 (2013).
- Kvach, M. V. *et al.* A convenient synthesis of cyanine dyes: Reagents for the labeling of biomolecules. *European J. Org. Chem.* 2107–2117 (2008). doi:10.1002/ejoc.200701190
- Laali, K. K. & Gettwert, V. J. Fluorodediazotiation in ionic liquid solvents: New life for the Balz-Schiemann reaction. *J. Fluor. Chem.* **107**, 31–34 (2001).
- Laughlin, S. T. & Bertozzi, C. R. Metabolic labeling of glycans with azido sugars and subsequent glycan-profiling and visualization via Staudinger ligation. *Nat. Protoc.* **2**, 2930–2944 (2007).
- Li, Z., Seo, T. S. & Ju, J. 1,3-Dipolar cycloaddition of azides with electron-deficient alkynes under mild condition in water. *Tetrahedron Lett.* **45**, 3143–3146 (2004).
- Lim, R. K. V & Lin, Q. Azirine ligation: fast and selective protein conjugation via photoinduced azirine-alkene cycloaddition. *Chem. Commun. (Camb.)* **46**, 7993–7995 (2010).
- Liu, L.-H. & Yan, M. Perfluorophenyl Azides : New Applications in. *Acc. Chem. Res.* **43**, 1434–43 (2010).
- Maki, Y., Takashi, F. & Suzuki, M. Photochemical Reactions. Part 10. Photolysis of o-Nitrobenzaldehyde N-Acylhydrazones leading to Benzyne and 5-Nitrophthalazines. *J. Chem. Soc. Perkins Trans. I* 553–557 (1979).
- Matsumoto, T., Hosoya, T., Katsuki, M. & Suzuki, K. New efficient protocol for aryne generation. Selective synthesis of differentially protected 1,4,5-naphthalenetriols. *Tetrahedron Lett.* **32**, 6735–6736 (1991).
- Mbua, N. E., Guo, J., Wolfert, M. a., Steet, R. & Boons, G. J. Strain-Promoted Alkyne-Azide Cycloadditions (SPAAC) Reveal New Features of Glycoconjugate Biosynthesis. *ChemBioChem* **12**, 1912–1921 (2011).

- McNulty, J., Keskar, K. & Vemula, R. The first well-defined silver(I)-complex-catalyzed cycloaddition of azides onto terminal alkynes at room temperature. *Chem. - A Eur. J.* **17**, 14727–14730 (2011).
- Nakanishi, K. *et al.* Photoaffinity labeling of rhodopsin and bacteriorhodopsin. *Biophys Chem* **56**, 13–22. (1995).
- Nuyken, O., Stebani, J., Lipped, T., Wokaun, A. & Stasko, A. Photolysis, thermolysis, and protolytic decomposition of a triazene polymer in solution. *Macromol. Chem. Phys.* **761**, 751–761 (1995).
- Papageorgiou, G., Ogden, D., Kelly, G. & Corrie, J. E. T. Synthetic and photochemical studies of substituted 1-acyl-7-nitroindolines. *Photochem. Photobiol. Sci.* **4**, 887–96 (2005).
- Poloukhine, A. a., Mbua, N. E., Wolfert, M. a., Boons, G. J. & Popik, V. V. Selective labeling of living cells by a photo-triggered click reaction. *J. Am. Chem. Soc.* **131**, 15769–15776 (2009).
- Prasad, G., Amoroso, J. W., Borketey, L. S. & Schnarr, N. A. N-Activated β -lactams as versatile reagents for acyl carrier protein labeling. *Org. Biomol. Chem.* **10**, 1992–2002 (2012).
- Prescher, J. A. & Bertozzi, C. R. Chemistry in living systems. *Nat. Chem. Biol.* **1**, 13–21 (2005).
- Riordan, J. F. & Vallee, B. L. Diazonium Salts as Specific Reagents and Probes of Protein Conformation. *Methods Enzymol.* 521–531 (1971).
- Roberts, J. D., Semenov, D. A., Simmons, H. E. & Carlsmith, L. A. The Mechanism of Aminations of Halobenzenes. *J. Am. Chem. Soc.* **78**, 601–611 (1956).
- Roberts, J. D., Simmons, H. E., Carlsmith, L. A. & Vaughan, C. W. Rearrangement in the Reaction of Chlorobenzene-1-C14 With Potassium Amide. *J. Am. Chem. Soc.* **75**, 3290–3291 (1953).
- Roglans, A., Pla-Quintana, A. & Moreno-Mañas, M. Diazonium salts as substrates in palladium-catalyzed cross-coupling reactions. *Chem. Rev.* **106**, 4622–43 (2006).
- Rostovtsev, V. V., Green, L. G., Fokin, V. V. & Sharpless, K. B. A stepwise Huisgen cycloaddition process: Copper(I)-catalyzed regioselective 'ligation' of azides and terminal alkynes. *Angew. Chemie - Int. Ed.* **41**, 2596–2599 (2002).
- Sandmeyer, T. Ueber die Ersetzung der Amid-gruppe durch Chlor, Brom und Cyan in den aromatischen Substanzen. *Berichte der Dtsch. Chem. Gesellschaft* **17**, 2650–2653 (1884).
- Schnapp, K. A. & Platz, M. S. A laser flash photolysis study of di-, tri- and tetrafluorinated phenylnitrenes; implications for photoaffinity labeling. *Bioconjug. Chem.* **4**, 178–83 (1993).
- Shi, F., Waldo, J. P., Chen, Y. & Larock, R. C. Benzyne click chemistry: synthesis of benzotriazoles from benzyne and azides. *Org. Lett.* **10**, 2409–2412 (2008).
- Sklar, L. a, Hudson, B. S. & Simoni, R. D. Conjugated polyene fatty acids as fluorescent probes: binding to bovine serum albumin. *Biochemistry* **16**, 5100–5108 (1977).
- Sletten, E. M. & Bertozzi, C. R. From Mechanism to Mouse: A Tale of Two Bioorthogonal Reactions. *Acc. Chem. Res.* **44**, 666–676 (2011).

- Song, W., Wang, Y., Qu, J. & Lin, Q. Selective functionalization of a genetically encoded alkene-containing protein via 'photoclick chemistry' in bacterial cells. *J. Am. Chem. Soc.* **130**, 9654–9655 (2008).
- Song, W., Wang, Y., Qu, J., Madden, M. M. & Lin, Q. A Photoinducible 1,3-Dipolar Cycloaddition Reaction for Rapid, Selective Modification of Tetrazole-Containing Proteins. *Angew. Chemie Int. Ed.* **47**, 2832–2835 (2008).
- Stiles, M., Miller, R. G. & Burckhardt, U. Reactions of Benzyne Intermediates in Non-basic Media. *J. Am. Chem. Soc.* **85**, 1792–1797 (1963).
- Tornøe, C. W., Christensen, C. & Meldal, M. Peptidotriazoles on solid phase: [1,2,3]-Triazoles by regiospecific copper(I)-catalyzed 1,3-dipolar cycloadditions of terminal alkynes to azides. *J. Org. Chem.* **67**, 3057–3064 (2002).
- Valenzeno, D. P., Pottier, R. H., Mathis, P. & Douglas, R. H. Photobiological Techniques. (1991).
- van Heyningen, E. 1,2,3-Benzotriazines. *J. Am. Chem. Soc.* **77**, 6562–6564 (1955).
- Vytla, D., Combs-Bachmann, R. E., Hussey, A. M., Hafez, I. & Chambers, J. J. Silent, fluorescent labeling of native neuronal receptors. *Org. Biomol. Chem.* **9**, 7151 (2011).
- Wang, M., Funabiki, K. & Matsui, M. Synthesis and properties of bis(hetaryl)azo dyes. *Dye. Pigment.* **57**, 77–86 (2003).
- Wang, X. *et al.* New method for effectively and quantitatively labeling cysteine residues on chicken eggshell membrane. *Org. Biomol. Chem.* **10**, 8082 (2012).
- Wang, Y., Hu, W. J., Song, W., Lim, R. K. V & Lin, Q. Discovery of long-wavelength photoactivatable diaryltetrazoles for bioorthogonal 1,3-dipolar cycloaddition reactions. *Org. Lett.* **10**, 3725–3728 (2008).
- Wang, Y., Song, W., Hu, W. J. & Lin, Q. Fast alkene functionalization in vivo by photoclick chemistry: HOMO lifting of nitrile imine dipoles. *Angew. Chemie - Int. Ed.* **48**, 5330–5333 (2009).
- Wang, Y., Rivera Vera, C. I. & Lin, Q. Convenient synthesis of highly functionalized pyrazolines via mild, photoactivated 1,3-dipolar cycloaddition. *Org. Lett.* **9**, 4155–4158 (2007).
- Wenk, H. H., Winkler, M. & Sander, W. One Century of Aryne Chemistry. *Angew. Chemie Int. Ed.* **42**, 502–528 (2003).
- Wilton, D. C. The fatty acid analogue 11-(dansylamino)undecanoic acid is a fluorescent probe for the bilirubin-binding sites of albumin and not for the high-affinity fatty acid-binding sites. *Biochem. J.* **270**, 163–6 (1990).
- Wittig, G. Phenyl-lithium, der Schlüssel zu einer neuen Chemie metallorganischer Verbindungen. *Naturwissenschaften* **30**, 696–703 (1942).
- Wittig, G. & Hoffmann, R. W. Dehydrobenzol aus 1.2.3-Benzothiadiazol-1.1-dioxyd. *Chem. Ber.* **95**, 2718–2728 (1962).

Wittig, G. & Krebs, A. Zur Existenz niedergliederiger Cycloalkine. *Chem. Ber.* **94**, 3260–3275 (1961).

Wittig, G. & Pohmer, L. Intermediäre Bildung von Dehydrobenzol (Cyclohexa-dienin). *Angew. Chemie* **67**, 348 (1955).

Yu, Z. & Lin, Q. Design of spiro[2.3]hex-1-ene, a genetically encodable double-strained alkene for superfast photoclick chemistry. *J. Am. Chem. Soc.* **136**, 4153–4156 (2014).

Yu, Z., Pan, Y., Wang, Z., Wang, J. & Lin, Q. Genetically encoded cyclopropene directs rapid, photoclick-chemistry-mediated protein labeling in mammalian cells. *Angew. Chemie - Int. Ed.* **51**, 10600–4 (2012).

Zhao, C.-J., Xue, D., Jia, Z.-H., Wang, C. & Xiao, J. Methanol-Promoted Borylation of Arylamines: A Simple and Green Synthetic Method to Arylboronic Acids and Arylboronates. *Synlett* **25**, 1577–1584 (2014).